

## ERRATA

### for "MEMOIRS OF THE KAKIOKA MAGNETIC OBSERVATORY SUPPLEMENTARY VOLUME I"

Page		Read	For
	CONTENTS (§ 2, Chapter IV)	Preliminary	Perlimentary
	CONTENTS ( 5, § 2, APPENDIX)	potential	patential
	CONTENTS ( 1, § 3, APPENDIX)	earth-currents	each-currents
	CONTENTS ( 2, § 3, APPENDIX)	earth-currents	each-currents
1	Line 14	radically	redically
4		Table 2	Table 12
9	Line 7 from bottom	(Fig. 1)	((Fig. 1)
20	Fig. 28	y: Mean for year	y: mean for yo
29	Line 4	$\bar{n}_x$	$n_x$
31	Line 2 (§ 5)	Sq of earth-currents	Sq earth-currents
35	Line 14	(Fig. 46)	(Fig. 16)
39	Line 3 from bottom	the preceding	thepreceding
51	Line 7	consistence	consistent
57	Line 7	Japan [52]. The	Japan [52] the
60	Line 12	this	his
62	Table 23	preliminary	prelimary
64	Line 12	impulse for	in impulse or
64	Line 5 from bottom	increases	inc reases
68	Line 2 from bottom	recently	ro ently

# UNIVERSAL EARTH-CURRENTS AND THEIR LOCAL CHARACTERISTICS

By  
TAKASABURO YOSHIMATSU

## CONTENTS

	Page
Introduction .....	1
Chapter I. Principal, or restricted direction of the variation of earth-currents	
§1. Distribution of the principal direction deduced from the diurnal variation..	2
§2. Principal direction observed in Japan.....	4
§3. Principal direction observed in the eastern part of U.S.A. ....	8
§4. Principal direction in some other places .....	9
§5. Summary of the observational results regarding the principal direction...	11
Chapter II. Time variations of the mode of Sq of earth-currents and solar activity	
§1. Introduction.....	13
§2. Correlation between maximum range of Sq of earth-currents and relative sunspot numbers .....	13
§3. Long period change of the mode of Sq in winter at Kakioka and sunspot numbers .....	21
§4. 4-year period change of the mode of Sq in winter at Kakioka .....	28
§5. Harmonic analysis of Sq of earth-currents .....	31
Chapter III. Magnitude of earth-current potential gradient and its local characteristics	
§1. World-wide data of Sq referred to some solar activity state .....	37
§2. Linear relationship between $C_{n,o}^N$ and $C_{n,o}^E$ .....	39
§3. Locality of $R_{n,o} = \sqrt{C_{n,o}^N{}^2 + C_{n,o}^E{}^2}$ and apparent resistivity $\rho_a$ .....	44
§4. Apparent resistivity $\rho_a$ and earth-resistivity $\rho_{obs}$ near the earth's surface...	47
§5. Presumed localities of underground electric structure in some places in Japan .....	51
§6. Anomalous amplitude of the harmonic waves of Sq near the sea-coast...	53
Chapter IV. Some characteristic features of the disturbance field of earth-currents observed in Japan	
§1. Introduction .....	60
§2. Preliminary changes of SSC and SI of earth-currents.....	60
§3. Diurnal variation of Ap and Sq.....	67
§4. Preliminary inverse impulse, or kick of SSC* of earth-currents .....	68
Chapter V. Conclusions.....	71
Acknowledgement .....	74
References.....	75

# APPENDIX

## The Measurement of Earth-Current Potentials and its Reliability

	Page
§1. Introduction .....	1
§2. Some experiments and notes on the measurement of earth-current potentials.	
1. Base length .....	2
2. Geomagnetic and atmospheric electric induction on the overhead line .....	3
3. Insulation .....	8
4. Contact resistances and their time variations .....	13
5. Variation of contact potentials.....	15
6. Comparison of universal earth-current potentials observed with different kinds of electrodes and apparatus .....	20
7. Polarization .....	24
§3. Measurements of earth-current potentials at the Magnetic Observatory (Kakioka) and its branch observatories	
1. Measurements of each-currents at Kakioka .....	25
2. Routine observations of each-currents at the observatories attached to the Magnetic Observatory (Kakioka) .....	28
Concluding remarks .....	28
References .....	29

## INTRODUCTION

So-called absolute values of earth-current potentials, which are meant by the potential differences themselves measured by some suitable method and apparatus between two points on the earth's surface, generally consist of various kinds of potentials due to different causes and circumstances in different localities, but generally speaking, they can be divided into two parts; the one is caused by some agencies prevailing in the higher atmosphere of the earth, while the other by ones seated in the earth including a number of extraneous effects near the electrodes.

The first part is mainly responsible for the so-called universal earth-currents, such as the daily variations, earth-current storms, micro-pulsations, various kinds of irregular disturbances and so on. These variations of earth-currents are all distinguishable from those of purely local origin and also observable simultaneously with those of the transient field of geomagnetism, but their local behaviors are remarkable indeed. The second part has been considered to be of radically local character itself, and actually, very little analysis has been done in rather specified localities probably on account of some observational troubles; for example, electrode performance, faulty insulation, variable contact potentials and so forth.

In this paper we dealt with their local characteristics as well as their world-wide natures of the first part of earth-currents, namely, so-called universal earth-currents, in respect to their spatial distributions and time variations. Since the very beginning of the history, many observations of this part of earth-currents have been carried out in various localities and in different epochs of the sunspot cycle. But owing to both defect of radical considerations of observational method and technique, and the complicated local natures of the earth's crust at the place where the observation is made, we are obliged yet to have little knowledge of their physical meanings, and even of their morphological basic facts as a world-wide phenomena. Therefore, in order to promote quickly this slow progress, as it holds good for the cases of other branches of science developed recently, it is strongly desired to observe them by using more modern techniques and apparatus at more well distributed stations all over the world. And then should be established their phenomenistic backbone of this branch of science. Unfortunately, it is a fact that even this self-evident requirement was not so easily realized. It is grateful, however, to have had recently many valuable material in several places in the world.

In the following chapters it is intended to make better understanding of remarkable local characteristics of universal earth-currents by using these available material as many as possible together with useful data of earth-resistivity and geomagnetism, and then to contribute to the investigation of earth-currents as a world-wide phenomena.

## CHAPTER I. PRINCIPAL, OR RESTRICTED DIRECTION OF THE VARIATION OF EARTH-CURRENTS

### §1. Distribution of the principal direction deduced from the diurnal variation

In the first place, in order to glance the general feature of the spatial distribution of universal earth-currents, so-called principal directions of potential gradients at several places over the earth's surface are summarized in Table 1, and shown in Fig. 1. Here, the principal direction is expressed by the nearest round number of degrees of the angle subtained between the geographical north and the direction of the major axis of a hodograph of the mean diurnal variation at each station, since available data at hand are all confined to the diurnal variation only. At some stations, each hourly vector does not always converge to any closely restricted direction, but makes more or less an oval figure, and somewhat differs this direction from that deduced from various kinds of short period variations mostly prevailing during the disturbances. We may be, however, satisfactory to demonstrate the general tendency, if any, of the spatial distribution of the direction of potential gradients. As it is seen in the figure, we have not so many points as a whole, and none in the middle parts of the North America, Africa and Asia, though relatively numerous in two regions, the eastern part of U. S. A. and Japan.

In the next paragraph we will first discuss the mode of distribution of the principal directions in these two regions from the topographical and geological points of views.

Table 1. Principal direction deduced from the diurnal variation.

Place	Principal direction	Lat.	Long.
Sodankylä [1]	N 90° W	67° 24' N	26° 30' E
Haparanda [2]	N 80 W	65 50 N	24 08 E
Lund [3]	N 60 W	55 42 N	13 11 E
Paris [1]	N 40 W	48 42 N	2 22 E
Berlin [4]	N 20 W	52 30 N	13 25 E
Greenwich [5]	N 10 E	51 44 N	0 0
Ebro [4]	N 20 W	40 49 N	0 33 E
Watheroo [4]	N 5 W	30 19.1 S	115 52.6 E
Fairbanks [4]	N 30 W	64 54 N	147 48 W
Tucson [4]	N 20 E	32 14.8 N	110 50.1 W
Huancayo [4]	N 50 W	12 02.7 S	75 20.4 W
Toyohara [6]	N 80 W	46 58 N	142 45 E
Kakioka [7]	N 60 E	36 14 N	140 11 E
Chesterfield [8]	N 50 W	63 20 N	90 42 W
Toledo [9]	N 60 E	39 53.1 N	4 02.7 W

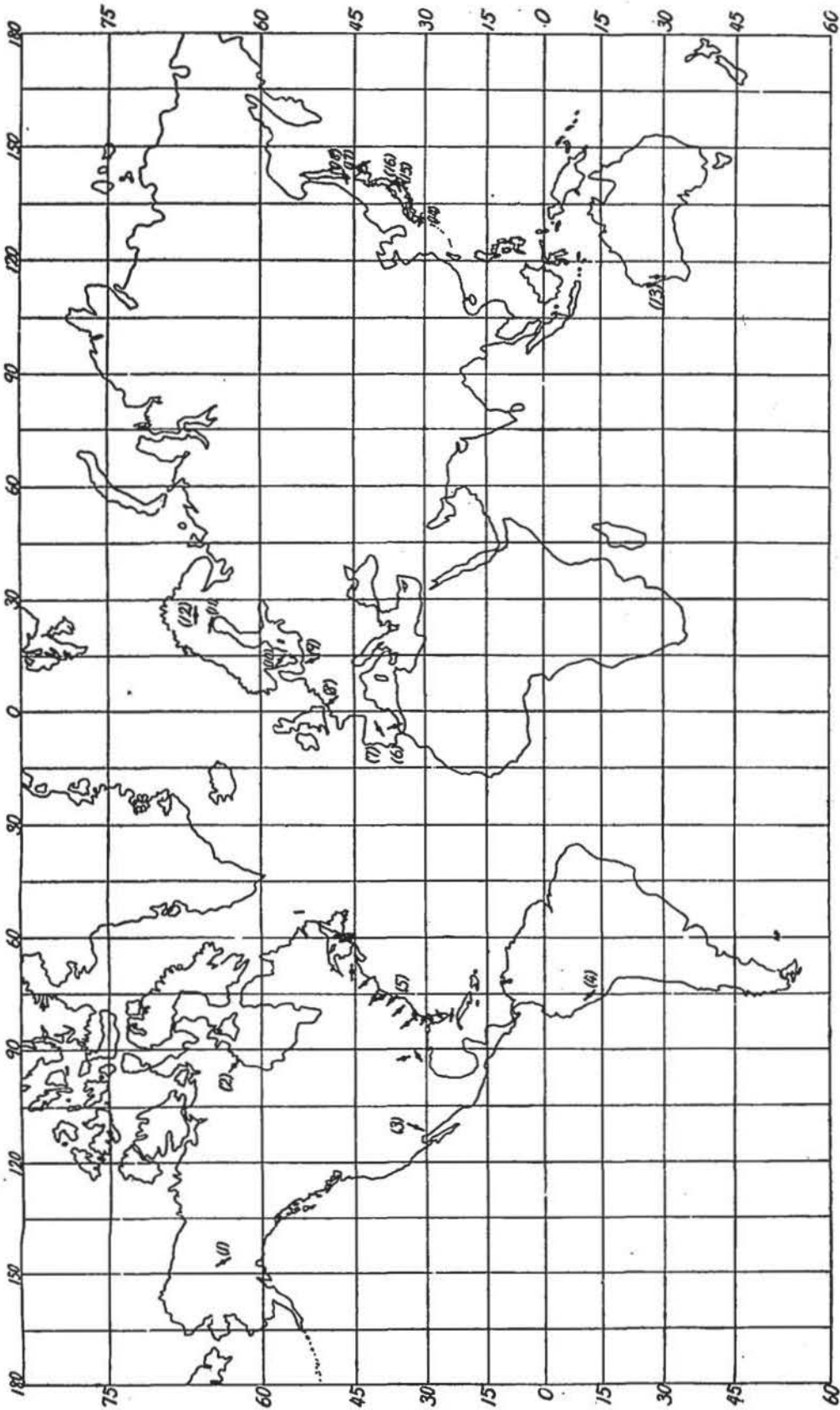


Fig. 1. Principal direction of earth-current potential gradients.  
 (1) Fairbanks (2) Chesterfield (3) Tucson (4) Huancayo (5) Houlton etc  
 (6) Ebro (7) Toledo (8) Paris (9) Berlin (10) Lund (11) Haparanda  
 (12) Sodankylä (13) Watheroo (14) Kanoya (15) Kakioka (16) Haranomachi  
 (17) Memanbetsu (18) Toyohara

## §2. Principal direction observed in Japan

## (A). Recent observations of earth-currents in Japan

In recent years, on the occasions of the total solar eclipses and destructive earthquakes we have had several lucky opportunities to obtain numerous available data of earth-currents at fixed and temporary stations all over the Japan Island. They could afford a chance to understand more precisely and more synthetically the characteristic distribution of earth-currents in different localities. These stations and their principal directions are shown in Fig. 2-17, and tabulated in Table 2. The values in this table

Table 12. Mean principal direction deduced from short period variations.

No.	Place	Lat. N	Long. E	Principal direction ( $\theta_0$ )	$\theta_0$	Period
1	Shirutori [10]	48° 36'	142° 50'	N 84°W	N 76°W	June 19—20, 1936
2	Toyohara	46 58	142 45	N 78 E	N 70 E	Mar., May, June, 1934 Sept., 1935
3	Memambetsu	43 55	144 12	N 43 E	N 43 E	June, 1936
4	Koshimizu [10]	43 52	144 28	N 30 E	N 20 E	June 19—20, 1936
5	Nemuro [12]	43 20	145 35	N 40 W	N 29 W	Jan., Feb., 1943
6	Obihiro	42 55	143 03	N 18 W	N 49 W	Jan., Feb., 1943
7	Ikutora	43 10	142 35	N 84 W	N 37 E	1947
8	Asamushi [10]	40 53	140 52	N 43 E	N 63 E	June 19—20, 1936
9	Morioka	39 42	141 01	N 54 E	N 74 E	Dec., 1946—Dec., 1947
10	Sendai [10]	38 15	140 52	N 39 W	N 61 W	June 19—20, 1936
11	Haranomachi	37 37	140 56	N 56 W	N 88 W	Dec., 1946—Dec., 1947
12	Kakioka	36 14	140 11	N 73 E	N 82 E	Dec., 1946—Dec., 1947
13	Miyakonojo	31 43	131 04	N 77 E	N 78 E	Dec., 1946—Dec., 1947
14	Heda	34 58	138 46	(A) N33W (B) N79W	N 25 W N 79 W	Aug., 1944
15	Owashi	34 04	136 12	N 76 E	N 66 E	Dec., 1946—Dec., 1947
16	Shikano [11]	35 27	134 04	N 13 E	0	Sept., 17—Oct., 2, 1943
17	Tanabe [15]	33 38	135 22	N 52 E	N 43 E	Jan.—Feb., 1947
18	Muroto [15]	33 17	134 17	N 55 E *(N 73 E)	N 55 E	Jan.—Feb., 1947
19	Kanoya	31 25	130 53	N 75 E	N 69 E	Dec., 1949 Jan.—Feb., 1950
20	Yamakawa [14]	31 12	130 38	N 15 E	N 15 E	May, Sept., 1950
21	Ishigaki [12]	24 20	124 10	N 56 W	N 50 W	Sept., 1941
22	Yonakuni [13]	24 28	123 00	N 34 E	N 30 E	Sept., 1941
23	Rebun	45 20	141 03	N 24 E	N 24 E	May, 1948
24	Fukui (Kawaimura) [16]	36 6.9	136 11.4	N 45 W	N 59 W	July, 1948

\* Values after the great earthquake, "Nankaidō Earthquake"

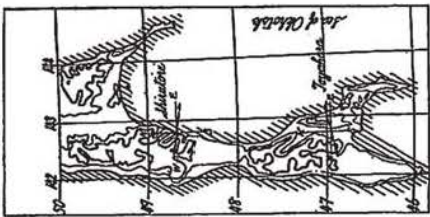


Fig. 2

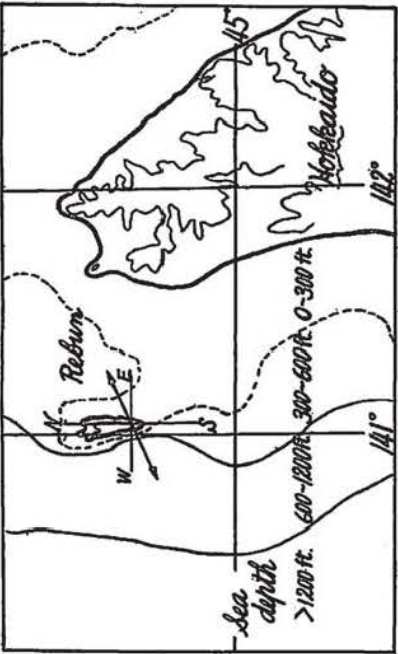


Fig. 3

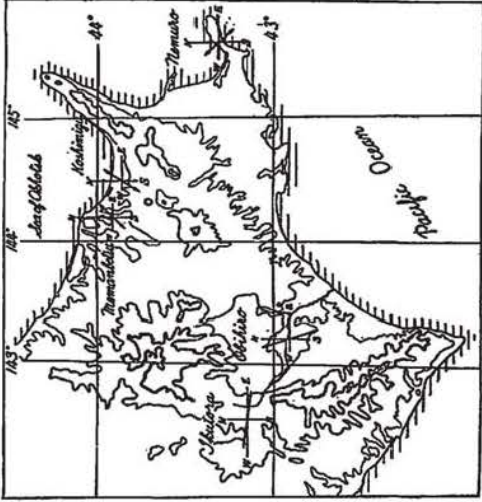


Fig. 4

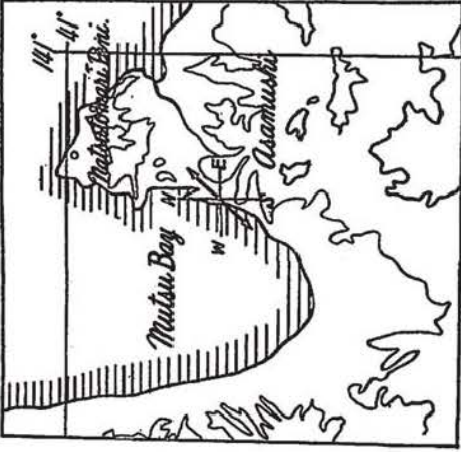


Fig. 5

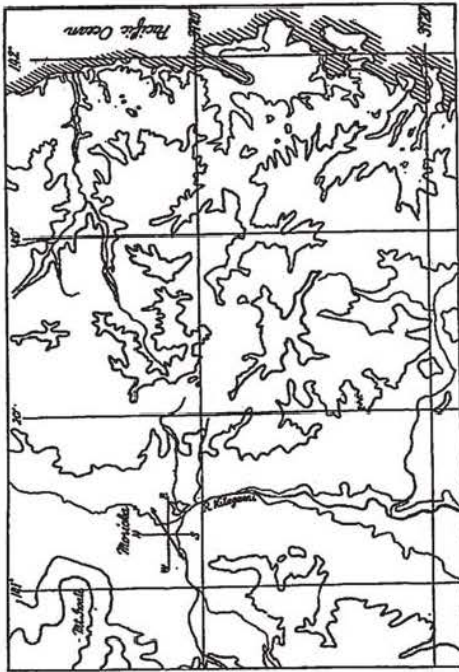


Fig. 6

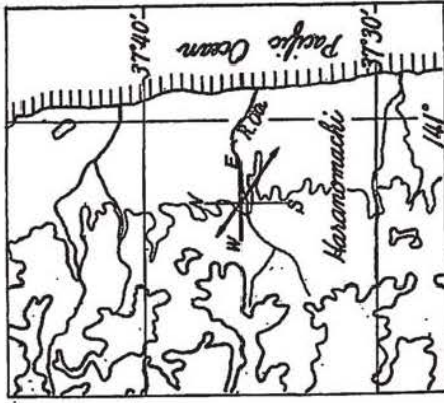


Fig. 8

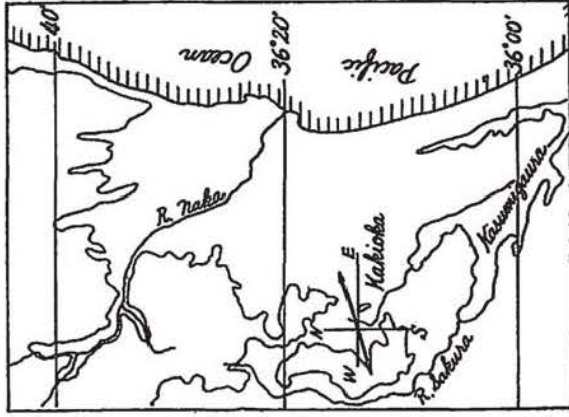


Fig. 9

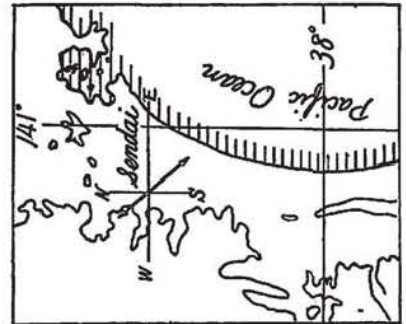


Fig. 7

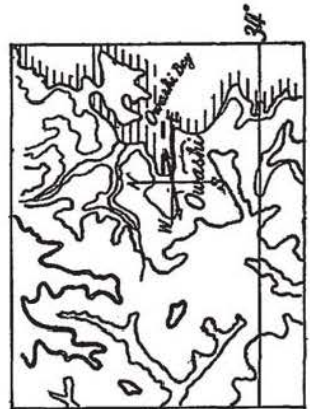


Fig. 10

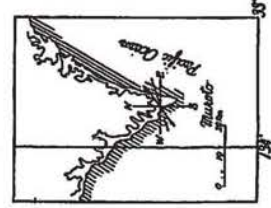


Fig. 12

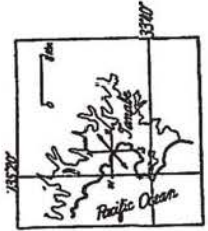


Fig. 11

Principal direction of earth-current potential gradients.

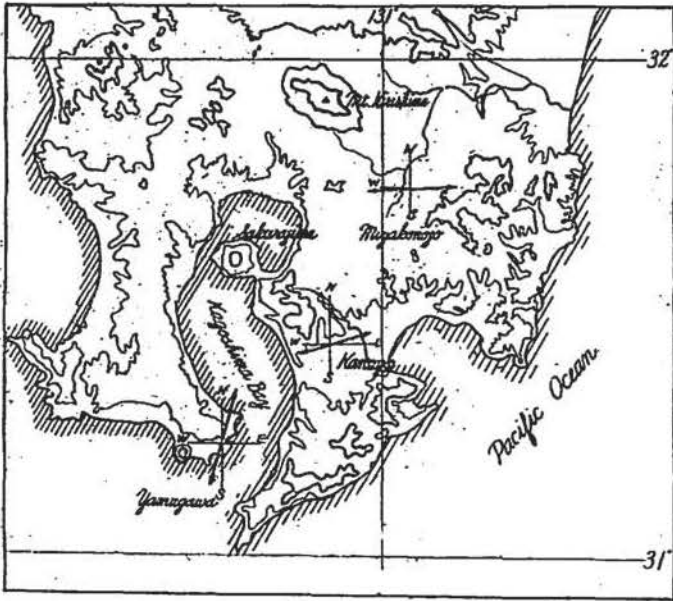


Fig. 13

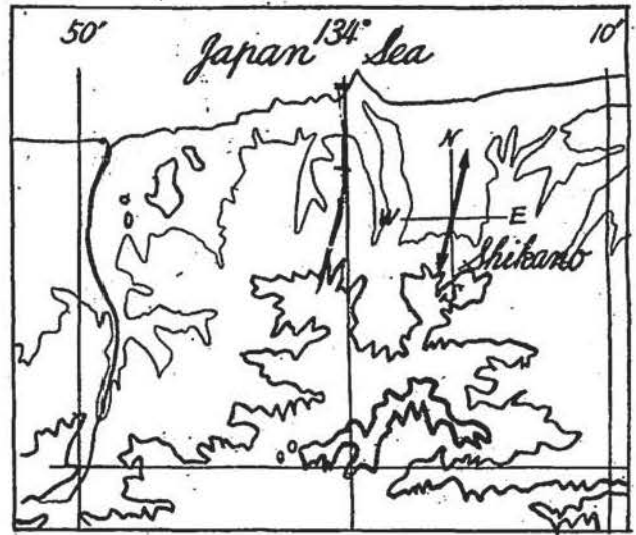


Fig. 14

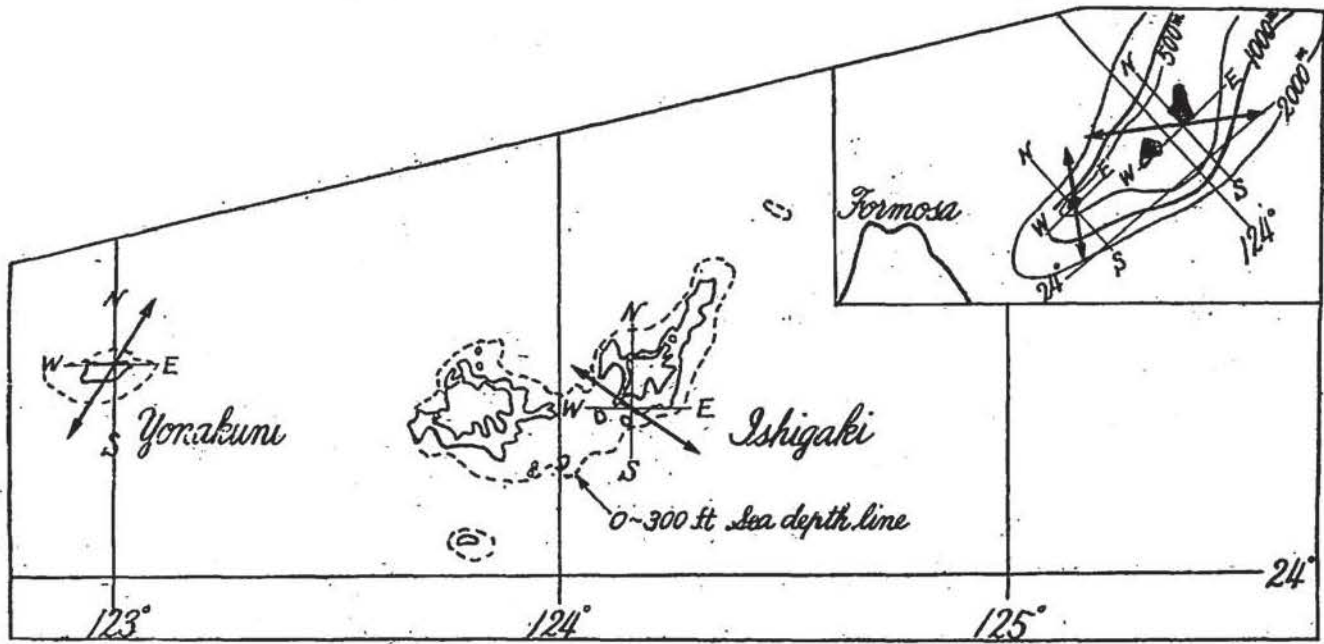


Fig. 15

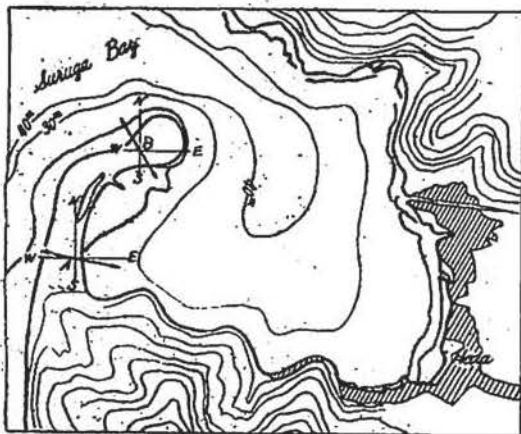


Fig. 16

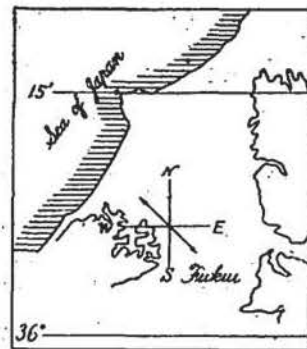


Fig. 17

Principal direction of earth-current potential gradients.

are almost deduced from the mean directions for many short period variations on account of the unpublished hourly values at most of stations and also troublesome gradual time variations of contact potentials. As it is seen in the table, since the epochs of observations are inevitably scattered in the interval of more than fifteen years, it may be hardly possible to avoid some errors due to time variations, if any, of the principal directions.

The short period variations adopted here are meant by ordinary fluctuations of universal earth-currents accompanied with simultaneous variations in the geomagnetic transient field. Most of the selected variations have so simple form that they make approximately linear changes lasting a few minutes to their extreme points. At Ikutora, however, the direction was exceptionally computed from the time variation between two successive hourly values during so disturbed intervals that they were hardly affected by the diurnal variation field, while at Rebun every ten minutes values were utilized.

(B). *Principal direction and topography in Japan*

As it is clearly seen in the figures above-mentioned, the mean principal direction in the Japan Island shows a characteristic distribution in respect to the topography in the vicinity of the station, or as contrasted with the relative distribution of land and sea. That is to say, for the most stations being situated near the coast, the directions are much more nearly at right angles to the coast line than along it. At some points in a narrow peninsula their principal directions coincide generally with the directions of shortest paths of the land at that points; Nemuro, Heda, Yamagawa and so on. The similar mode can be also seen at a station in a small island when the adjacent shallow portion of the sea is taken into account; Rebun, Ishigaki, Yonakuni and so on.

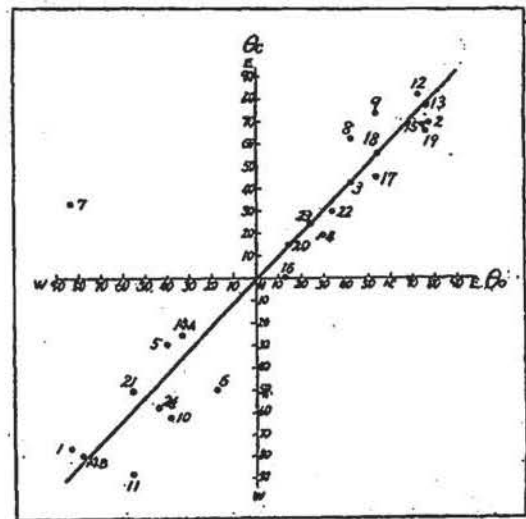


Fig 18 Relation between  $\theta_0$  and  $\theta_c$

Furthermore, in order to show the above-mentioned fact clearly, the observed principal direction  $\theta_0$ , which is reckoned from the geographical north, is compared with the calculated angle  $\theta_c$  sustained between the north and the line connecting the station to its

nearest point on the coast line, provided that at a station near the top of a narrow peninsula the latter line is taken perpendicularly to the length of the peninsula. The result is shown in Fig. 18. As mentioned above, the angles  $\theta_0$ 's are approximately equal to  $\theta_c$ 's in spite of wide range of  $\theta_0$ 's except only one station, Ikutora, which is situated in the high mountained part of the Hokkaido District and far remote from the sea-side. It may be, however, worthy to note that the direction of the shortest linear path in this district passing through Ikutora is N 70° W, while  $\theta_0$  is N 84° W.

It may be worthy further to remark that the residual,  $\theta_0 - \theta_c$  seems to be distributed more or less in regular manner as shown in Fig. 19. That is to say, 13 positive values out of 24 points are appeared in the larger part of the islands, while 7 negative ones

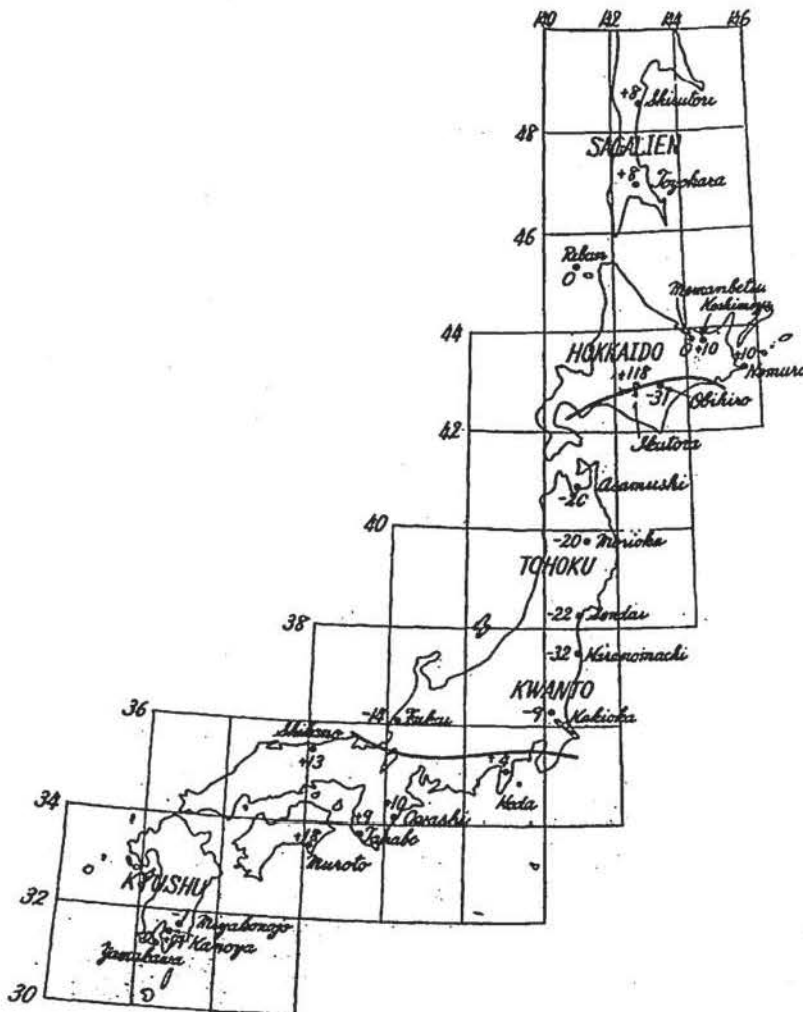


Fig. 19. Distribution of  $\theta_0 - \theta_c$ .

are all crowded in the limited zone in the middle and northeastern parts of Japan. The rest 4 are zero or nearly zero. In the Sagalien all stations show positive values in spite of its northerly elongated figure like that of the Tohoku District. On the other hand, it can be noted that the negative area of  $\theta_0 - \theta_c$  seems to coincide approximately with the well-known geological structure zone in Japan, "North-East Japan". At any rate, it may be then suggested that these facts may afford a clue to investigate the relationship between earth-currents and geological structure in rather large scale, though it is desired to have more stations to decide it, especially on the coasts of both the Sea of Japan and Seto Inner Sea, together with those in the central mountained regions.

### §3. Principal direction observed in the eastern part of U.S.A.

In the preceding paragraph, we described observational facts regarding characteristic local distribution of the principal direction in Japan and her vicinity. As another example to examine the minute feature of the mode of distribution of the principal direction, in this paragraph are treated the results obtained in the eastern United States.

During the second polar year, 1932-1933, G.C. Southworth[17] observed the earth-current potentials at about a dozen points crowded in this region. According to his report, near the coast, especially near and in the peninsula Florida including Key West, which is located in a small island laid between the peninsula and Havana (Cuba), earth-current potential gradients mostly tend to direct perpendicularly to the nearest coast-line, or to the length of the peninsula including the adjacent shallow part of the sea (Fig. 1). This general tendency of the distribution of the principal direction is very similar with that obtained in Japan, although the directions here are deduced from the diurnal variations. It is to be noted, however, that at two points, Denmark and Houlton, the potential gradients are of relatively small amplitude and their principal directions deviate markedly from this general tendency. They suggest apparently some local behaviours of the electrical conductivities near the stations, though we have no data of resistivities of their subterranean masses.

At an inland station, Wyanet (Illinois) the hourly vectors do not show the similar northwest-southeast direction, but make more rotary variations than those at other stations. It is somewhat notable that along this section of Mississippi Valley as pointed out by Southworth the principal direction seems to become more northerly, or more perpendicularly to the coast-line of the Gulf of Mexico. But the latter point should be

discussed from other possible points of views.

#### §4. Principal directions in some other places

Here is also examined whether any apparent relation does exist between their principal directions and topographies at some of the well-known observatories which are already given in Table 1 .

At Ebro and Chesterfield, which are respectively located near the Mediterranean Sea and the Hudson Bay, their principal directions are more perpendicular than parallel to the coast. And it is also noted that the principal direction at the former place is nearly along the part of the river Ebro near it. The similar mode can be found at San Miguel in Argentine (Fig. 20). Haparanda is situated near the coast of the so jugged Gulf of Bothnia that its principal direction seems to be not so simply relatable to the topography, but takes more or less similar mode with that at a station near the coast (Fig. 21)\*. The principal direction at Greenwich is not directed to the mouth of the Thames, but deviates slightly from the north. It coincides approximately with the direction of the shortest path in the island at the station, from the English Channel to the North Sea, including its adjacent shallow part of the Sea (Fig. 22). But it is possible to suppose that the principal direction may be controlled by the southern, or north-eastern hilly region provided its larger resistivity in the northern direction than that perpendicular to it. At Lund the direction runs northwest-southeasterly across the top of the peninsula in the direction of approximately the shortest path of the land (Fig. 23).

In the next place, we will examine the subject at some other stations more remote from the coast. At Paris the principal direction runs towards  $N 40^{\circ} W$  along the route of the river Seine. However, it may be considered to be rather perpendicular to the coast of the English Channel ((Fig. 1). The well-known result at Berlin by Weinstein also shows the similar mode with that at a station near the coast (Fig. 1 ). The principal direction,  $N 20^{\circ} W$ , at this place does not take the general direction, northwest-southeast, of the topographical features; that is, routes of the rivers Elbe and Oder or trend of mountain ranges in the southern part of Berlin.

At Huancayo in Peru, where the high mountain system of Andes runs northwest-southeasterly along the coast, the principal direction is directed towards  $N 50^{\circ} W$  along

---

\* Even at a station as high as Scoreby Sund, Greenland (Lat.  $70^{\circ}30'$ ), its principal direction shows this type.

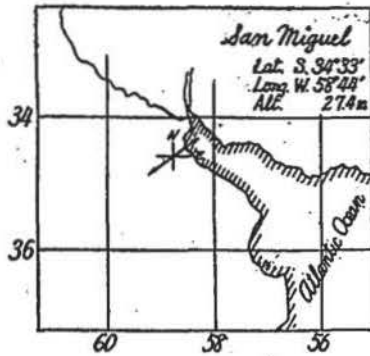


Fig. 20

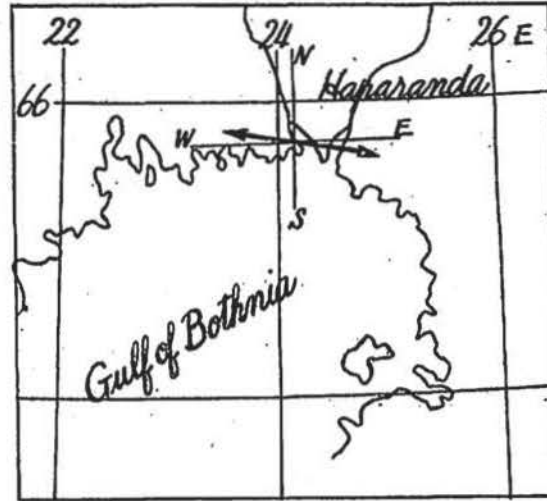


Fig. 21



Fig. 22

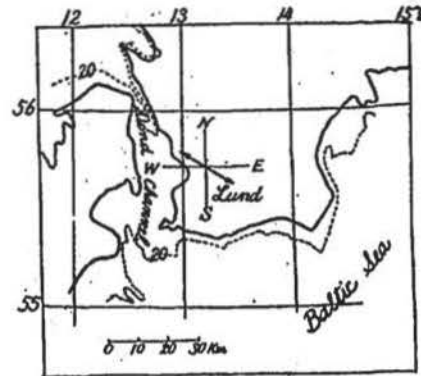


Fig. 23

Principal direction of earth-current potential gradients.

this trend, or the valley of the river Mantaro, but not perpendicular to the coast line. It is more or less similar with that at Toledo in Spain, where the principal direction,  $N 60^\circ E$ , is nearly along the general trend of the river Tajo, or mountain chains in this vicinity. The result of the second polar year's observations at Fairbanks shows the similar manner as those given above. The principal direction,  $N 30^\circ W$ , at this place merely remains in the same northwestern quadrant as the general direction of the Tanana, a branch river of the Yukon, or its valley, but deviates rather by large angles from it.

At Watheroo the principal direction,  $N 5^\circ W$ , coincides approximately with that of the mountain-ranges running along the coast of the Indian Sea, at the eastern margin of

which is situated the observatory. But the principal direction does not tend towards the general direction of the rivers, or their valleys, which are mostly originated in these mountained regions. Then, in this case the direction of the river, or its valley, itself seems to take no important role apparently for the distribution of the principal direction. It is, however, to be noted that the rivers in this region are all of minor scale. On the other hand, according to the resistivity survey (18) near the observatory the values in the northern part are about three times larger than those in the eastern one as it may be expected from the topographical views. Then it is not surprising that we have such order of amplitude ratio of the north-component to the east one. In the vicinity of Tucson the Rocky mountains generally appears to run northerly or northeasterly, and joins the Sierra Madre Occidental running northwesterly on the coast of the Gulf of California. The principal direction,  $N 20^{\circ} E$ , is rather parallel to the running direction of the former mountains.

At Sodankylä the mode of the diurnal variations on quiet days are quite different from those on disturbed days, that is, in the former case the east-component is predominant, while north-component so in the latter case. Then, any further description can not be done based on the same idea as that regarding the stations in the middle or low latitudes.

##### §5. Summary of the observational results regarding the principal direction

From the topographical point of view, general features of the distribution of the principal direction above-mentioned are summarized as follows.

*Coast-type.* At a station located near the coast its principal direction appears frequently to be more perpendicular to the nearest coast line than along it.

*Peninsula-type.* When a station is situated in a narrow peninsula its principal direction runs approximately perpendicularly to the length of it. And similar manner can be seen at a station being situated near the top of a peninsula, or in a small island, when the adjacent shallow part of the sea is taken into consideration. In other words, the principal direction coincides approximately with direction of the shortest path of the region considered passing through that point.

*Inland-type* The principal direction at an inland station far remote from the coast seems to take its own way characterized by the surrounding topography, probably

electrical conditions of the subterranean mass. As a whole, however, the principal direction is apt to be parallel to the general trend of the mountained regions in rather vast area including the station ; say, Huancayo, Toledo, Fairbanks. Watheroo and so on.

It is a fact that at present there are few local measurements of resistivity, and it is much difficult to make so large scale electrical survey that effective portions of the earth controlling the earth-current flow at the very point can be satisfactorily examined and located. Of course, it is not seldom to have remarkable distortion of the potential gradient due to the heterogeneous distribution of the electrical conductivity in the adjacent part of one electrode or one component only. But, actually above-mentioned classification based on so many available data at present can picture up more substantially the locality of the principal direction than hitherto done.

On the other hand, it is well known that the transient fields of both geomagnetism and earth-currents can be governed by the fundamental electromagnetic equations in and out of the ionospheres and solid earth, both having corresponding anisotropic structure of the electric conductivity. The geomagnetic contribution from the induced current in the shallow part of the earth is actually so small that the observed universal earth-current can be primarily considered as an induced electric phenomena in the superficial layer. If the intensity of induced currents in the earth is determined in a world-wide scale, the potential drop at any point should be remarkably localized according to the heterogeneous conductivity at the very point.

From this point of view, the principal direction of universal earth-currents at any point will be interpreted by assuming a reasonable spatial distribution of the conductivity in some area around the station, where the conductivity may be mathematically expressed in tensor from.

## CHAPTER II. TIME VARIATIONS OF THE MODE OF $S_q$ OF EARTH-CURRENTS AND SOLAR ACTIVITY

### §1. Introduction

In the preceding chapter has been studied experimentally the problem of the principal direction of earth-currents observed at several stations over the world. As a next step the local characteristics of the magnitude of universal earth-currents are to be clarified by using available data as many as possible. However, before treating with this problem it is needed at first to see to what extent the magnitude of earth-currents can be variable under different conditions of the solar activity in order to make clearly the statement of the problem.

On the other hand, this is also useful not only for the investigation of the solar and terrestrial relationships from the side of earth-currents, but also for the purpose of studying any other kind of local or world-wide phenomena, not suffered from the solar influence. In this chapter will be discussed various subjects in such a field of interest with respect to the time variations of the mode of  $S_q$  at many stations over the world, especially at Kakioka.

### §2. Correlation between maximum range of $S_q$ of earth-currents and relative sunspot number

#### [A]. *Statistics for calm days*

In recent years relatively long continued observations of earth-currents have been carried out, or continuing up to date at the following four observatories, Tucson, Arizona, U. S. A.; Huancayo, Peru; Watheroo, West Australia and Kakioka, Japan.

L. A. Bauer[19] has studied something about the solar and terrestrial relationships from the side of earth-currents observed at Ebro, Tortosa, Spain, during the interval 1914-1918. For the present investigation as a measure of the solar influence upon the potential gradient of the daily variation is simply adopted the maximum range,  $R$ , of each annual mean  $S_q$ , because it is simple and sufficient for the present purpose. By this means the relationship between  $R$  and annual sunspot number  $S$  (Zürich) was studied by using the available data at these observatories during the latest one or two sunspot cycles. At first the following three possible expressions for the correlation between  $R$  and  $S$  are examined in respect to the maximum range of east-component for all days at Kakioka in the period from 1934 to 1951,

$$R_1 = \alpha_1 + \beta_1 \cdot S, \quad R_2 = \alpha_2 + \beta_2 \cdot S + \gamma_2 \cdot S^2, \quad R_3 = a(S+b)^{1/2}$$

The various constants contained in  $R$ 's and  $\sum \left| \frac{\text{cal.} - \text{obs.}}{\text{obs.}} \right| / 18$  are calculated as follows in unit of mV/km,

	$\alpha$	$\beta$	$\gamma$	$a$	$b$	$\sum \left  \frac{\text{cal.} - \text{obs.}}{\text{obs.}} \right  / 18$
$R_1$	16.6	0.0462				0.059
$R_2$	16.8	0.0255	$0.012 \cdot 10^{-2}$			0.054
$R_3$				1.37	143	0.058

where one can find no superiority of any one expression as compared with others as far as these data are concerned.

Therefore, for the sake of simplicity the linear expression given by  $R_1$  will be used for the following statement.

The results shown in Fig. 24 are written as follows,

$$R_B^c = R_{O,B}^c + \alpha_c^B \cdot S$$

$$R_N^c = R_{O,N}^c + \alpha_c^N \cdot S,$$

where  $R_B^c$  and  $R_N^c$  are respectively the annual mean maximum ranges given in mV/km for east-component

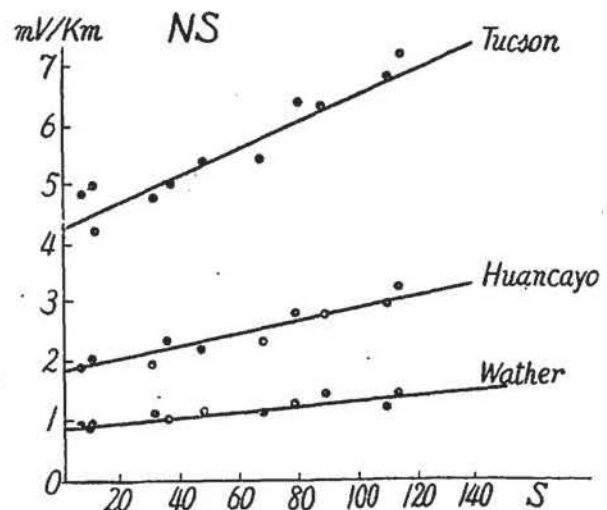


Fig. 24(A). Relationship between maximum range  $R_N^c$  of the annual mean  $S_q$  (10 least disturbed days) and relative sunspot number  $S$ , 1932~1942.

and north-component, while  $R_{0,E}^c$  and  $R_{0,N}^c$  are meant by fictional similar quantities which would be appeared when  $S=0$ . By the method of least square the coefficients  $\alpha_c$  s and  $R_0^c$ 's are calculated as given in Table 3(a), to which some material at Toyohara[20] Saghalien, is added.

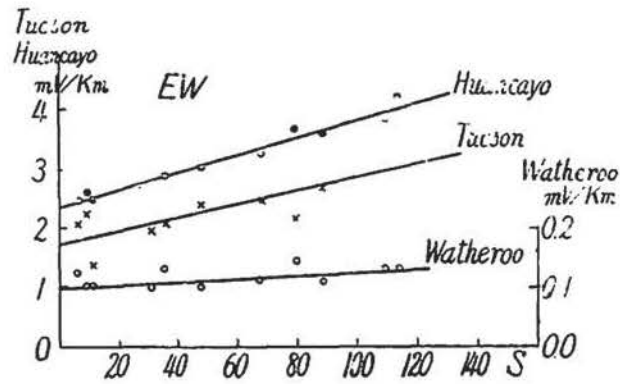


Fig. 24(B). Relationship between maximum range  $R_N^c$  of the annual mean Sq (10 least disturbed days) and relative sunspot number S, 1932~1942.

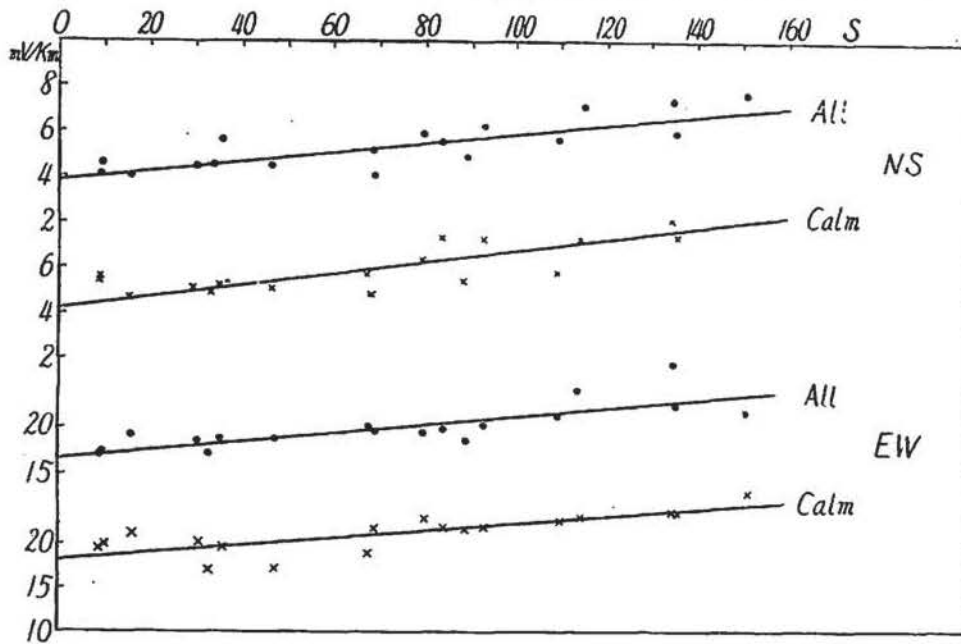


Fig. 24(C). Relationship between maximum ranges  $R_N$  and  $R_E$  of the annual mean Sq and relative sunspot number S, Kakioka. Calm days : 1934~1945. All days : 1934~1951.

Table 3. Relationship between the maximum ranges of the annual mean Sq and relative sunspot number(Zürich).

(a) Calm days.

Station	Latitude	$R_{0,N}^c$	$R_{0,E}^c$	$100 \alpha_c^N$	$100 \alpha_c^E$	Period
Watheroo	30° 19.1' S	0.86	0.10	0.49	0.02	} 10-calm days, 1932-1942
Huancayo	12 02.7 S	1.89	2.36	1.12	1.46	
Tucson	32 14.8 N	4.37	1.75	2.36	1.10	
Kakioka	36 13.9 N	4.20	18.0	2.63	4.00	5-calm days, 1934-1951
Toyohara	46 58 N	2.60	6.60	0.99	3.23	5-calm days, 1933-1936



component at Kakioka, however, deviates so much from the line that it shows no such distinct relationship, but for the summer season it holds fairly good. On this point a precise discussion will be made in later paragraphs.

On the other hand, if one looks more precisely at the distribution of points in these figures, apart from the general feature mentioned above, one notices some interesting mode of changes, for example, yearly rate of change of  $R_e$  does not seem to be constant, but slightly differs for different solar cycles, and even for components. And also during some intervals, namely, near the maximum or minimum epoch of  $S$  when the curve of  $S$  changes slowly, observed values fluctuate more remarkably than others. The latter seems to be more conspicuous at Tucson and especially so at Kakioka, and this point will be also retouched in latter paragraphs.

[B]. *Statistics for all days*

Regarding the case for all days' mean the result is given in Table 3 (b) and graphically shown in Fig. 25 (B), adding the similar data at three stations in Japan; Haranomachi, Kanoya and Memambetsu, where earth-currents observations have been continued up to date for some years (Fig. 26).

The expression corresponding to  $R_e$  is given as follows,

$$R_a = R_0^a (1 + m_a \cdot S), \quad m_a = 0.54 \cdot 10^{-2},$$

where the values of east-component at both Kakioka and Haranomachi are excluded from the computation of  $R_a$  because of the same reason as mentioned above in the case for calm days. Comparing (A) statistics with (B), it is safely said that there is no appreciable difference between two solar proportional constants  $m_e$  and  $m_a$  as far as the present statistics are concerned.

[C]. *Seasonal changes of Sq of earth-currents and geomagnetic field at Kakioka*

In order to clarify the apparent dis-

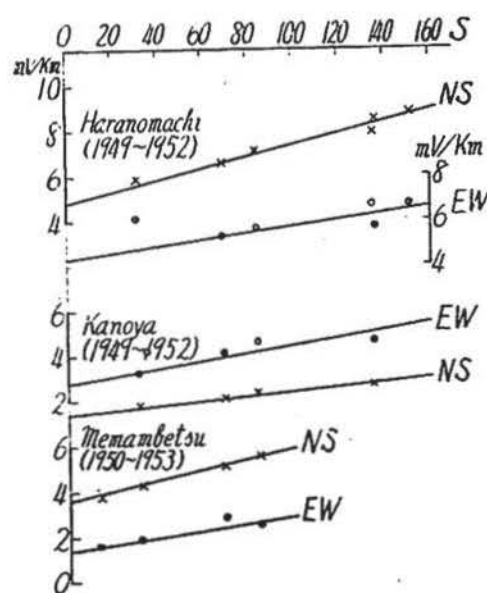


Fig. 26. Relationship between maximum ranges of the annual mean Sq for all days and relative sunspot number, Haranomachi, Kanoya and Memambetsu, Japan.

crepancy of east-component in relationship between  $R$  and  $S$  at Kakioka and in its vicinity, it is necessary to ascertain whether or not the same relation holds for each season. The maximum ranges of east component at Kakioka are given in Table 4, classifying into three seasons, equinox (III, IV, IX, X), summer (V, VI, VII, VIII,) and winter (I, II, XI, XII) for each year, 1934~1951. The calculated values of  $R_{0,E}^c$  and  $\alpha_c^E$  are given in Table 5.

From these tables one can easily accept that in the winter season  $R$  varies in wide range, and consequently  $\alpha_c^E$  amounts merely to  $1/3 \sim 1/4$  times those of other seasons. Furthermore, it seems that there exists no connection between  $R$  and  $S$  in the last sunspot cycle, 1934~1944, and only appears a slight correlation in the present cycle. Contrary to these winter characteristics of the amplitude of  $S_q$ , the relation is closer in equinox, showing no definite difference between two cycles except for

Table 4. Maximum range of the solar daily variation of earth-currents for each season for east-component at Kakioka, 1934-1951. (calm days)

Year	Summer	Winter	Equinox	Year	Summer	Winter	Equinox
1934	mV/km 20.2	mV/km 19.3	mV/km 25.7	1943	mV/km 19.6	mV/km 15.1	mV/km 31.5
35	19.7	18.7	20.2	44	26.1	18.4	21.5
36	30.4	17.5	25.6	45	18.5	19.2	16.8
37	24.9	19.4	27.6	46	20.7	21.5	22.2
38	27.4	17.6	24.6	47	31.1	22.5	27.6
39	25.6	13.8	30.4	48	32.7	22.9	26.8
40	23.8	19.9	23.4	49	30.9	27.6	27.0
41	18.4	18.4	20.5	50	25.5	23.3	25.1
42	22.9	18.9	20.6	51	27.9	21.9	24.8

Table 5.  $R_{0,E}^c$  and  $\alpha_c^E$  for each season at Kakioka, 1934-1951.

	Summer	Winter	Equinox
$R_{0,E}^c$	18.0 mV/km	18.6 mV/km	18.4 mV/km
$\alpha_c^E$	$9.5 \cdot 10^{-2}$	$2.4 \cdot 10^{-2}$	$6.6 \cdot 10^{-2}$

two larger values of  $R$ 's in 1934 and 1943, these values being omitted from the computation of Table 5. In summer, however,  $\alpha_c^E$  becomes as large as four times that of winter, and consequently it agrees fairly well

with the value expectable from the diagram ( $\alpha_c^E, R_{0,E}^c$ ), as shown in Fig. 25(A). The

inequality of the solar effect said above can be also detectable in other terrestrial phenomena, for example, at Washington [21] the noon value of  $f^oF_2$  in winter shows about 20% smaller  $\alpha$  in the epoch 1944 ~ 1952 than that in 1935~1943 provided the linear correlation with  $S$ . It is concluded, there-

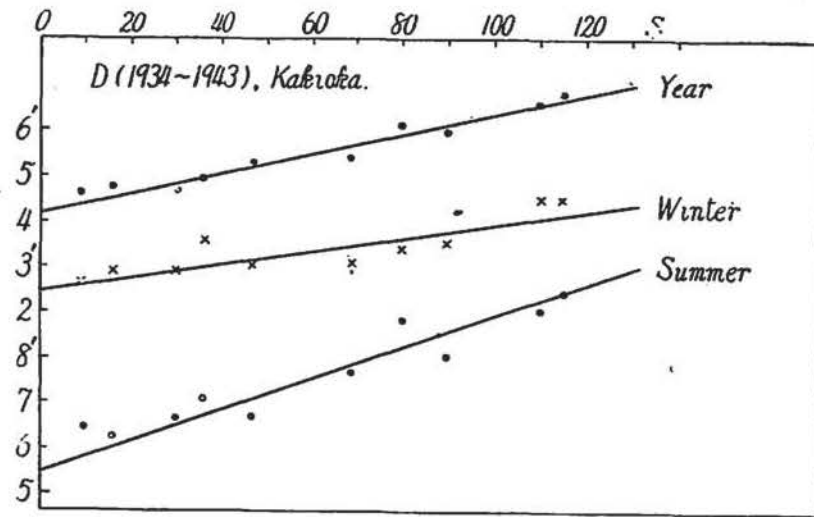


Fig. 27 (A). Relationship between maximum range of geomagnetic Sq for calm days at Kakioka and relative sunspot number. (A) : Declination. (B) : Horizontal intensity.

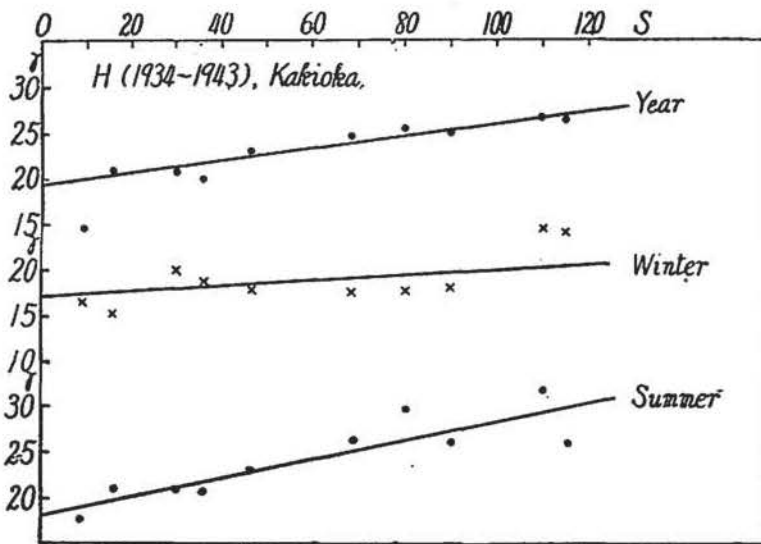


Fig. 27 (B).

fore, that Sq at Kakioka makes a remarkable seasonal change in respect to east-component, and consequently one may prefer summer to the other seasons for some investigations of the solar and terrestrial relationships in the vicinity of Kakioka.

Further, in order to support the statement

before-mentioned a similar correlation between  $S$  and the maximum range of the geomagnetic Sq-field was examined at Kakioka.

As seen easily from Table 6 and Table 7, or Fig. 27, there is scarcely a linear correlation between  $S$  and  $R_H^c$ , maximum range of Sq of the geomagnetic horizontal intensity in winter season, while a fairly good connection can be seen between  $S$  and  $R_D^c$ , maximum range for declination. The former just corresponds to the case of east-

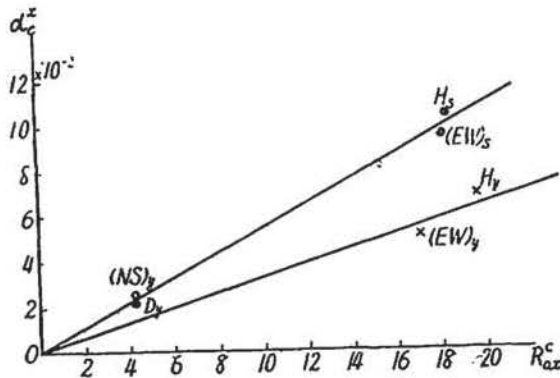


Fig. 28 Relation between  $\alpha_c^z$  and  $R_{O,x}^c$  for geomagnetic and earth-current Sq variations.

Suffix  $x$ : H, D, East- and North-component, respectively.  
 $y$ : Mean for year  
 $s$ : Mean for summer

component of earth-currents, while the latter does to that of north-component. And it is also to be noted that in summer the horizontal intensity shows the closest correlation with  $S$  as east-component of earth-currents does. In Fig. 28 is shown such a correspondence between earth-currents and geomagnetic field with respect to  $\alpha_c^z$ 's, where suffix  $x$  represents H, D, Z, E and N, respectively.

This intimate connection between earth-currents and geomagnetic field

obtained here confirms that an abnormally small amplitude of east-component of Sq at Kakioka or in its vicinity is not caused by any extraneous effect depending on observational conditions, but does link into more significant geophysical circumstances in the region considered.

Table 6. Maximum range of the solar daily variation of geomagnetic elements at Kakioka, 1934-1943 (calm days)

Year	Summer			Winter			Year		
	H	D	Z	H	D	Z	H	D	Z
1934	17.6 <sup>y</sup>	6.47 <sup>s</sup>	23.1 <sup>y</sup>	16.6 <sup>y</sup>	2.66 <sup>s</sup>	11.5 <sup>y</sup>	14.5 <sup>y</sup>	4.60 <sup>s</sup>	17.1 <sup>y</sup>
35	20.6	7.02	27.6	18.8	3.60	15.0	20.1	4.89	20.0
36	29.9	8.81	31.9	17.7	3.40	20.3	25.5	6.11	26.7
37	25.8	9.44	33.4	24.3	4.49	25.0	26.6	6.80	28.8
38	32.2	9.01	30.8	24.7	4.48	21.8	26.9	6.56	25.7
39	26.2	8.03	28.3	18.1	3.53	17.8	25.1	5.95	23.4
40	26.4	7.70	22.9	17.7	3.09	17.3	24.8	5.39	21.0
41	23.0	6.70	21.2	17.9	3.01	16.4	23.1	5.29	18.3
42	21.0	6.67	20.7	20.1	2.90	16.8	20.8	4.64	19.1
43	21.1	6.25	18.6	15.0	-2.92	13.4	21.1	4.76	17.0

Table 7.  $R_{0,x}^c$  and  $\alpha_c^z$  for the geomagnetic three elements at Kakioka ( $x$ :H,D,Z).

	Summer			Winter			Year		
	H	D	Z	H	D	Z	H	D	Z
$R_{0,x}^c$	17.5	5.5	18.7	17.3	2.5	11.7	19.5	4.2	14.6
$100\alpha_c^z$	11.2	3.4	11.3	2.7	1.4	9.3	6.9	2.2	11.5

### §3. Long period change of the mode of Sq in winter at Kakioka and sunspot number

#### (A). Introduction

In connection with the phenomena of abnormally decreasing amplitude of east-component of earth-currents at Kakioka, it seems to be important to touch further some characteristic changes of the mode of Sq in the course of long years.

Kakioka may be probably a typical station in the middle latitude encountering with different mode of distribution of the northern focus of the equivalent overhead current system of Sq. And it has been recently established[22] by using the data of the Second Polar Year that the intensity and position of foci of Sq frequently make remarkable changes. The matter, however, has been scarcely known yet about how does this mode change in the long course of time, especially with respect to the solar activity. Although the following statistics are mainly based on the data at Kakioka during the latest two sunspot cycles, they may contribute a new information to the question stated above.

#### (B). Long period change of $T_{min}^E$ , time of occurrence of the extreme minimum of Sq of earth-currents, in winter at Kakioka

The form of Sq at Kakioka is such as shown in Fig. 29, in which positive sense is used when the current flows eastwards or northwards. It should be, however, emphasized that the form of Sq shown in the figure, that is, the mode of occurrence

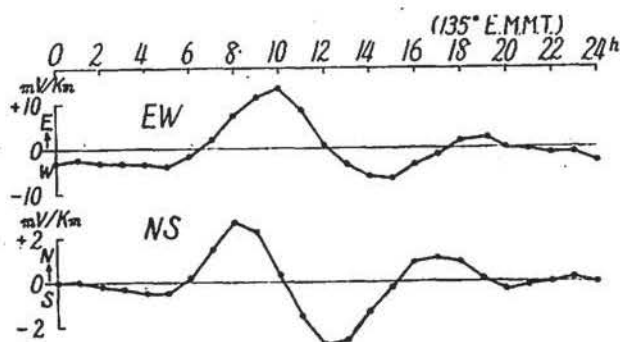


Fig. 29. Yearly mean Sq of earth-current potential gradient at Kakioka, 1934~1944 (five calm days).

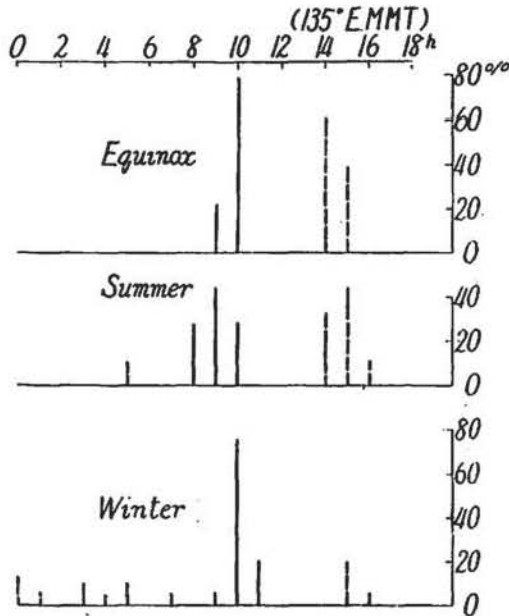


Fig. 30. Hourly frequencies of occurrence of extreme maximum and minimum of Sq for east-component, 1934-1951, (calm days).

Solid line : extreme maximum.

Broken line : extreme minimum.

winter, therefore, the extreme minimum of Sq appears for the most time in early morning, contrary to the mode of Sq in summer or equinox. The time variations of  $T_{max}^E$  and  $T_{min}^E$  for each annual mean Sq are shown in Fig. 31, denoting by the marks max. and min., respectively. It is clearly seen in the figure that out of total twenty years only five years show the extreme minimum of Sq in the afternoon. Furthermore, it should be noticed that all these five years are situated in the increasing phases of sunspot numbers as far as the latest two sunspot cycles are concerned. As a whole,  $T_{min}^E$  undergoes a remarkable long period change with the maximum about two years before the maximum year of S, but the form of the curve is dissimilar with that of S itself. Concerning this point, however, it was found out that there is a good parallelism between the curve and that of  $\Delta S/\Delta t = S_{n+1} - S_n$ , successive difference of annual sunspot numbers, which are plotted for the middle of two consecutive years. In other words, it is found out that even in winter there exists an intimate connection between R and S, if such a new measure is taken into consideration for the inequality of the form of Sq.

At last it may be worthy to touch again the problem of  $T_{min}^E$  in winter in an

of the extreme values does not remain constant in the course of the sunspot cycle.

For the first time a remarkable difference between winter and the other two seasons can be seen in the hourly frequency distribution of  $T_{min}^E$ , as shown in Fig. 30. This seasonal inequality is most conspicuous for east-component in winter.

Concerning  $T_{max}^E$ , occurrence time of the extreme maximum, one can find no such a thing. Then, in the following statement one may confine himself to  $T_{min}^E$  of east-component in winter only. The frequency of occurrence of  $T_{min}^E$  in the forenoon hours amounts to 75% of the total number during the period 1934~1951. In

another way. Let the number of months satisfying  $T_{min}^E > T_{max}^E$  out of four winter months be denoted by  $n$ , and its year-to-year change is examined. In Fig. 32 (A) is shown the yearly change of  $n$  for east-component, manifesting a similar long period change as seen already in Fig. 31. Of course, we have a similar change for north-component, though  $n$  is larger but less amplitude of variation than east-component.

The smoothed solid curves in the figures are drawn by using four years' running average of  $n$ .

(C). Long period change of the mode of geomagnetic Sq at Kakioka

In order to ascertain the result obtained above in another interval of years, geomagnetic Sq at Kakioka will be examined for the period 1925~1945.

**Horizontal intensity H :** The hourly frequency of  $T_{min}^H$  and  $T_{max}^H$  are shown in Fig. 33. The distribution of  $T_{min}^H$  is almost steady in each season within a limit of two hours of fluctuations, though there is a slight tendency in winter to occur within a few hours before the midnight. On the contrary to this, the monthly mean extreme maximum occurs during 6~9 hours by 38% of the total months in winter. In harmony with the case of earth-currents, the number of months satisfying  $T_{max}^H > T_{min}^H$  out of four winter months is denoted by  $n$ , and its yearly change is shown by  $H_{max}$  in Fig. 34. The smoothed curve shows two maxima, a predominant maximum in 1927

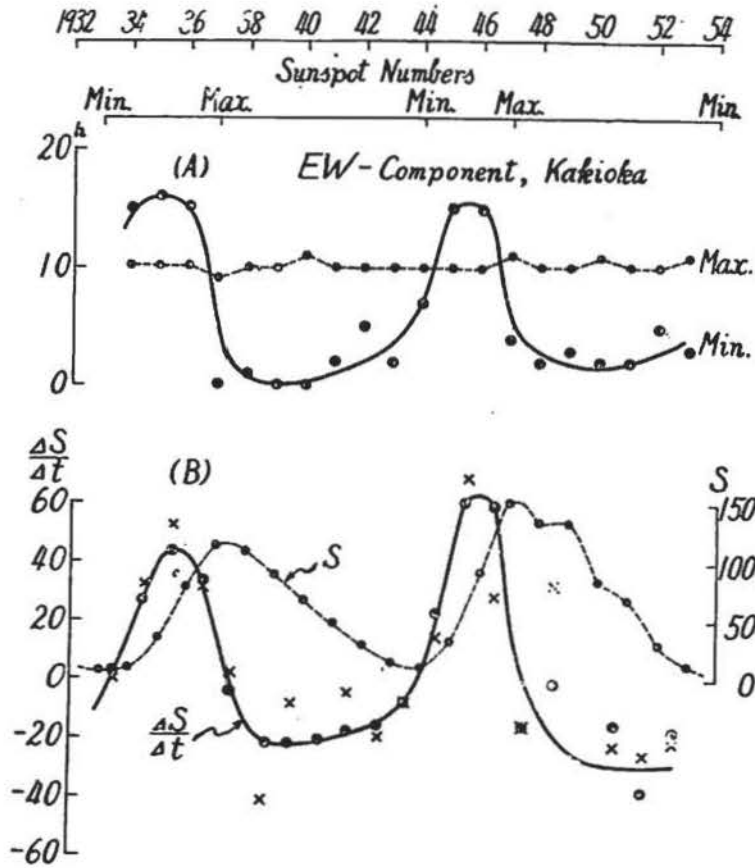


Fig. 31. Long period change of  $T_{min}^E$  of Sq for east-component in winter at Kakioka (A) and time gradient of relative sunspot number  $\Delta S/\Delta t$ , where  $\Delta t$  is one year (B).  $\Delta S/\Delta t$ 's for annual and winter means of  $S$  are expressed by black circles and cross marks, respectively.

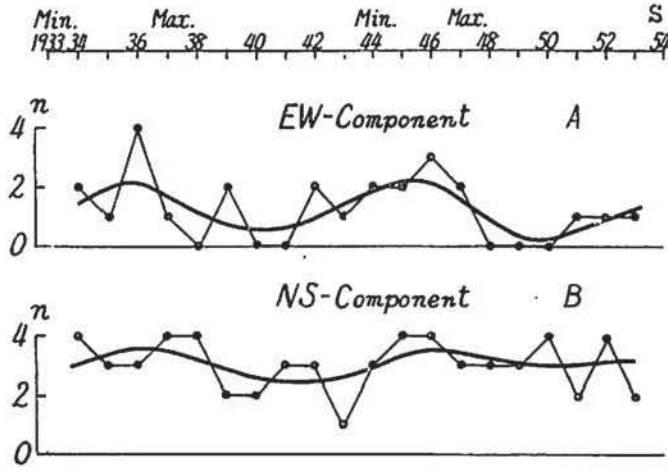


Fig. 32 Long period change of  $n$ , namely, number of months satisfying  $T_{min}^E > T_{max}^E$ , out of four winter months for each year at Kakioka (calm days).

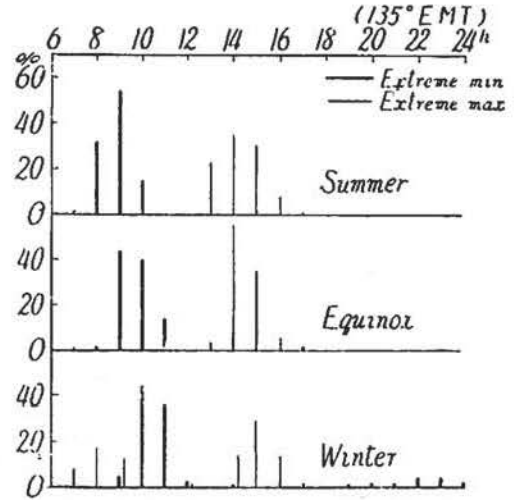


Fig. 33 Hourly frequencies of extreme maximum and minimum of geomagnetic Sq for the horizontal intensity  $H$  at Kakioka, 1925~1945 (calm days).

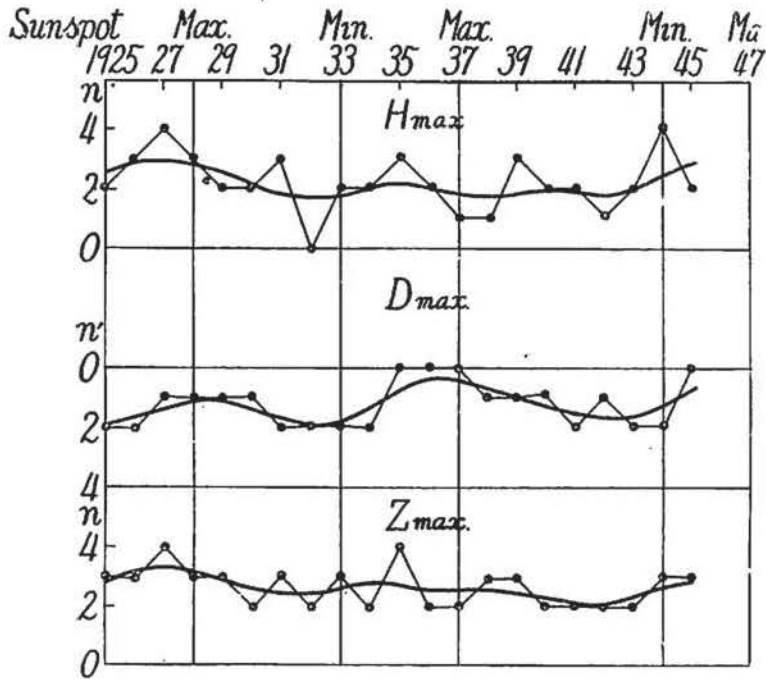


Fig. 34 Long period changes of the mode of geomagnetic Sq in winter for the horizontal intensity  $H$ , declination  $D$  and vertical intensity  $Z$  at Kakioka.

and less one in 1935; each occurs one or two years earlier than the maxima of  $S$ . This general tendency is in harmony pretty well with that of earth-currents.

**Declination  $D$ :** Comparing with  $H$ , the form of Sq of  $D$  is remarkably stable, and the maximum and minimum occur almost at 13hr and 9hr, respectively. The frequencies of  $T_{max}^D$  and  $T_{min}^D$  are such as given in Table 8. If the number of months in winter, of which daily maxima occur earlier or later than 13 hr, the most frequent time of occurrence, be denoted by  $n'$ , the year-to-year variation of  $n'$  is of a similar curve with  $H_{max}$  as shown by  $D_{max}$ .

and less one in 1935; each occurs one or two years earlier than the maxima of  $S$ . This general tendency is in harmony pretty well with that of earth-currents.

**Declination  $D$ :** Comparing with  $H$ , the form of Sq of  $D$  is remarkably stable, and the maximum and minimum occur almost at 13hr and 9hr, respectively. The frequencies of  $T_{max}^D$  and  $T_{min}^D$  are such as given in Table 8.

in Fig. 34. But the sense of variation is such that the more frequently  $H$  shows the summer-or equinox-type, the more nearly  $T_{max}^D$  approaches to 13 hr. In other words, deviations of  $T_{max}^D$  from the most frequent value, 13 hr, seem to be controlled by the same agency as governing the fluctuations of  $T_{max}^H$ .

Table 8. Frequency (%) of  $T_{max}^D$  and  $T_{min}^D$  at Kakioka, 1925-1945.

	8	9	10	11	12	13	14 <sup>h</sup>
$T_{max}^D$	—	—	—	—	15	69	15
$T_{min}^D$	12	77	11	—	—	—	—

*Vertical intensity Z*:  $T_{min}^Z$  appears in the interval 8 hr~11 hr, namely, 50% at 9 hr, and 83% in 9 hr~10 hr, while  $T_{max}^Z$  appears in two groups of hours, 4 hr~8 hr and 13 hr~16 hr, respectively. The time variation of  $n$ , which is calculated for the afternoon maximum, is given by the lowest curve in Fig. 34, showing a similar tendency with the other two magnetic elements.

(D). Relationship between  $n$  and frequency of so-called "E-type" of Sq in winter at Kakioka

At last the variation of  $n$  of any element said above, say, east-component of earth-currents is directly compared with that of frequency of "E-type" of Sq in winter,  $N$ , the result being shown in Fig. 35 during the latest sunspot cycle, 1944~1953. It is natural to find a good parallelism between two curves, because characteristics

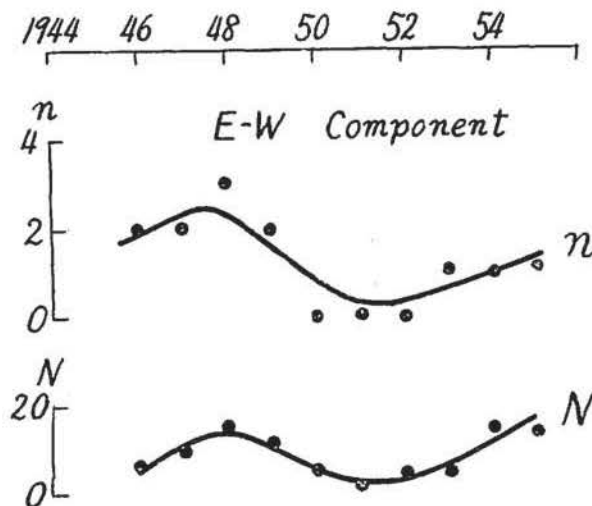


Fig. 35. Long period variations of  $n$  and  $N$  in winter at Kakioka.

of  $n$  ought to be controlled by  $N$ . The criterion for classifying the type of the solar daily variation has been discussed by the Ionosphere Research Committee, Science Council of Japan, to which larger parts of the present data of "E-type" have been presented by the Kakioka Magnetic Observatory. Now, considering the connection between  $n$  and  $\Delta S/\Delta t$  obtained above, the frequency  $N$  of "E-type" of Sq should

also be understood in the sense of  $\Delta S/\Delta t$ , but not  $S$  itself. On the other hand, as to the average state of Sq, the position of focus in the northern hemisphere attains its most northern latitude in the forenoon with respect to G.M.T.[23], while the intensity of focus in the southern hemisphere raises nearly to the maximum value. Hence, even at a station far remote from the focus, "E-type" variations may manifest themselves when the northward wandering motion of foci is strengthened. The variation of  $N$  at Kakioka, therefore, seems to be apparently due to the remarkably intensified ionization, or enlarged integrated conductivity, of the ionosphere in the southern hemisphere. But, from ionospheric observational results and others, the yearly change of ionization of the ionosphere, or magnitude of integrated conductivity, seems to depend solely upon  $S$  itself, but not  $\Delta S/\Delta t$ . Hence, it may be apparently suggested that if the sun does not emit some special kinds of short waves during the rapidly raising interval of  $S$ , namely one or two years before the maximum of  $S$ , the ionospheric motion would be subjected by some unknown mechanism in the ionosphere to intensify the equivalent current system with the same long period as  $n$  or  $N$ . Nevertheless, at present one has no sufficient observations such as to be able to check possible considerations said above.

At any rate, however, these facts obtained in the vicinity of variable locus of foci of Sq may throw a light on the theory of Sq, especially its secular change. At the same time some predictable informations of the type of Sq will become useful for some practical geomagnetic and geoelectric workers.

[E]. *Long period change of the mode of Sq of earth-currents in winter at Tucson*

A similar treatment with Sq was carried out for an another middle latitude station, Tucson, Arizona, U.S.A.[24] of which material covers the former sunspot cycle 1932 ~1944, but not long enough for the present object. The seasonal variation of earth-current potential gradients at Tucson has been already discussed by W. J. Rooney[25], while the present treatment is confined itself to the behavior of Sq in winter months only in comparison with the result at Kakioka. The form of the solar daily variation at Tucson is such as shown in Fig. 36.

In Table 9 are given the average values of  $T_{max}^E$  and  $T_{min}^E$  for each month as well as the frequency of deviations from the corresponding average values. The average

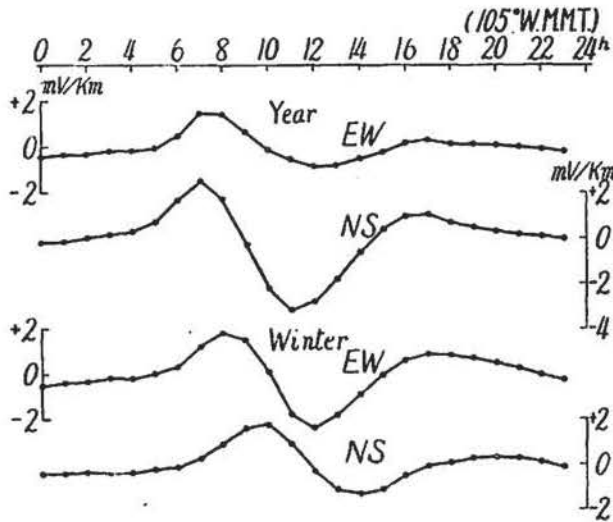


Fig. 36. Sq for 10 least disturbed days per month at Tucson, 1932~1942.

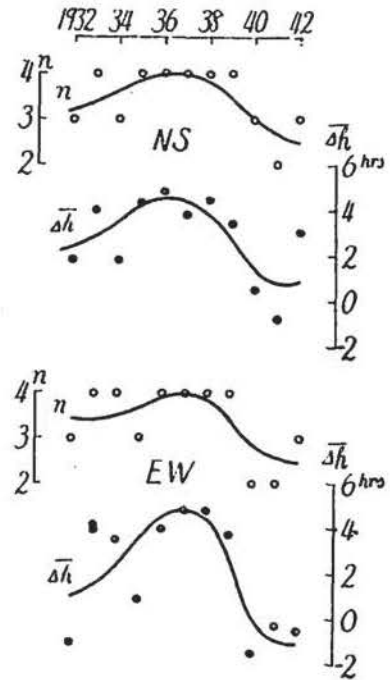


Fig. 37. Long period changes of  $n$  and  $\Delta h$  at Tucson.

values of  $T_{max}^B$  and  $T_{min}^B$  are nearly constant for each month in respect to the whole period as well as an individual year.

The number of months  $n$ , in which average time of occurrence of the extreme

Table 9. Frequencies of time of occurrence of the extreme values of  $S_q$  in winter at Tucson, 10 least disturbed days, 1932~1942.

Component	Average time of occurrence of the extreme values for each month. (1)			Number of months corresponding to the following deviations of hours from (1).													
	Extreme value	Month	Average time (hr)	-14	-12	-3	-2	-1	0	1	2	6	7	8	9	10	11
NS	min.	I	12 ~ 13						1	8	2						
		II	12 ~ 13						1	9	1						
		XI	12 ~ 13		1				3	6			1				
		XII	12 ~ 13							8	3						
NS	max.	I	9 ~ 10						3	8							
		II	8 ~ 9						2	5	1			2	1		
		XI	7 ~ 8							8	2	1					
		XII	9 ~ 10						5	4				2			
EW	min.	I	14 ~ 15						1	9	1						
		II	14 ~ 15						2	2							
		XI	15 ~ 16				1		3	2							
		XII	15 ~ 16		1				3	2	1						
EW	max.	I	10 ~ 11						1	9	1					1	
		II	9 ~ 10						2	1	2	3	1			1	
		XI	8 ~ 9			1				3	5	2					
		XII	10 ~ 11						3	5	3						

minimum lags behind that of the extreme maximum, is distributed as shown in Fig. 37, where  $n \geq 2$  for both components. In the figure is also shown a quantity  $\Delta h$ , which is the average value of  $\Delta h = T_{\min}^n - T_{\max}^n$ . Comparing these results with those at Kakioka, a similar tendency can be found, but less remarkable at Tucson. This is probably due to the inequality of their relative positions to the focus of the Sq current system in spite of their nearly same geographical coordinate of latitude.

#### §4. 4-year period change of the mode of Sq in winter at Kakioka

##### (A). Shorter periodic changes of $n$ of earth-currents and geomagnetic field

Following the preceding paragraph a further detailed analysis of the time variation of the occurrence time of the extreme values will be performed in this paragraph.

It is easily found out in Fig. 32 or Fig. 34 that there may exist some shorter periodic variations superposed on the long period change mentioned above. Since apparently fluctuations with about 4-year period can be seen in these figures, the

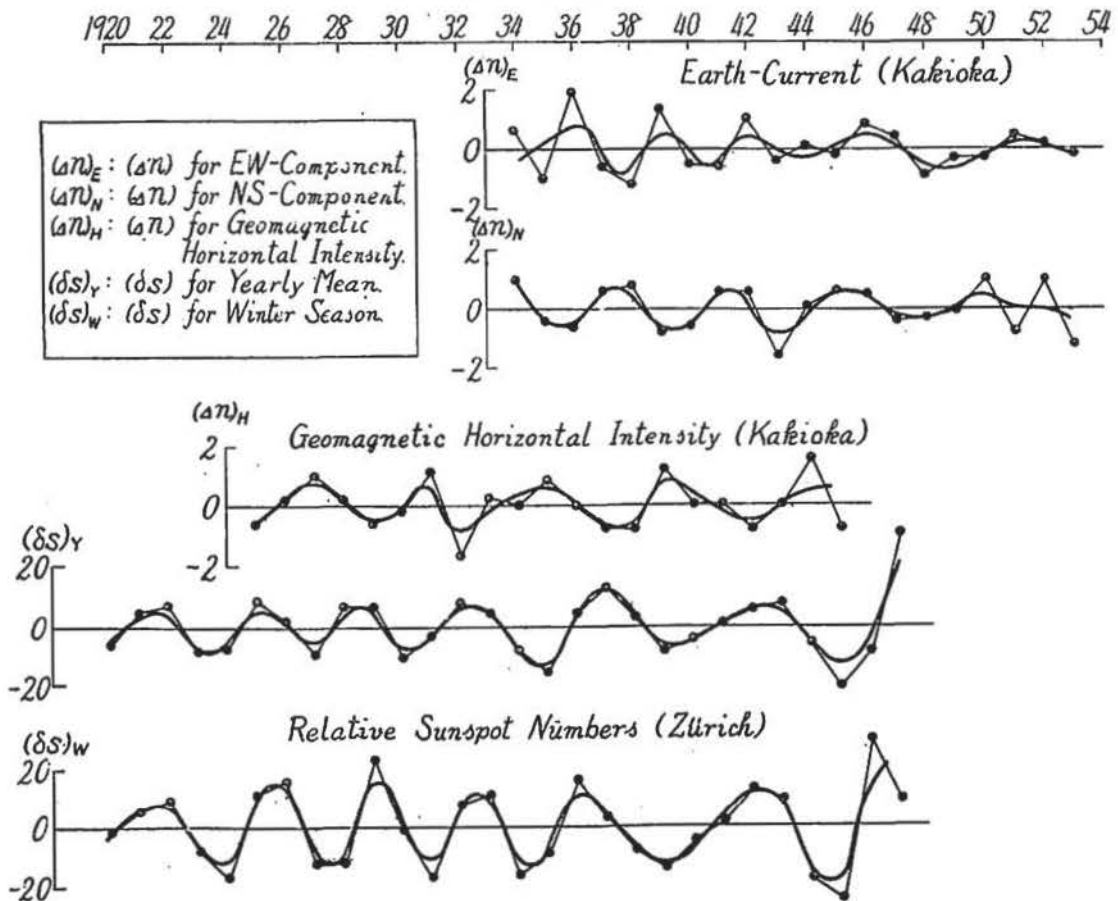


Fig. 38. 4-year period change of the mode of Sq in winter at Kakioka and its connection with that of  $S$

residuals  $(\Delta n)_x = n_x - \bar{n}_x$  are calculated for the convenience of the study of shorter periodic changes, where the suffix  $x$  is to be read as  $N$ ,  $E$  and  $H$  for north-component, east-component of earth-currents and geomagnetic horizontal intensity, respectively,  $n_x$  being the 4 years' running average of  $n$ . They are shown in Fig. 38.

$(\Delta n)_N$ : During the interval from 1934 to 1949 4-year period is apparent, while in the period 1951~1953 observational points are more or less scattered and tend to show longer period as well as increasing amplitude. At least, 4-year period in the interval 1934~1949 is statistically significant by 1.3% level of the criterion of the periodogram analysis.

$(\Delta n)_E$ : In the interval 1934~1940, 3-or 4-year period are seen, and generally in an opposite sense of variation against  $(\Delta n)_N$ .

$(\Delta n)_H$ : 4-year period is apparent, and in later years the period seems to grow longer. The variation is approximately in opposite sense against  $(\Delta n)_N$ .

Referring to the geomagnetic vertical intensity  $Z$ ,  $(\Delta n)_Z$  shows no distinct periodicity because of small amplitude.

From these facts it is evident that there is contained a predominant periodic change with period about 4 years in the time variation of  $\Delta n$  for both earth-current and geomagnetic field during the recent thirty years.

[B].  $\Delta n$ ,  $fF_z$  and  $S$

It is interesting to know whether or not such a periodic change stated above does exist in the time variations of annual relative sunspot numbers  $S$ . The lowest two curves of  $\delta S$  in Fig. 38 will answer to this question. In order to eliminate 11-year period five years' running average of  $S$  is subtracted from  $S$ . But for convenience of treatment of data, the same process of average is repeated twice more. The final residual  $\delta S$

is calculated for two cases,  $(\delta S)_Y$  for annual mean and  $(\delta S)_W$  for winter, respectively. The connection between  $\delta S$  and  $\Delta n$ , say,  $(\Delta n)_H$  is shown in Fig. 39 of which all points

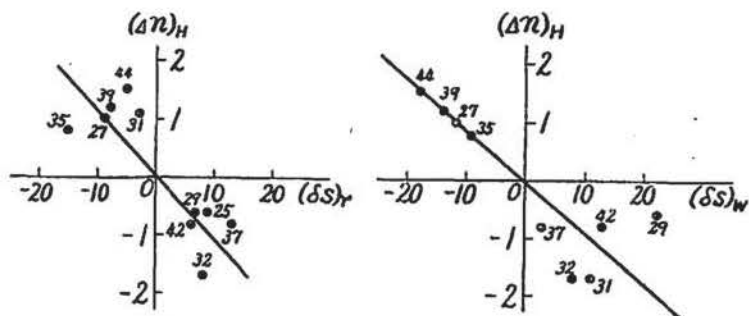


Fig. 39. Values of  $(\Delta n)_H$  at Kakioka corresponding to maxima and minima of  $\delta S$ .

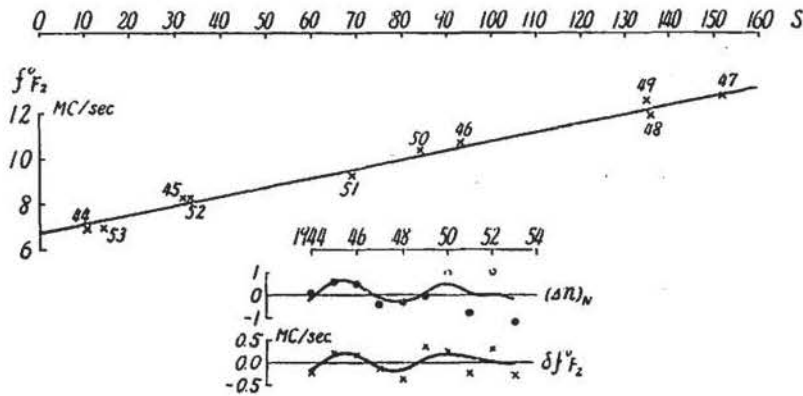


Fig. 40. Correlation between  $S$  and  $f_{F_2}^o$  in winter at Kokubunji, Japan.

correspond to the maxima and minima of  $\delta S$ .

There is seen clearly an inverse sense of variation between two quantities, though the numerical values do not always show so good connection, which is inevitable in such a case of treatment.

On the other hand

it is also interesting to see whether or not the corresponding shorter periodic change does exist in the time variations of the ionospheric elements. For example, in Fig. 40 are shown the correlation between  $f_{F_2}^o$  at Kokubunji, Tokyo[26] and  $S$ , together with that between  $(\Delta n)_N$  and  $\delta f_{F_2}^o$ . Here,  $f_{F_2}^o$  is the average noon value for each winter, and  $\delta f_{F_2}^o$  the deviation of  $f_{F_2}^o$  from a linear expression  $f_{F_2}^o = 6.7 - 0.041 \cdot S$  which is calculated by the method of least square. As seen in the figure a fairly good positive correlation can be found between  $(\Delta n)_N$  and  $\delta f_{F_2}^o$ , showing that the ionosphere over Kokubunji in winter may be simultaneously changeable in a similar way as Sq field, since Sq is mainly originated in the  $E$ -layer. A similar change of  $\delta f_{F_2}^o$  can be more or less found at Washington[27] and other middle latitude ionospheric stations.

At last it may be worthy to add some remarks that if the calculation of  $(\delta S)_Y$  is extended to the former century, almost all large peaks of the maximum values of  $(\delta S)_Y$  fall on the respective sunspot maximum years (Table 10). Moreover, it is likely that  $(\delta S)_Y$  contains some longer periods, say, two or four times the

Table 10. Maximum values of  $(\delta S)_Y$ .

Year	$(\delta S)_Y$	Year	$(\delta S)_Y$	Year	$(\delta S)_Y$
1832	11	1974	3	1909	7
36	31	77	12	12	8
41	4	81	10	17	21
45	3	84	7	22	7
48	25	89	5	25	9
52	8	92	13	28	8
54	1	98	1	32	13
59	15	1900	7	37	8
64	11	5	8	43	31
70	30				

primary sunspot period, 11 years.

§5. Harmonic analysis of Sq earth-currents

(A). Harmonic analysis of Sq of earth-currents at Kakioka

The results of harmonic analysis of Sq up to the fourth harmonics are given in Table 11 for each years(28). Fourier terms are expressed by  $E(N) = \sum_n C_n \sin(nT + \varphi_n)$ , where  $\varphi_n$  is measured from the midnight of the universal time  $T$ .

In the first place, the correlation between  $C_n^a$  for all days and  $S$  can be approximately expressed as follows from Table 12 and Fig. 41,

$$C_n^a = C_{n,0}^a + \beta_n^a \cdot S = C_{n,0}^a (1 + m_a' \cdot S), \quad m_a' = 0.38 \cdot 10^{-2},$$

where the fourth term is excluded from the calculation because of small amplitude. The value of  $m_a'$  is nearly equal to  $0.34 \times 10^{-2}$  calculated from Fig.28 for yearly maximum range, and also to  $0.42 \times 10^{-2}$ , mean value for east- and north- component in Table 3.

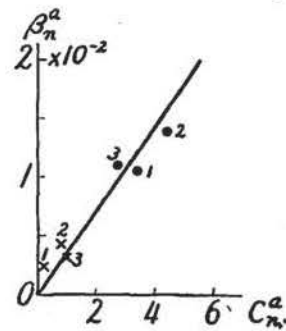


Fig. 41. Relationship between  $\beta_n^a$  and  $C_{n,0}^a$  of Sq at Kakioka, 1934~1944. Black circle : East-component. Cross mark : North-component.

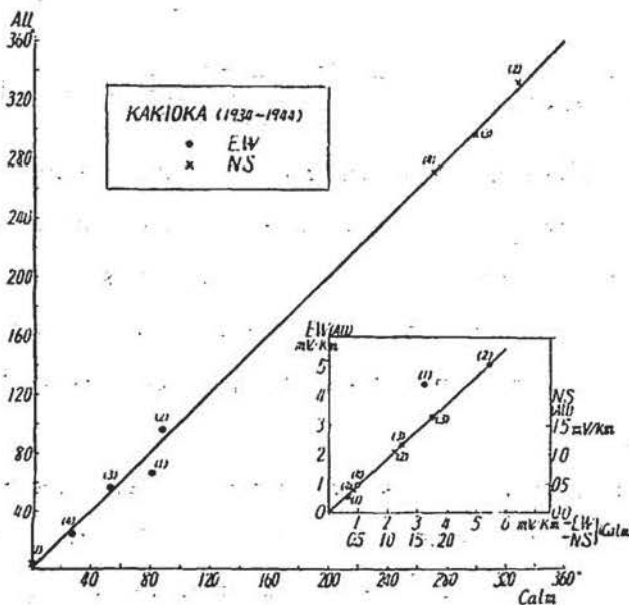


Fig. 42. Comparison of Fourier coefficients of Sq for all days and calm days at Kakioka, 1934~1944.

The comparison of Fourier terms for all days with those for calm days is graphically shown in Fig. 42 for the average value in the interval 1934~1944. As seen from the figure, there is no appreciable difference between them except for the diurnal wave of east-component, though for each individual year the matter does not always hold good so because of some accidental irregularities. The amplitude of the diurnal wave of east-component is

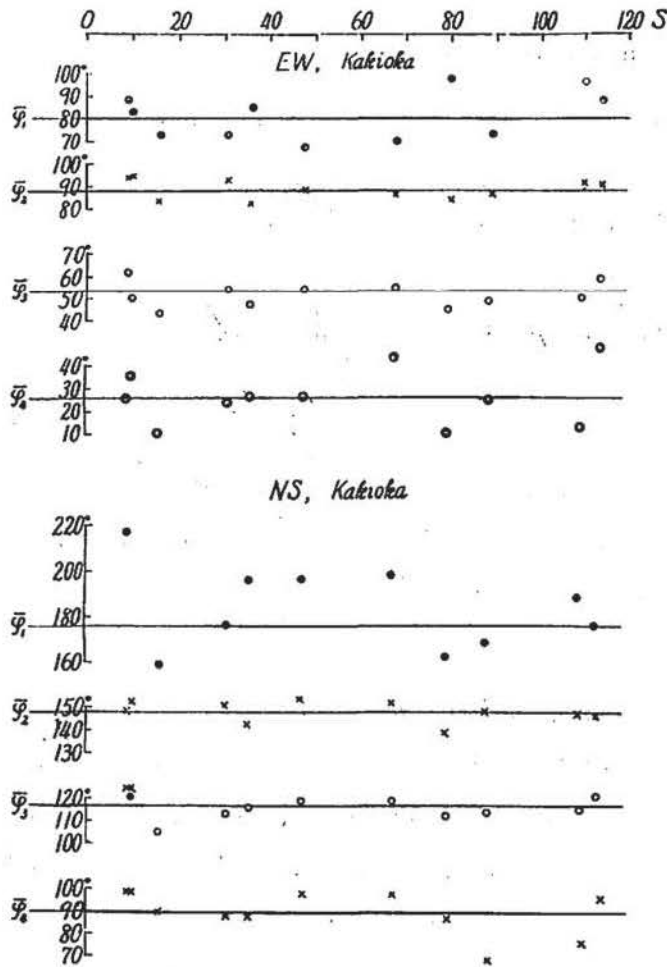


Fig. 43. Relation between phase angle  $\varphi_n$  of Sq for calm days at Kakioka and  $S$ , 1934~1944.

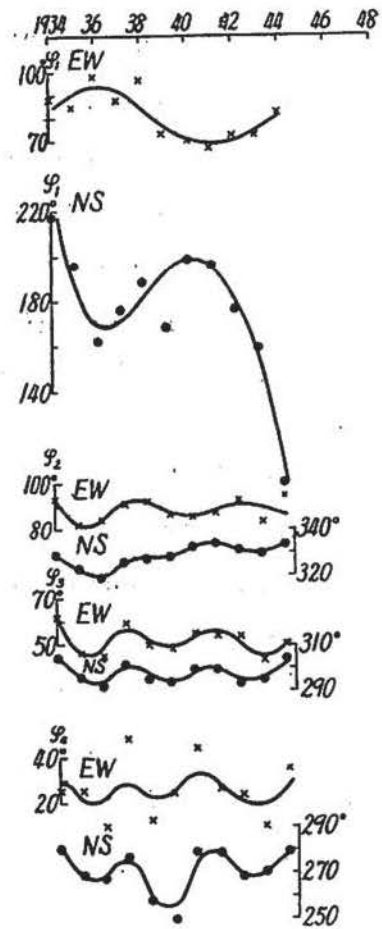


Fig. 44. Year-to-year change of  $\varphi_n$  of Sq for calm days at Kakioka, 1934~1944.

relatively larger for all days, while the phase angle shows only a minor difference.

Referring to this point, it may be worthy to raise a question that whether or not the solar flare effects would be intensified during prevailing disturbances as compared with those on calm days. From the result obtained here it seems to be no appreciable difference as a whole between two cases, and if any, it may be probably responsible for a contribution from the diurnal term.

In the second place, the correlation between phase angles for calm days and  $S$  is graphically shown in Fig. 43, in which  $\varphi_n$  represents the mean value for the  $n$ -th harmonic wave. It is easily seen that there is no appreciable connection between  $S$  and the phase angles of the second and third harmonic waves, the former being the largest wave of Sq. The values of  $\varphi_1$  manifest apparently random large

fluctuations especially in north-component, and as a whole, there is no definite correlation between  $\varphi_1$  and  $S$ .

Table 11. Fourier coefficients of  $S_q$  of earth-currents at Kakioka, 1934-1944.

$$E(N) = \sum_n C_n \sin(nT + \varphi_n). \quad \text{Unit: } 0.01 \text{ mV/km and degree.}$$

c: Five calm days; a: All days. +: Higher potential electrode.

Year	EW+				NS+				EW+				NS+				
	$C_1$	$C_2$	$C_3$	$C_4$	$C_1$	$C_2$	$C_3$	$C_4$	$\varphi_1$	$\varphi_2$	$\varphi_3$	$\varphi_4$	$\varphi_1$	$\varphi_2$	$\varphi_3$	$\varphi_4$	
1934	c	308	545	299	78	34	155	128	39	89	84	62	26	217	149	124	99
	a	388	480	254	59	21	97	112	34	74	95	57	30	262	154	123	93
35	c	311	515	291	66	28	101	118	34	85	82	47	26	196	143	116	88
	a	416	510	323	81	43	112	119	40	75	99	54	46	191	152	119	94
36	c	359	578	356	84	61	136	137	36	98	84	45	10	162	139	112	87
	a	435	514	321	98	60	126	123	35	72	93	46	9	162	141	111	78
37	c	324	586	451	125	64	151	157	60	88	91	59	48	176	146	121	96
	a	489	672	452	154	62	149	156	53	73	93	66	40	174	150	121	94
38	c	270	591	391	69	49	121	131	35	97	92	50	13	188	147	115	77
	a	462	602	347	59	31	121	127	31	74	95	50	6	195	149	118	83
39	c	325	599	404	125	30	118	125	39	73	87	48	25	168	148	114	69
	a	499	508	338	69	28	104	113	32	62	101	56	358	201	156	115	77
40	c	356	528	355	116	54	107	120	49	70	86	55	44	198	152	119	98
	a	512	499	367	89	38	100	117	40	64	88	54	44	210	151	111	99
41	c	364	415	317	37	36	102	110	42	67	88	54	27	196	154	119	98
	a	416	476	323	151	31	90	104	38	58	104	66	12	202	154	114	17
42	c	373	528	352	117	29	106	111	42	73	93	54	24	176	151	113	88
	a	398	478	322	122	25	87	106	39	63	104	60	12	201	153	116	52
43	c	287	517	332	114	14	97	108	46	73	13	43	11	159	150	105	90
	a	521	417	258	68	19	89	92	37	61	88	47	17	69	146	113	101
44	c	272	541	316	94	28	80	102	46	83	95	50	36	100	153	124	99
	a	341	494	311	89	26	80	100	44	64	104	62	33	72	165	127	98
1934~1944	c	317	539	350	97	36	113	122	41	81	89	52	27	180	148	118	91
	a	422	511	327	90	27	106	115	38	67	97	57	24	184	152	117	92

On the other hand, if year-to-year changes of  $\varphi_n$  are drawn in Fig. 44, there is seen a corresponding systematic change for each  $\varphi_n$ , but a remarkable inequality between  $\varphi_1$  and others. This is ready to remind of contrast of variation between  $n$  and  $\Delta n$  as already mentioned. That is to say, the mode of time variation of  $\varphi_1$  corresponds to that of  $n$ , while that of each other  $\varphi_n$  to that of

Table 12. Amplitude of Fourier coefficients at Kakioka. (mV/km)

$n$	$C_{n,0}^a$		$100\beta_n^a$	
	NS	EW	NS	EW
1	0.22	3.38	0.24	1.05
2	0.81	4.37	0.43	1.39
3	1.00	2.67	0.32	1.10

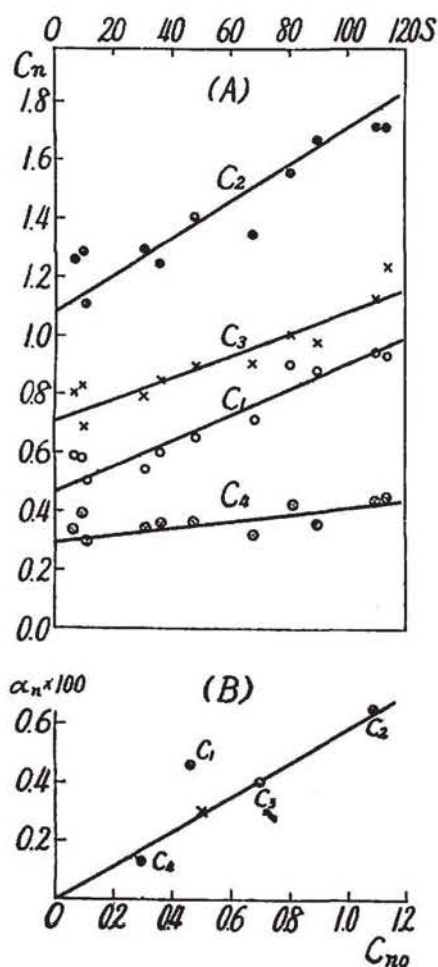


Fig. 45. Correlation between Fourier coefficients  $C_n$ 's of Sq at Tucson and  $S$ .

$\Delta n$ . In other words, the periodic change with 4-year period of  $\Delta n$  may be primarily responsible for higher harmonic waves, but not for the diurnal one. On the contrary the long period change of  $n$  or  $N$ , which bears a striking resemblance to that of  $\Delta S/\Delta t$ , may be substantially responsible for the first harmonic wave.

(B). *Harmonic analysis of Sq of earth-currents at Tucson*

For the comparison with the results at Kakioka the results of harmonic analysis of Sq deduced from 10-least disturbed days' mean at Tucson are given in Table 13 for the interval 1932~1942. The correlation between  $C_n$  and  $S$  is graphically shown in Fig. 45 (A), which is of less closeness in both maximum and minimum sunspot periods as already seen at Kakioka. As a whole, however, it can be expressed as follows,

Table 13. Harmonic analysis of north-component of Sq of earth-currents at Tucson, 1932~1942 (10-least disturbed days).  $N = \sum_n C_n \sin(nt + \varphi_n)$ ,  $t$ : 105° W. M. M. T.

		1932	1933	1934	1935	1936	1937	1938	1939	1940	1941	1942
Amplitude (mV/km)	$c_1$	0.50	0.59	0.58	0.60	0.90	0.94	0.95	0.88	0.71	0.65	0.54
	$c_2$	1.11	1.26	1.29	1.25	1.56	1.71	1.72	1.67	1.35	1.41	1.30
	$c_3$	0.69	0.80	0.83	0.85	1.01	1.24	1.14	0.98	0.91	0.90	0.80
	$c_4$	0.39	0.34	0.39	0.36	0.42	0.46	0.44	0.36	0.32	0.36	0.34
Phase (degree)	$\varphi_1$	93	82	80	74	75	68	75	73	86	89	92
	$\varphi_2$	278	276	275	274	273	272	270	270	275	279	279
	$\varphi_3$	121	118	120	116	119	117	116	118	120	127	125
	$\varphi_4$	336	333	331	330	352	338	344	342	338	347	343

$$C_n = C_{n,0} + \alpha_n \cdot S \equiv C_{n,0}(1 + m' \cdot S), \quad m' = 0.58 \cdot 10^{-2},$$

where the diurnal term is omitted from the calculation because of large deviation from this expression. This large deviation is responsible for the maximum period of S, 1936~1939, and if the values of these years are excluded from the calculation of the mean value,  $C_1$  falls just on the line as shown by a cross mark in Fig. 45 (B); there might be something to intensify the diurnal term in this period. The value  $m' = 0.58 \cdot 10^{-2}$  is nearly equal to  $m_c = 0.54 \cdot 10^{-2}$  deduced from the (R, S) correlation, and can be reasonably expected because  $\varphi_n$  does not change remarkably throughout the period except for the diurnal wave.

As compared with the time variations of phase angles at Kakioka,  $\varphi_n$  at Tucson shows a remarkable difference in the following point (Fig. 16). The matter is that there appears no shorter periodic change, 4-year change, in each phase angle at Tucson, keeping a nearly constant respective value each other throughout the period except for  $\varphi_1$ , which shows a similar long period change at both stations as already

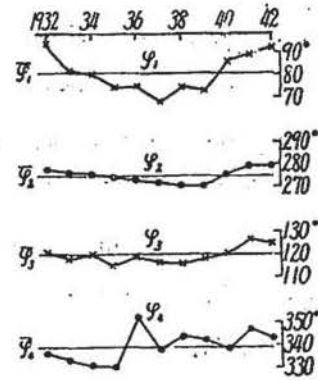


Fig. 46. Year-to-year changes of phase angles  $\varphi_n$ 's of Sq at Tucson.

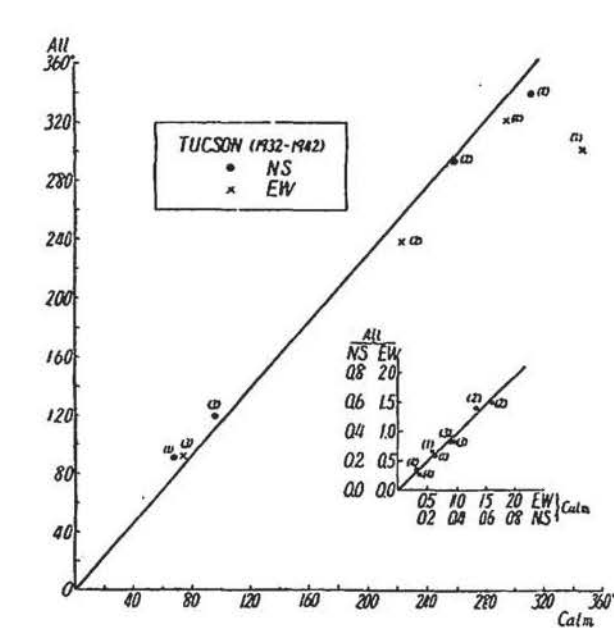


Fig. 47. Comparison of Fourier coefficients of Sq for all days' mean and calm days' one at Tucson, 1932~1942.

mentioned. It seems likely that the ionosphere over Tucson exerts a different kind of action upon the mode of year-to-year change of Sq as compared with that over Kakioka. Regarding this discrepancy between two observatories, it may be somewhat worthy to note that the yearly rate of time variation  $\delta f^{\circ} R_2$  is remarkably larger in winter at Kokubunji, while there is no appreciable difference between winter and annual means at Washington. It is desired to examine this inter-

esting behavior of the secular change of Sq field by using as many data at stations in similar situations as possible. From the same point of view, further continued observations of earth-currents at Tucson, if possible, will play an important role for clarification of such long period changes of Sq and other transient phenomena, some of which may contain some multiple harmonics of 11-year period of sunspot numbers.

The comparison of Sq for calm days' mean with that for all days' mean is graphically shown in Fig. 47, in which no appreciable difference can be seen between them except for  $\varphi_1$ .

## CHAPTER III. MAGNITUDE OF EARTH-CURRENT POTENTIAL GRADIENT AND LOCAL CHARACTERISTICS

### §1. World-wide data of Sq referred to some solar activity state

The results of harmonic analysis of potential gradient of Sq observed at various stations over the world are given in Table 14, where north- and east-component are expressed as follows,

$$N = \sum_n C_n^N \sin (nt + \alpha_n), \quad E = \sum_n C_n^E \sin (nt + \beta_n),$$

and  $t$  is measured from midnight of the local standard time, positive direction being reckoned towards east and north. These data, however, are based on various kinds of sources, that is, different interval of observations, different epoch of the solar activity, different character of adopted days and so forth. So, they are not suitable for the synthetic study of any phenomena over the world without making reductions of the data to some standard state of activity.

For the present purpose to treat with the general aspect of the characteristics of amplitude of Sq, the following three criteria are allowable,

(1). Amplitude difference between all days' mean and calm days' one is to be neglected.

(2). Solar influence can be generally deduced from the linear expression,

$$C_n^{N(E)} = C_{n,0}^{N(E)} (1 + m \cdot S), \quad m = 0.58 \cdot 10^{-2}, \text{ while for east components at Kakioka and Haranomachi, } m = 0.38 \cdot 10^{-2}.$$

(3). Fourier coefficients are satisfactorily taken up to the 4th or 5th harmonic.

In order to check the third condition an example of the result of synthetic process of Fourier series is shown in Fig. 48 for east-component at Kakioka. As seen from

Table 14(A). Harmonic analysis of Sq of earth-currents.  $N = \sum_n C_n^N \sin(n\lambda + \alpha_n)$ ,  $E = \sum_n C_n^E \sin(n\lambda + \beta_n)$ .

Positive direction of currents : northward and eastward.

Unit : mV/km and degree.

 $\bar{S}$  : Annual mean sunspot numbers during the interval of observation.

Place	$\phi$	$\lambda$	$C_1^N$	$C_2^N$	$C_3^N$	$C_4^N$	$\alpha_1$	$\alpha_2$	$\alpha_3$	$\alpha_4$	$C_1^E$	$C_2^E$	$C_3^E$	$C_4^E$	$\beta_1$	$\beta_2$	$\beta_3$	$\beta_4$
Alaska	65° 54' N	147° 48' W	0.7	6.0	1.5	0.7	90	308	221	355	3.1	2.9	0.4	0.2	227	108	21	300
Canada	63° 20' N	90° 42' W	0.5	4.2	0.6	0.2	282	76	231	76	4.2	3.0	0.4	0.4	56	252	75	336
Europe	Toledo	39° 53' N	0.067	0.136	0.085	0.027	77	314	132	349	0.092	0.183	0.217	0.119	256	333	142	321
	Ebro	40° 49' N	5.34	9.02	3.84	1.07	141	296	124	335	2.09	3.63	1.41	0.38	231	117	306	171
U. S. A.	32° 15' N	110° 50' W	0.79	1.51	0.95	0.33	79	272	119	339	0.33	0.68	0.37	0.13	4	188	94	314
South America	Huancayo	12° 03' S	0.77	0.63	0.32	0.09	350	168	358	217	0.88	0.74	0.39	0.13	166	352	187	35
	San Miguel	34° 33' S	3.11	2.49	1.66	0.40	48	108	310	292	2.67	2.60	0.77	1.66	85	86	43	312
Saghalien	46° 58' N	142° 45' E	0.44	0.52	0.66	0.15	113	296	84	266	1.00	1.79	1.62	0.57	347	202	44	253
Japan and South-West Pacific region	Memambetsu	43° 55' N	0.56	0.95	1.01	0.30	44	256	76	285	0.26	0.42	0.52	0.12	339	238	59	259
	Nemuro	43° 20' N	13.1	7.9	7.8	6.3	350	313	275	226	10.3	6.2	7.0	4.7	175	134	95	43
	Morioka	39° 42' N	1.12	2.75	2.14	0.56	331	225	46	261	3.32	3.36	2.53	0.29	290	167	357	192
	Haranomachi	37° 37' N	1.44	1.53	1.46	0.50	84	293	113	310	1.44	1.20	1.09	0.38	287	148	317	155
	Kakioka	36° 14' N	0.36	1.12	1.21	0.38	56	241	71	268	4.50	5.31	3.38	0.89	294	186	12	205
	Owashi	34° 04' N	1.58	0.83	0.87	0.26	15	232	61	266	1.04	0.58	0.67	0.25	282	182	323	90
	Kanoya	31° 25' N	0.37	0.24	0.66	0.25	22	263	59	259	1.34	0.58	0.79	0.36	229	106	290	115
	Ishigaki	24° 20' N	3.3	0.5	1.8	0.7	302	263	192	198	3.1	1.1	1.0	0.6	77	34	71	6
Australia	30° 19' S	111° 53' E	0.159	0.333	0.195	0.048	65	223	54	214	0.0027	0.0375	0.0170	0.0068	345	42	241	42

Table 14 (B).

Place		Interval	Character of adopted days	Time	$\bar{S}$
Alaska	Fairbanks	Oct., 1932- Sep., 1933	all days	150° W. M. M. T.	9
Canada	Chesterfield	1932~1933 (81 days)	calm days	90° W. M. M. T.	9
Europe	Toledo	1948	all days	G. M. T.	136
	Ebro	1914~1918	calm days	G. M. T.	60
U. S. A.	Tucson	1939~1940	calm days	105° W. M. M. T.	79
South America	Huancayo San Miguel [29]	1927~1929	all days	75° W. M. M. T.	71
		1951~1952	all days		50
Saghalien.	Toyohara	1934~1936	all days	135° E. M. M. T.	42
Japan and South-West Pacific region	Memambetsu	1950~1953			50
	Nemuro	Jan.-Feb., 1943			(21)
	Morioka	1947			152
	Haranomachi	1950			84
	Kakioka	1934~1941			69
	Owashi	1947			152
	Kanoya	1950			84
	Ishigaki	Sep.-Oct., 1941			(56)
Australia	Watheroo	1924~1927	all days	120° E. M. M. T.	49

the figure the third condition may be allowable for an ordinary synthesis of harmonic series, while the other two criteria have been already stated so as to be acceptable.

Table 15 is thus prepared for the estimated amplitudes  $C_{n,o}^N$  and  $C_{n,o}^R$ , which would manifest themselves when  $S$  were absent, provided that the second condition is valid up to the extreme value when  $S=0$ .

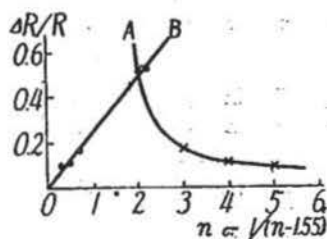


Fig. 48. Relative errors of synthetic values of Fourier coefficients of  $S_q$  due to neglected higher harmonics. (East-component at Kakioka)  
 $R$ : Sum of hourly absolute values of the daily variation.  
 $\Delta R$ : Sum of absolute values of differences between observed hourly values and those of synthetic values up to the  $n$ th harmonic.  
 $A: (\Delta R/R, \bar{n}), B: (\Delta R/R, 1/\bar{n}-1.55)$ .

## §2. Linear relationship between $C_{n,o}^N$ and $C_{n,o}^R$

It is in regard to the daily vector hodograph that in the preceding paragraphs we have treated with the principal direction of earth-currents. So it may be natural to retouch here the same problem taking individual harmonic wave into consideration.

Table 15. Values of  $C_{n,o}^2$   
 unit : mV/km and  $\gamma$ .  $p : N, E, X$  and  $Y$ , respectively.

Place	$C_{1,0}^N$	$C_{2,0}^N$	$C_{3,0}^N$	$C_{4,0}^N$	$C_{1,0}^B$	$C_{2,0}^B$	$C_{3,0}^B$	$C_{4,0}^B$	$C_{1,0}^X$	$C_{2,0}^X$	$C_{3,0}^X$	$C_{4,0}^X$	$C_{1,0}^Y$	$C_{2,0}^Y$	$C_{3,0}^Y$	$C_{4,0}^Y$
Fairbanks	0.7	5.7	1.4	0.7	2.9	2.8	0.4	0.2					5.4	11.9	3.3	2.3
Chesterfield	0.5	3.8	0.6	0.2	4.0	2.9	0.4	0.4	17.2	14.3	2.4	0.9	5.4	11.9	3.3	2.3
Toledo	0.037	0.076	0.045	0.015	0.051	0.102	0.121	0.066	5.5	2.5	0.3	0.6	9.5	7.3	4.0	1.1
Ebro	3.96	6.69	2.85	0.78	1.55	2.69	1.05	0.28	3.0	1.2	1.3	0.8	9.5	8.5	5.0	1.6
Tucson	0.54	1.04	0.65	0.23	0.23	0.47	0.25	0.09	1.6	2.5	1.4	0.4	8.5	8.3	4.2	1.4
Huancayo	0.55	0.45	0.23	0.06	0.62	0.53	0.28	0.09	3.2	1.6	9	3	60	35	18	3
San Miguel	2.41	1.93	1.29	0.21	2.06	2.02	0.60	0.90								
Toyohara	0.35	0.42	0.53	0.12	0.81	1.45	1.31	0.46	5.8	5.2	3.2	1.1	9.7	6.5	3.6	0.9
Memambetsu	0.43	0.74	0.78	0.23	0.20	0.33	0.40	0.09								
Morioka	0.60	1.46	1.14	0.30	1.77	1.79	1.35	0.15								
Haranomachi	0.97	1.03	0.98	0.34	1.09	0.91	0.83	0.29								
Kakioka	0.26	0.80	0.86	0.27	3.57	4.21	2.68	0.71	1.3	3.1	2.5	0.7	8.8	7.2	4.6	1.4
Owashi	0.84	0.44	0.46	0.14	0.71	0.31	0.42	0.13								
Kanoya	0.25	0.16	0.44	0.17	0.90	0.39	0.53	0.24								
Nemuro	10.8	6.5	6.4	5.2	8.5	5.1	5.8	3.9								
Ishigaki	2.5	0.4	1.4	0.5	2.3	0.8	0.8	0.5								
Watheroo	0.124	0.259	0.152	0.037	0.0021	0.0292	0.0132	0.0053	3.8	1.9	0.6	0.2	8.9	8.7	3.8	1.1

As seen in Fig. 49 the connection between  $C_{n,o}^N$  and  $C_{n,o}^E$  is approximately linear, as a whole, and stations can be classified into three groups from a standpoint of degree

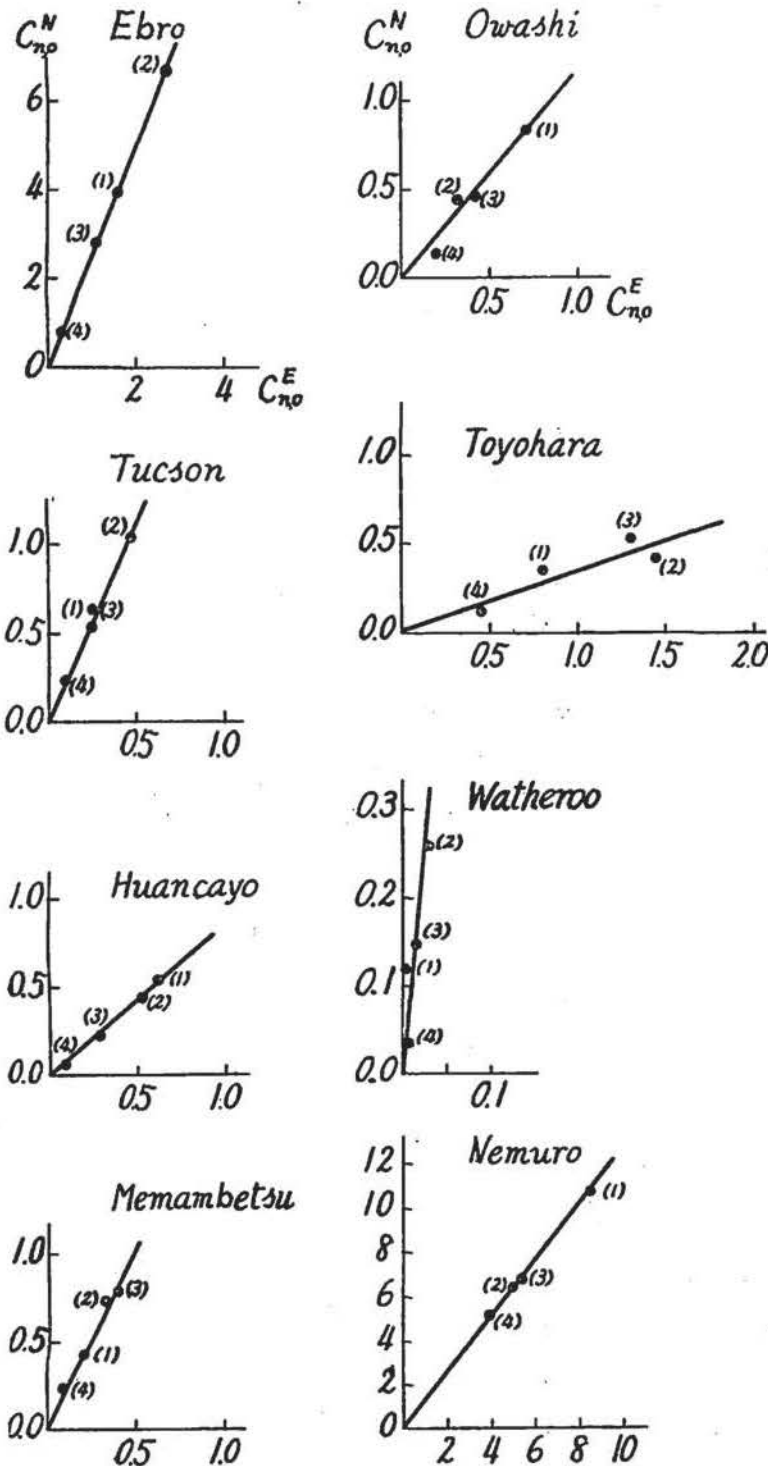


Fig. 49. Linear relationship between  $C_{n,o}^E$  and  $C_{n,o}^N$ . -First group.

of linearity.

(i). *First group:*

First of all the best linearity can be seen, and in other words, each wave persuades its principal axis of the elliptic hodograph in nearly the same direction. And the most predominant wave at any station is common for both east- and north-component as given in Table 15 or Fig. 49. The stations which belong to this group are as follows; Toyohara, Memambetsu, Nemuro, Owashi, Watheroo, Ebro, Tucson and Huancayo.

(ii). *Second group:*

This group is distinguished from the first group in the following point that some one wave, practically the first wave only, deviates remarkably below the straight line determined by the other waves. Morioka, Hara...

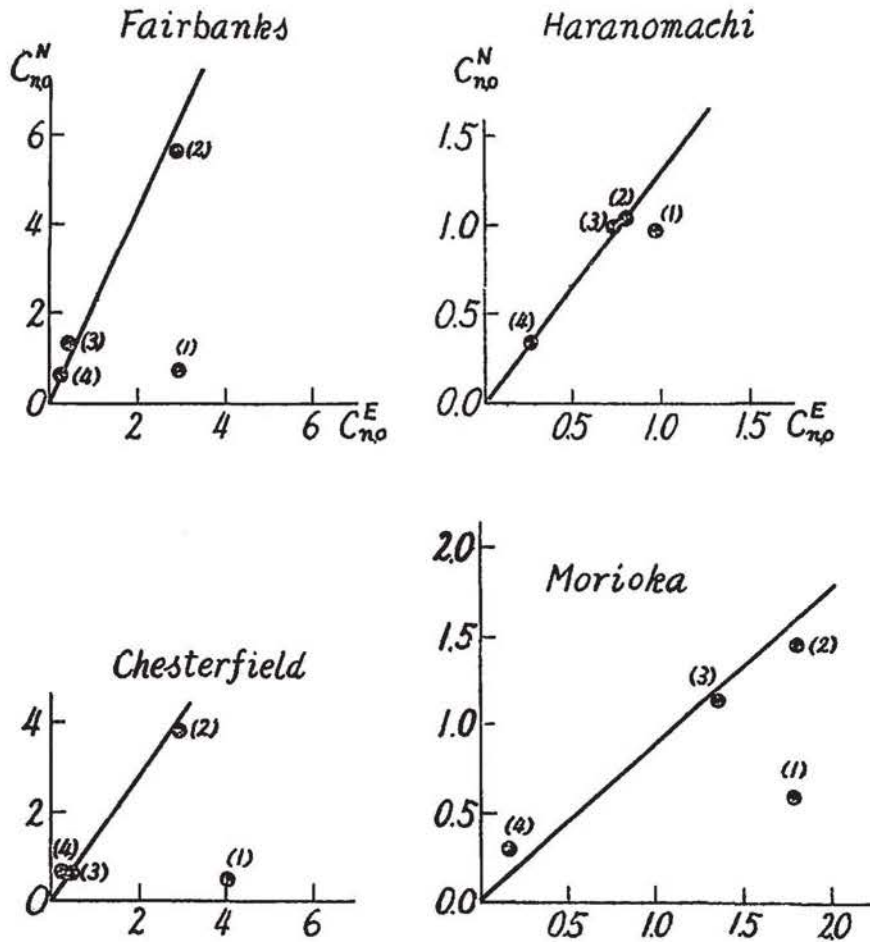


Fig. 49. Linear relationship between  $C_{n,o}^E$  and  $C_{n,o}^N$  -Second group.

Fig. 65. Linear relationship between  $C_{n,o}^E$  and  $C_{n,o}^N$  -Second group.

nomachi, Fairbanks and Chesterfield belong to this group. The most predominant wave is diurnal for all east components, but not always so for north-component. So the vector of the first wave exceptionally approaches to the east-west direction.

(iii). *Third group*: This is of less definite linear distribution as compared with the other two groups, and the most predominant wave appears independently of the base line direction. Kakioka, Kanoya, Ishigaki, San Miguel and Toledo belong to this group.

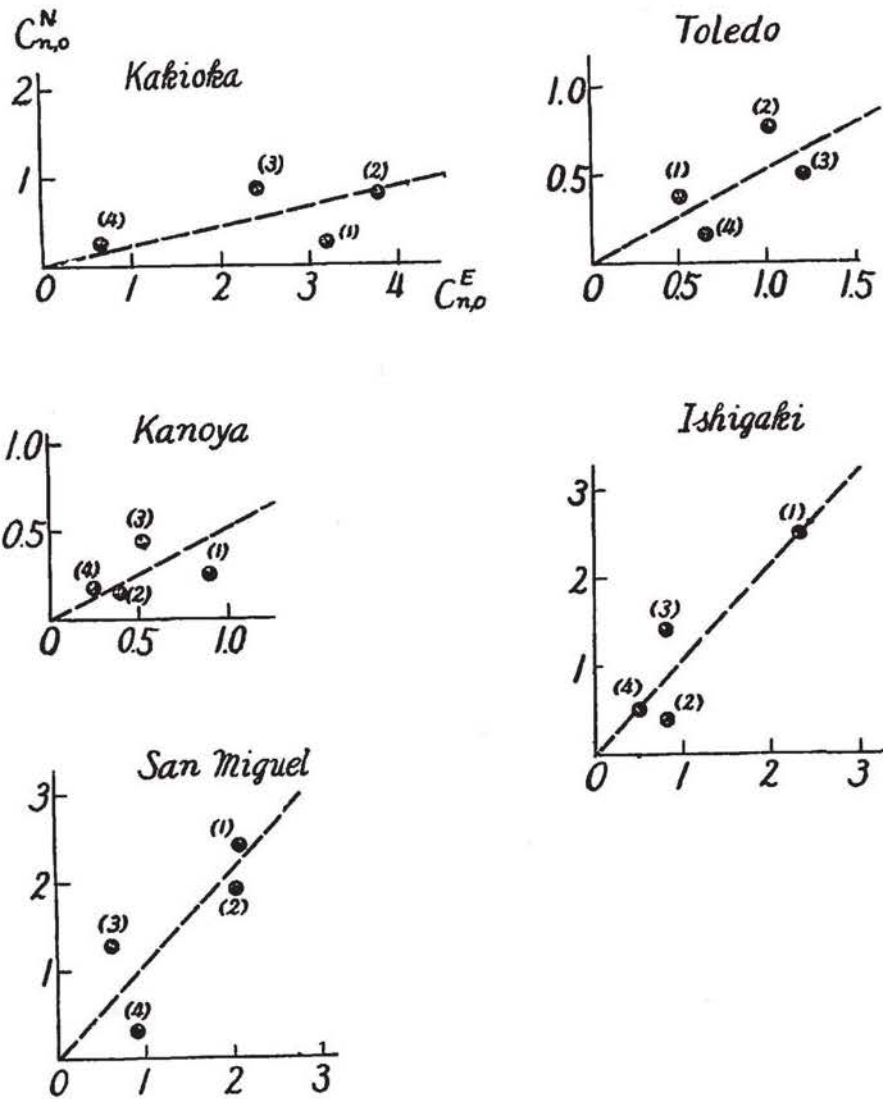


Fig. 49. Linear relationship between  $C_{n,o}^E$  and  $C_{n,o}^N$  -Third group.

As to the spatial distribution of these three groups, it is to be remarked that the second group seems to appear frequently in both high and middle latitudes especially  $30^\circ \sim 40^\circ$  parallels. In Japan and her vicinity it distributes from the north to south in the successive order of the first, second and third group except for Owashi. The mode of distribution may relate to the electric state of the underground structure, but at some middle latitude stations at least, it is probably responsible to some extent for the irregular distribution of foci of Sq current system. For example, at Kakioka the annual mean state of Sq is remarkably controlled by the corresponding mode of appearance of the first and second waves in winter as shown in Fig. 50, while higher

waves of  $n \geq 3$  are independent of any season. As to the higher latitude distribution of the second group,  $S_D$  current system may be taken into consideration.

At any rate, it may be pointed out

that the statement said above becomes necessarily when minute features of the principal direction of earth-currents are to be examined for some quantitative discussions.

§3. Locality of  $R_{n,o} = \sqrt{C_{n,o}^N{}^2 + C_{n,o}^E{}^2}$  and apparent resistivity  $\rho_a$

For the convenience to treat with the first approximate features of localities of amplitudes, the resultant  $R_{n,o} = \sqrt{C_{n,o}^N{}^2 + C_{n,o}^E{}^2}$  is examined instead of treating separately with  $C_{n,o}^N$  or  $C_{n,o}^E$ , putting any consideration about inhomogeneity of the earth's conductivity aside. As seen in Table 16, magnitude of  $R_{n,o}$  is of order of some millivolts per kilometer at most except for exceptionally small values at Toledo and large ones at Nemuro, and as regards the average  $R_{n,o}$  no appreciable difference can be seen among three groups of stations mentioned above. At Huancayo, where geomagnetic Sq manifests a well-known equatorial type of variation with large amplitude, one can find no corresponding large  $R_{n,o}$  as compared with others, which may strongly suggest an underground structure with sufficient high electric conductivity so as to give rise to rather small amplitude of earth-currents. As a reference of a general conception about the magnitude of  $R_{n,o}$ , average values for 12 middle latitude stations, except for Fairbanks, Chesterfield, Nemuro, Ishigaki, and Huancayo in Table 16, are given in Table 17.

In view of the well-known electromagnetic induction theory of earth-currents within the earth with uniform conductivity, the amplitude ratio of the horizontal component of electric field  $E_x$  to that of magnetic field  $H_y$  perpendicular to the  $x$ -axis can be expressed by the following simple equation,

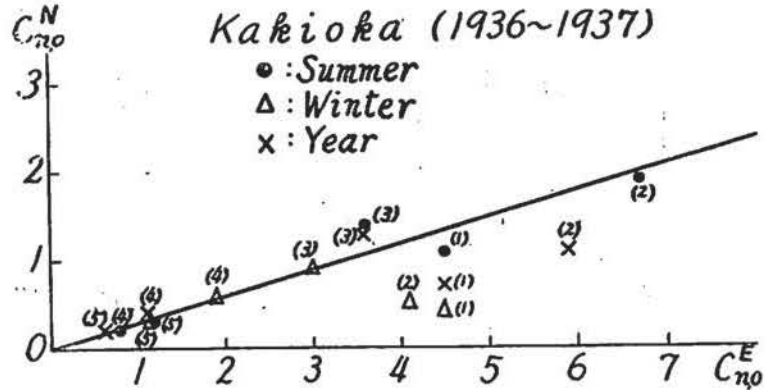


Fig. 50. Seasonal change of correlation between  $C_{n,o}^N$  and  $C_{n,o}^E$  at Kakioka, 1936~1937.

Table 16.  $R_{n,o} = \sqrt{C_n^X^2 + C_n^Y^2}$  and  $H_{n,o} = \sqrt{C_{n,o}^X^2 + C_{n,o}^Y^2}$ 

Place	(mV/km)				(γ)			
	$R_{1,0}$	$R_{2,0}$	$R_{3,0}$	$R_{4,0}$	$H_{1,0}$	$H_{2,0}$	$H_{3,0}$	$H_{4,0}$
Fairbanks	3.0	6.4	1.5	0.7				
Chesterfield	4.0	4.8	0.7	0.4	18.0	18.6	4.1	2.5
Toledo	0.063	0.126	0.141	0.069	11.0	7.7	4.0	1.2
Ebro	4.25	7.20	3.04	0.83	9.9	8.6	5.2	1.8
Tucson	0.59	1.14	0.69	0.25	8.6	8.7	4.4	1.4
San Miguel	3.17	2.84	1.42	0.95				
Toyohara	0.88	1.51	1.42	0.48	11.3	8.3	4.8	1.4
Memambetsu	0.47	0.81	0.88	0.25				
Morioka	1.87	2.32	1.77	0.34				
Haranomachi	1.46	1.37	1.28	0.45				
Kakioka	3.58	4.29	2.81	0.76	8.9	7.8	5.2	1.6
Owase	1.11	0.53	0.62	0.19				
Kanoya	0.93	0.40	0.68	0.29				
Nemuro	1.37	8.3	8.6	6.5				
Ishigaki	3.4	0.9	1.6	0.7				
Watheroo	0.124	0.261	0.153	0.038	9.7	8.9	3.8	1.1
Huancayo	0.84	0.69	0.36	0.11	68	38	20	4

 Table 17. Mean values of  $R_{n,o}$  and  $H_{n,o}$ .

 $\bar{R}_{n,o}$  : Mean for 12 stations.

 $\bar{H}_{n,o}$  : Mean for 6 stations.

$$E_x/H_y = \sqrt{\rho/2T}, \quad \rho = 1/\sigma,$$

$T$	$\bar{R}_{n,o}$	$\bar{H}_{n,o}$	$\bar{R}_{n,o}/\bar{H}_{n,o}$
hr	mV/km	γ	
24	1.54	9.9	0.155·10 <sup>5</sup>
12	1.90	8.3	0.229
8	1.24	4.6	0.269
6	0.41	1.4	0.293

where  $T$  is a period of variation and  $\sigma$  the uniform conductivity of the earth. The conductivity  $\sigma$ , or specific resistance  $\rho$  of the earth is not practically uniform at all, but may be a complex

function of space co-ordinates  $x, y, z$  and generally even time, although for the mathematical convenience  $\sigma$  is frequently assumed in a tensor form. When the earth is assumed to consist of several horizontal layers with respective uniform conductivity, the matter becomes simpler; for example, in the case of two horizontal layers the amplitude ratio  $E_x/H_y$  and phase difference  $\theta$  are expressed as follows, if it is treated as a two dimensional problem[38],

$$E_x/H_y = \sqrt{\rho_1/2T} \cdot F(\rho_1, \rho_2, h, T) \equiv \sqrt{\rho_a/2T},$$

$$\tan\theta = (1 - 2Ke^{-y} \sin y - K^2 e^{-2y}) / (1 + 2Ke^{-y} \sin y - K^2 e^{-2y}),$$

$$F(\rho_1, \rho_2, h, T) = (1 + 2Ke^{-y} \cos y + K^2 e^{-2y})^{1/2} / (1 - 2Ke^{-y} \cos y + K^2 e^{-2y})^{1/2},$$

$$K = (\sqrt{\rho_2} - \sqrt{\rho_1}) / (\sqrt{\rho_2} + \sqrt{\rho_1}), \quad y = 4\pi h / \sqrt{\rho_1 T},$$

where  $\rho_1$  and  $\rho_2$  are specific resistances of the upper layer and substratum, respectively, and  $h$  the thickness of the upper layer and  $\rho_a$  apparent resistivity called hereafter. When  $T$  is sufficiently large, namely,  $y$  is so small, the ratio  $E_x/H_y$  is mainly controlled by the presence of substratum and *vice versa*. The phase difference can take any value within the limit of  $0 - \pi/2$  by suitable combination of three quantities,  $\rho_1$ ,  $\rho_2$  and  $h$ , while for the uniform earth the phase difference takes a constant value  $\pi/4$ .

On the other hand some available geomagnetic data at hands corresponding to that of earth-currents are given in Table 15 and Table 18, where  $C_n^{X(X')} = C_n^{X(X')}(1 + m \cdot S)$ ,  $m = 0.58 \cdot 10^{-2}$  is used for the all reductions except  $m = 0.38 \cdot 10^{-2}$  at Kakioka. At Tucson, however, they are given for 1919~1920 because of no corresponding available data in our hands, during which interval sunspot number shows a similar phase of the cycle as that in the interval 1939~1940. The value of  $H_{n,0} = \sqrt{C_{n,0}^X + C_{n,0}^Y}$  and the average for the six middle latitude stations excluding Chesterfield and Huancayo are given in Table 16 and Table 17.

Table 18. Harmonic analysis of geomagnetic Sq field,  $X = \sum_n C_n^X \sin(nt + \delta_n)$ ,  
 $Y = \sum_n C_n^Y \sin(nt + \gamma_n)$ . Unit:  $\gamma$  and degree.

Place	$C_1^X$	$C_2^X$	$C_3^X$	$C_4^X$	$C_1^Y$	$C_2^Y$	$C_3^Y$	$C_4^Y$	$\delta_1$	$\delta_2$	$\delta_3$	$\delta_4$	$\gamma_1$	$\gamma_2$	$\gamma_3$	$\gamma_4$	Positive direction	Period
Chesterfield[30]	18.1	15.0	2.5	0.9	5.7	12.5	3.5	2.4	80	198	342	169	230	140	156	341	N W	Oct., 1932- Sep., 1933 (calm days)
Toledo[31]	9.8	4.5	0.6	1.0	17.1	13.1	7.1	1.9	48	209	291	84	42	210	51	255	N E	1948(all days)
Ebro[32]	4.1	1.6	1.8	1.1	12.8	11.4	6.7	2.2	99	236	199	61	35	220	53	246	N E	1914-1918 (calm days)
Tucson[33]	2.4	3.6	2.1	0.5	12.5	12.1	6.1	2.0	99	328	172	34	11	194	26	234	N E	1919-1920 (calm days)
Toyohara[34]	7.2	6.4	4.0	1.3	12.0	8.1	4.5	1.1	100	328	161	18	217	46	226	56	N W	1934-1936 (all days)
Kakioka[35]	1.7	3.9	3.2	0.9	12.3	10.0	6.4	2.0	48	335	158	7	211	42	227	68	N W	1934-1941 (all days)
Watheroo[36]	4.9	2.4	0.8	0.2	11.4	11.2	4.7	1.4	26	247	48	53	184	358	194	12	N E	1924-1927 (all days)
Huancayo[37]	45	22	12	4	85	49	25	3	343	122	342	188	272	102	247	340	N E	1927-1929 (all days)

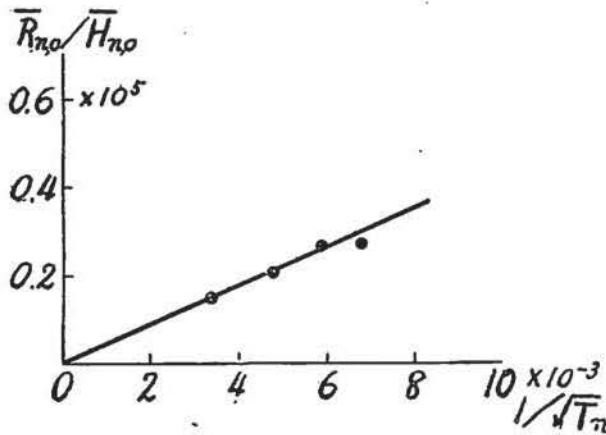


Fig. 51(B). Relationship between  $R_{n,o}/H_{n,o}$  and  $1/\sqrt{T_n}$  for Sq.

At any rate, taking a simple theoretical result mentioned above into consideration it was tried to see in what manner  $R_{n,o}/H_{n,o}$  does correlate to  $1/\sqrt{T_n}$ , and the result is graphically shown in Fig. 51(A). Here the observed values of  $H_{n,o}$  at Toyohara and Kakioka are assumed to be equal to  $H_{n,o}$ 's which would be observed

at Memambetsu and the other all Japanese earth-current stations, respectively. And also for Fairbanks and San Miguel are used  $H_{n,o}$ 's observed at Chesterfield and the middle latitude average value given in Table 17, respectively. As seen in the figures, as a whole, there is a nearly linear correlation between  $R_{n,o}/H_{n,o}$  and  $1/\sqrt{T_n}$ , although unfortunately, the present material of earth-currents and geomagnetic forces is not always supplied from the same station, and also intervals of observations or epochs of the sunspot activity differ each other at some stations. As far as the average values given in Table 17 are concerned, a fairly good connection can be found as shown in Fig. 51(B). So it is confirmed that the amplitude ratio  $R_{n,o}/H_{n,o}$  is proportional to  $1/\sqrt{T_n}$  for the first approximation in many places over the world in spite of their supposed different modes of structure of the ground as far as such a range of period that covers those of principal harmonics of the Sq variation is concerned. Nevertheless, at some stations, where there is seen scarcely a linear relation, we may have such special ground structures that, say, for the two layers' structure  $\rho_2$  is very larger than  $\rho_1$  and the ratio  $R_{n,o}/H_{n,o}$  shows no dependency on  $1/\sqrt{T_n}$ . On the contrary when  $\rho_2 \ll \rho_1$  and  $y$  is very small, the amplitude ratio may become proportional to  $1/T_n$ , showing a concave curve in Fig. 51(A).

§4. Apparent resistivity  $\rho_a$  and earth-resistivity  $\rho_{obs}$  near the earth's surface

Assuming such a simple structure of the earth as said above,  $\rho_a$ 's are calculated from  $R_{n,o}/H_{n,o} = \sqrt{\rho_a/2T_n}$  and given in the second column of Table 19. They are of order of  $10^4 \Omega \cdot \text{cm}$  at nine stations out of fifteen, and as small as  $3 \sim 4 \cdot 10^3 \Omega \cdot \text{cm}$  at Huancayo and Toledo. The average value of  $\rho_a$  corresponding to Fig. 51(B) gives

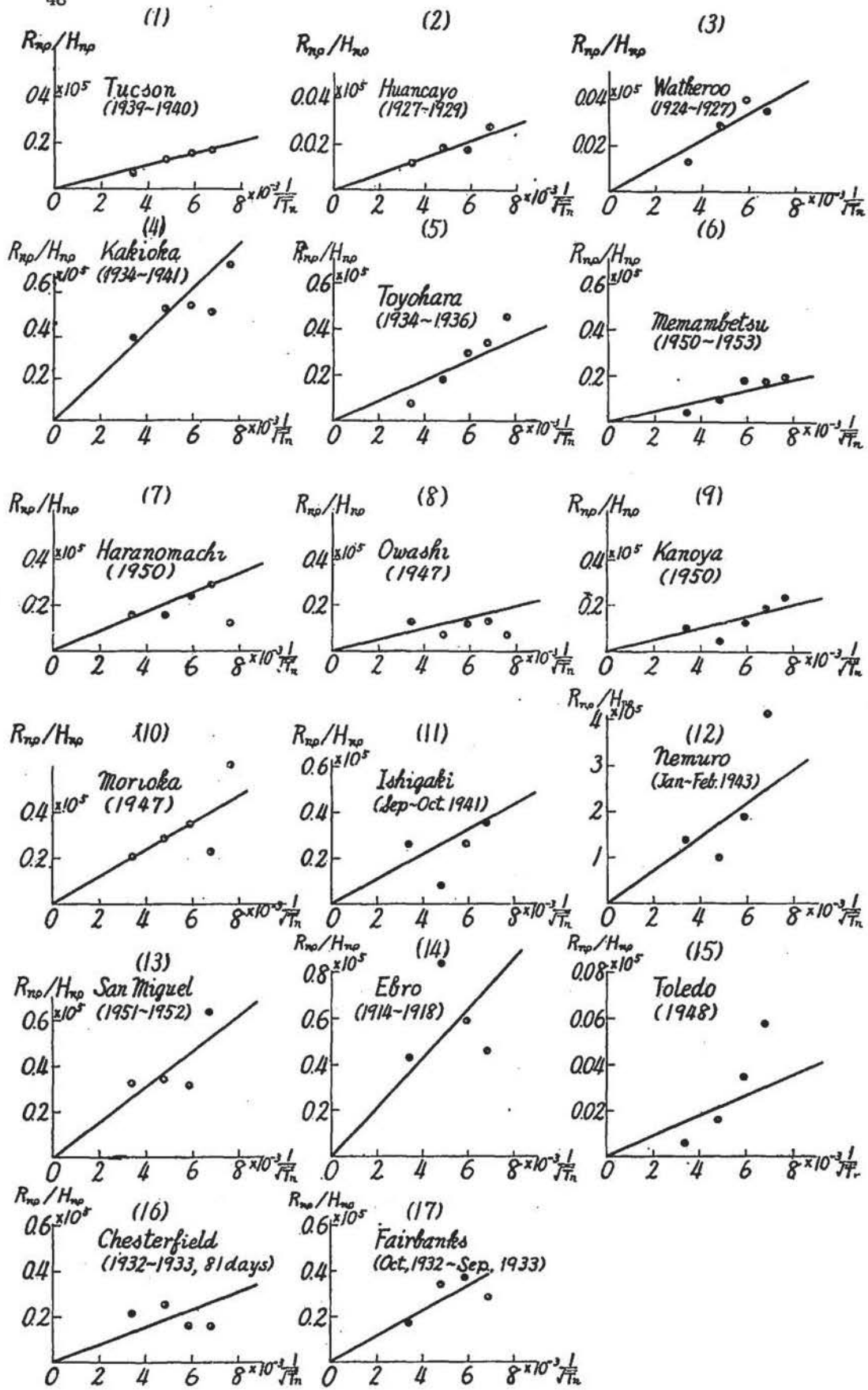


Fig. 51 (A). Relationship between  $R_{n0}/H_{n0}$  and  $1/\sqrt{T_n}$  for  $S_q$  at each station.

Table 19. Estimated apparent resistivity  $\rho_a$  and earth-resistivity  $\rho_{obs}$  measured by Wenner-Gish-Looney method.

Station	$\rho_a$	$\rho_{obs}$
	$\Omega \cdot \text{cm}$	$\Omega \cdot \text{cm}$
Fairbanks	$6.4 \cdot 10^4$	
Chesterfield	$2.9 \cdot 10^4$	
Toledo[39]	$0.4 \cdot 10^3$	$2 \cdot 10^3$
Ebro[40]	$2.3 \cdot 10^5$	$11 \cdot 10^3$
Tucson[41]	$1.5 \cdot 10^4$	$3 \cdot 10^3$
Toyohara	$3.9 \cdot 10^4$	$4 \cdot 10^3$
Memambetsu	$1.1 \cdot 10^4$	
Morioka	$6.7 \cdot 10^4$	$4 \cdot 10^3$
Haranomachi	$3.8 \cdot 10^4$	$5 \cdot 10^3$
Kakioka	$1.9 \cdot 10^5$	$14 \cdot 10^3$
Owashi	$1.2 \cdot 10^4$	
Kanoya	$1.4 \cdot 10^4$	$33 \cdot 10^3$
Huancayo[42]	$0.3 \cdot 10^3$	$13 \cdot 10^3$
Watheroo[43]	$0.6 \cdot 10^3$	$1.5 \cdot 10^3$
San Miguel	$1.2 \cdot 10^5$	

$4 \cdot 10^4 \Omega \cdot \text{cm}$ . The remarkable variety of  $\rho_a$  indicates clearly the locality of universal earth-currents.

On the other hand, at some of the stations considered here have been carried out some earth-resistivity surveys with different scale and depth of penetration, but almost the same Wenner-Gish-Looney method was used. These observed earth-resistivities, denoted by  $\rho_{obs}$  here, are given in the third column of Table 19, of which effective depth corresponding to the inner electrode span,  $a$ , is about 200 meters. Of course,

$\rho_{obs}$  is generally different in different direction and depth, sometimes largest values being crowded in relatively small area in the vicinity of a station. In practice, however, most of surveys have been carried out to the effective depth corresponding to  $a=200 \sim 300$  meters at most. Now  $\rho_{obs}$  at  $a=200$  meters is assumed to be more or less representative for the average state of  $\rho_{obs}$  near the earth's surface in relatively wide area around the station. It becomes then interesting to know whether or not any connection does exist between  $\rho_a$ , and  $\rho_{obs}$ , the result being graphically shown in Fig. 52 in logarithmic scale. Excepting Huancayo and

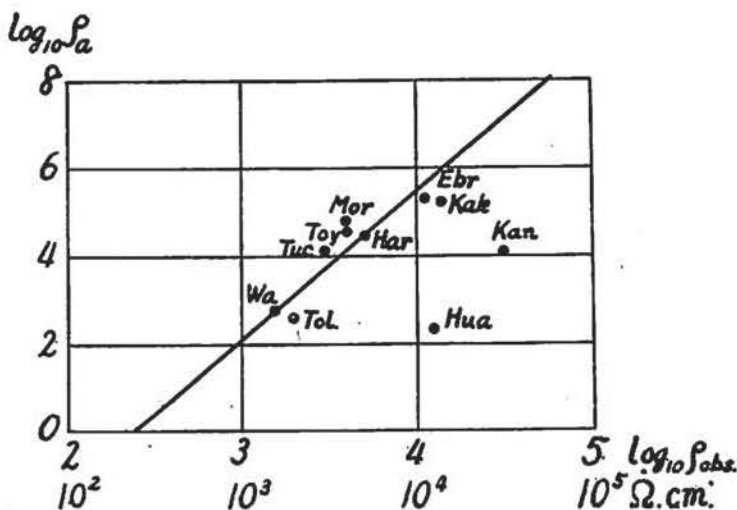


Fig. 52. Relationship between  $\rho_a$  and observed earth-resistivity  $\rho_{obs}$ .

Kanoya, remaining eight points approximately fall on a straight line,  $\rho_{obs}$ 's at these two stations being as large as about ten times those expectable from this linear expression. As seen from the depth distribution of  $\rho_{obs}$  given in Table 20,

Table 20. Earth-resistivity  $\rho_{obs}$  at Kanoya.  
(Wenner-Gish-Looney method)

a	EW	NS
300m	$2.37 \cdot 10^4 \Omega \cdot \text{cm}$	$2.40 \cdot 10^4 \Omega \cdot \text{cm}$
200	3.13	3.61
100	5.12	5.70
70	6.78	6.21
40	6.72	4.40

$\rho_{obs}$  at Kanoya decreases so rapidly with increasing depth that if the upper high resistivity layer be ignored, the average  $\rho_{obs}$  of deeper portions may fall to some thousand ohm. cm. This is near to a reasonable magnitude expectable from the figure.  $\rho_{obs}$  at Huancayo decreases in a similar way with increasing depth, namely, it attains to  $5 \cdot 10^3 \Omega \cdot \text{cm}$  at about  $a=600$  meters and seems further to decrease gradually. So two exceptionally deviated values of both Kanoya and Huancayo would approach to the line in Fig. 52, provided that some plausible  $\rho_{obs}$  is taken in place of the present  $\rho_{obs}$  corresponding to  $a=200$  m. So as far as these stations are concerned, contribution of the uppermost part of the earth to  $\rho_a$  may be approximately expressed as follows,

$$\rho_a = 10^{-8.1} (\rho_{obs})^{3.4} \Omega \cdot \text{cm}.$$

Summarizing the results obtained above, it is found out that there exists a fairly close connection between apparent resistivity  $\rho_a$ , presumed from earth-currents

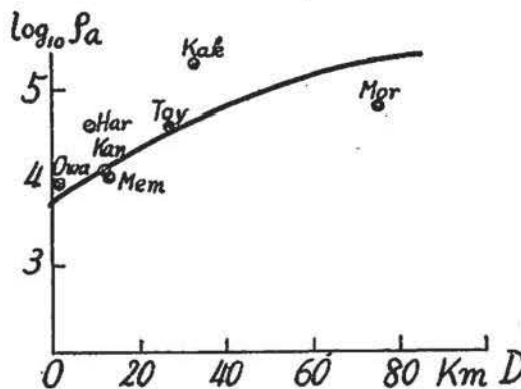


Fig. 53. Variation of apparent resistivity  $\rho_a$  with regard to the distance  $D$  from the nearest sea-coast to the station, Japan.

and geomagnetic field, and average earth-resistivity  $\rho_{obs}$ , observed in the upper portion of the earth up to some hundred meters or more below the surface. And the matter is not of mere chance, but actually the upper portion of the earth near any station may contribute more or less in similar manner to the magnitude of earth-currents observed. Then, it is easy to understand such a well-known experience in applied geophysics, or electric

surveys that magnitude of natural earth-currents observed in a small area, in which geomagnetic potential is considered to be constant, increases with increasing earth-resistivity. It is also natural to expect a systematic distribution of  $\rho_a$ , or magnitude of earth-currents in a limited area such as the Japanese Island, of which mountainous portions are probably of higher earth-resistivity and lower near the coast, as a whole. Actually, as shown in Fig. 53,  $\rho_a$  increases gradually with increasing distance from the coast. And the large  $\rho_a$  at Kakioka is also in consistent with high earth-resistivity observed, which is due to the upper portion of rocky substratum of the Tsukuba mountain block. At any rate, since there has been no synthetic statement about the role of observed earth-resistivity to act upon the observed earth-currents, the results obtained here will be useful not only for the interpretation of earth-currents variations, but also for directions of earth-resistivity measurements, as far as the first approximate considerations of the electric structure of the earth are concerned.

#### §5. Presumed localities of underground electric structures in some places in Japan

At last it may be practically interesting to estimate some plausible structure of the shallow part of the underground mass from an electromagnetic point of view. Here, the matter is treated simply as a two-layer problem in two dimensions as mentioned above, and the underground structure will be estimated very roughly by using the amplitude ratio  $R_n/H_n$ , because of combining some material for short period variations. Of course, more complicated mathematical treatment may be possible, but it belongs to a multiple values' problem and besides, few observational back grounds for it have been reported. The diagrams,  $(R_n/H_n, 1/\sqrt{T_n})$ , at some stations in Japan are shown in Fig. 54 (A)-(D), where at Toyohara[44]  $C_n^B/C_n^X$  is used in place of  $R_n/H_n$ , because the average amplitude of the short period variation corresponding to a specified period at Toyohara is given for various kinds of variations of  $X$  and east-component. The values marked by black circles in Fig. 54(D) are calculated from nearly periodic variations chosen from many available records. The other short period variations referred are all *SSC's*, for which  $T_n$ 's are taken twice times the duration from the beginning to the maximum value of the geomagnetic horizontal intensity. These figures show that all curves change convexly with increasing  $1/\sqrt{T_n}$ , namely, indicating  $\rho_2 \gg \rho_1$ ,

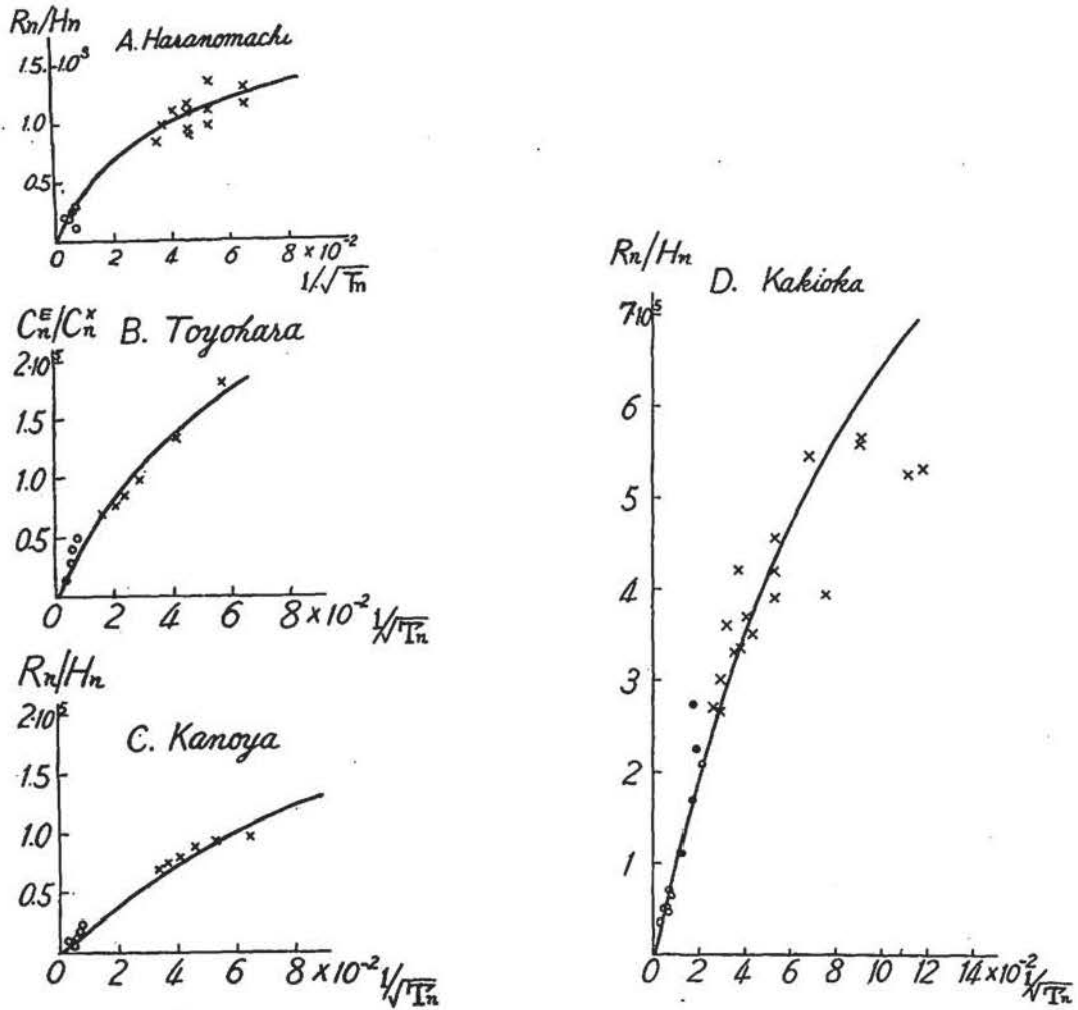


Fig. 54(A)-(D). Relationship between  $R_n/H_n$  and  $1/\sqrt{T_n}$  at four stations in Japan when both  $Sq$  and some short period variations are taken into consideration.

while they are approximately linear as already mentioned within the range of period corresponding to those of principal harmonics of  $Sq$ . So we may presume more or less reasonably the specific resistance of the substratum  $\rho_2$  from  $Sq$  analysis presented here. After some trials, considering the correlation between  $\rho_a$  and  $\rho_{obs}$ , an adjusted theoretical curve is drawn by a solid curve for each figure of Fig. 54, showing a fairly good agreement with observations.

Although we have no observational evidence to check the plausibility of these quantities obtained from the other geophysical points of view, it may be interesting to note that in the vicinity of Tokyo the propagation velocity of earthquake waves in the upper

Table 21. Presumed values of  $h$ ,  $\rho_1$ , and  $\rho_2$  in some places in Japan.

Station	$h$	$\rho_1$	$\rho_2$
	km	$\Omega \cdot \text{cm}$	$\Omega \cdot \text{cm}$
Toyohara	5	$2.0 \cdot 10^3$	$55 \cdot 10^3$
Haranomachi	5	1:4	22
Kakioka	6	8.0	200
Kanoya	3	1.0	11

layer of a few kilometers in thickness can be distinguished from that of the lower part[45]. The values of  $h$ ,  $\rho_1$  and  $\rho_2$  used for calculations are tabulated in Table 21, and it should be remembered that the matter is not

always uniquely determined.

§6. Anomalous amplitude of the harmonic waves of Sq near the sea-coast

Following the preceding paragraph, here something about irregularities of the distribution of observed points in Fig. 51 will be treated. In

the first place, one can notice that some stations in Japan, such as Kanoya, Ishigaki and etc., show the remarkably small semi-diurnal waves. So if the deviation of observed  $R_{2,0}/H_{2,0}$  from the corresponding value  $(R_{2,0}/H_{2,0})_0$  on the straight line in the figure be denoted by  $\Delta(R_{2,0}/H_{2,0}) = (R_{2,0}/H_{2,0}) - (R_{2,0}/H_{2,0})_0$ , the ratio  $\Delta(R_{2,0}/H_{2,0}) / (R_{2,0}/H_{2,0})_0$  is almost negative, and monotonously distributed as shown in Fig 55 (A) in respect to the distance  $D$  measured from the

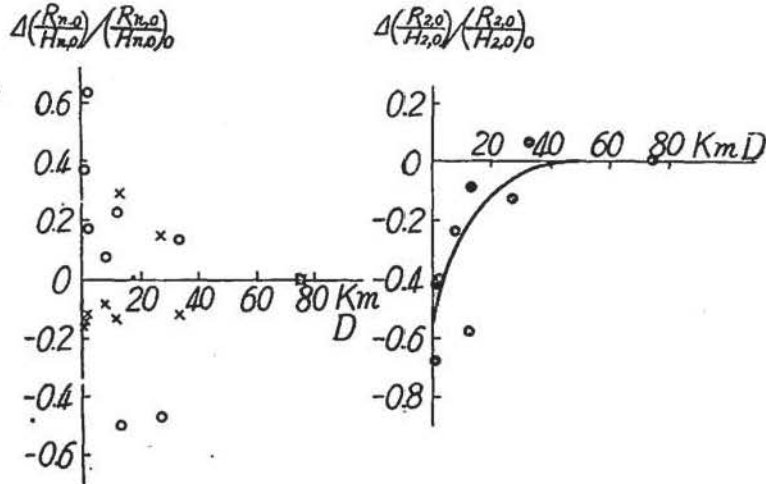


Fig. 55 (A). Variation of  $\Delta\left(\frac{R_{n,0}}{H_{n,0}}\right) / \left(\frac{R_{n,0}}{H_{n,0}}\right)_0$  with  $D$  in Japan.  
 White circle : first wave.  
 Black circle : second wave.  
 Cross mark : third wave.

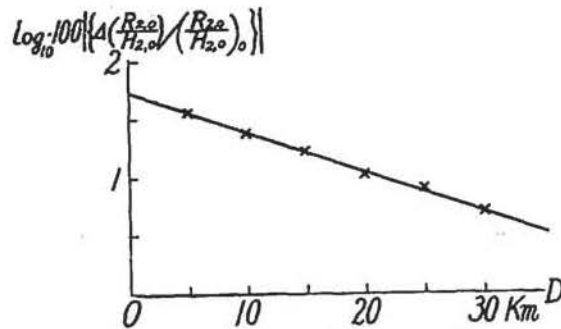


Fig. 55(B): Relation between  $\Delta\left(\frac{R_{2,0}}{H_{2,0}}\right) / \left(\frac{R_{2,0}}{H_{2,0}}\right)_0$  and  $D$ .

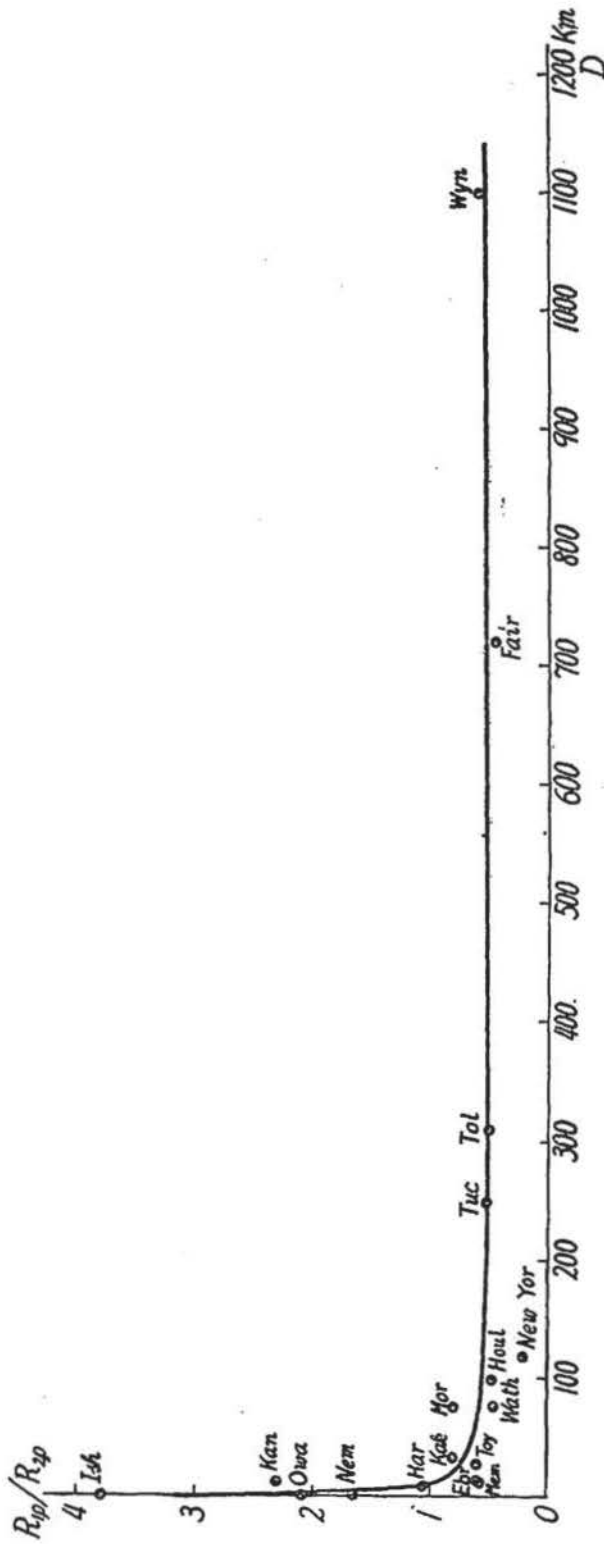


Fig. 56. Variation of  $R_{1,0}/R_{2,0}$  with  $D$  at several stations in the world.

Wyn : wyanet (U.S.A.)

New Yor : New York (U.S.A.)

Houl : Houlton Me. (U.S.A.)

Fair : Fairbanks (Alaska); Tol ; Toledo (Spain) ; Tuc : Tucson (U.S.A.) ;

Wath : Watheroo (Australia) ; Mor : Morioka (Japan) ; Toy : Toyohara (Saghalien) ;

Kak : Kakioka (Japan) ; Ebr : Ebro (Spain) ; Mem : Memambetsu (Japan) ;

Har : Haranomachi (Japan) ; Nemuro (Japan) ; Owa : Owashi (Japan) ; Kan : Kanoya (Japan) ; Ish : Ishigaki (Japan).

nearest sea-coast to the respective station. The numerical value of the ratio rapidly increases near the sea-coast in a fairly regular form, of which average curve may be expressed approximately as follows as shown in Fig. 55(B),

$$\Delta(R_{2,0}/H_{2,0}) / (R_{2,0}/H_{2,0})_0 = -Ae^{-\gamma \cdot D},$$

$$A=0.54, \quad \gamma=0.078,$$

where the distance  $D$  is measured in unit of km. In the second place, however, it is examined in vain to get such a regular distribution as said above for the other waves, showing remarkable fluctuations at some stations. (Fig. 55(A))

On the other hand, the ratio  $R_{1,0}/R_{2,0}$  observed in various places over the world is shown in Fig. 56 in order to check the anomalous distribution of the amplitude before-mentioned within more wide range of  $D$ . The ratio falls also very rapidly within the interval from the coast to 20~30 km distance, and tends to a nearly constant value  $R_{1,0}/R_{2,0} \approx 0.5$  as far as 1000 km from the coast. Therefore, the anomalous behavior of the second wave is characterized within very small distances from the coast, and so its origin may be attributed to some phenomena related directly with the sea.

In respect to this point it may first lead us to remind of the lunar daily variation of earth-currents, of which available data seem to be so scanty at present to establish

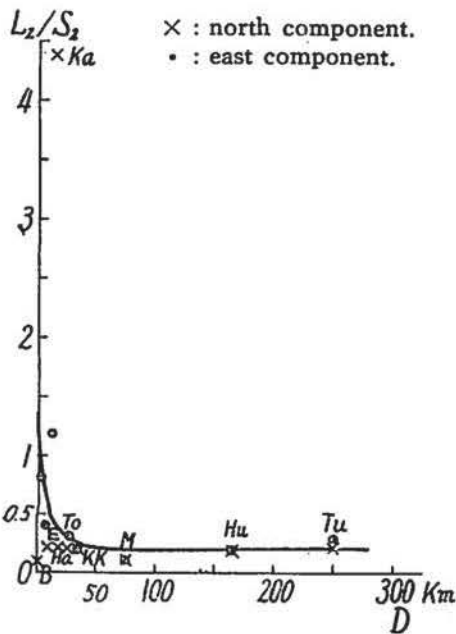


Fig. 57. Relation of  $L_2/S_2$  of earth-currents to  $D$ .

any definite picture of the phenomena. However, it is a fact that the value of  $L_2/S_2$ , ratio of the semidiurnal amplitude of the lunar daily variation to that of  $S_q$  is only about 1/15 for the geomagnetic field, while for earth-currents it has been known to be as large as three or four times the former. Furthermore, the results of recent observations given in Table 22 or Fig. 57 strongly suggest that the lunar daily variation of earth-currents should be discussed first of all from the local standpoint of view, taking the relative distribution of land and sea into consideration. In other words, this suggests also some similar local origins for the anomalous

amplitude of the second wave of  $S_q$ , since these systematic anomalous effects can be found only for the semi-diurnal wave and of comparatively large magnitude. In the following some possible explanations will be put forth.

The first is that the solar semi-diurnal ocean tide in the permanent geomagnetic field

produces the corresponding e. m. f. in the sea, which may have its leakage circuit in the land. The relative amplitude of the solar semi-diurnal component of the tide is about 0.32 when that of lunar semi-diurnal tide is taken as unity, while that of the solar diurnal component is 0.11(51). So any electric field due to such a kind of origin ought to be most predominant in the semi-diurnal term, the situation being thus favourable to the present problem. The second is that under the same circumstance some electrochemical potential, say, a kind of concentration cell may be formed near the coast due to permeating sea-water into the land, or retarded underground water streaming into the sea. They are subjected to a semi-diurnal change of concentration with raising and falling sea-level. At some stations situated so near the sea-side, remarkable contact potentials can be set up at the electrodes due to direct contact with concentric saline solution of the ground adjacent to them. On the other hand, regarding the motion of the soil liquid the third possible cause is pointed out such as that an appreciable magnitude of so-called streaming potential may be changed or newly produced under suitable conditions between the sea-coast and the inner part of the land. For example, when the sea-water raises upwards, expectable geomagnetic induction currents may flow nearly westwards in the vicinity of Japan, and at the same time soil liquid may become sufficiently concentrative near the coast to yield an appreciable magnitude of electromotive force which is likely to direct towards less concentrated inner parts of the land.

At any rate, if the proper semi-diurnal wave of earth-currents, say east-component be expressed by  $E_2^0 \cdot \sin(2t + \varphi_2^0)$ , positive sense reckoned eastwards, and that of

Table 22.  $L_2/S_2$  at several stations over the world.

Station	NS	EW
Tucson[46]	0.2	0.3
Huancayo[46]	0.2	0.2
Ebro[47]	0.2	
Kakioka[48]	0.2	0.2
Toyohara[49]	0.2	0.3
Beppu[49]	(0.1)	0.8
Kanoya[50]	4.4	1.2
Haranomachi[50]	0.2	0.4
Morioka[50]	0.1	0.1

local earth-currents said above by  $-E_1^1 \sin(2t + \varphi_1^1)$ , combined value becomes as follows,

$$e_2 = E_2^0 \sin(2t + \varphi_2^0) - E_1^1 \sin(2t + \varphi_1^1) = E_2 \sin(2t + \varphi_2),$$

$$E_2 = E_2^0 \sqrt{1 - 2(E_1^1/E_2^0) \cos(\varphi_2^0 - \varphi_1^1) + (E_1^1/E_2^0)^2},$$

$$\tan \varphi_2 = \frac{1 - \frac{E_1^1}{E_2^0} \cdot \frac{\sin \varphi_1^1}{\sin \varphi_2^0}}{1 - \frac{E_1^1}{E_2^0} \cdot \frac{\cos \varphi_1^1}{\cos \varphi_2^0}} \cdot \tan \varphi_1^1.$$

On the other hand, at several inland stations far remote from the sea-coast  $\varphi_2$ 's are approximately equal to  $\pi$ , and an average phase angle of the solar semi-diurnal wave of the tide is also near  $\pi$  in the vicinity of Japan[52] the semi-diurnal oscillation of the atmospheric pressure change is known so as to have its two maxima at about 9 hr and 21 hr in local time. Furthermore, concerning observed semi-diurnal phase angles there is found no such a definite connection with  $D$  as seen in the case of amplitude distribution (Table 14). So we may assume  $\varphi_2^0 = \varphi_1^1$ , and furthermore when  $(E_1^1/E_2^0)^2 < 1$ ,  $e_2$  can be approximately written as follows,

$$e_2 = E_2^0 (1 - E_1^1/E_2^0) \sin(2t + \varphi_2^0).$$

Hence the amplitude deviation of  $e_2$  from  $E_2^0$ , is given as follows,

$$\frac{e_2 - E_2^0}{E_2^0} = -\frac{E_1^1}{E_2^0}$$

It is natural to consider the decreasing amplitude of  $E_2^0$  with increasing distance  $D$  from the sea-coast, and if  $E_2^0 = (E_2^0)_{D=0} \cdot e^{-\alpha D}$  is assumed, as seen in the case of permeating water level in the land adjacent to a water channel[53], then,

$$\frac{e_2 - E_2^0}{E_2^0} = -\frac{(E_1^1)_{D=0}}{E_2^0} \cdot e^{-\alpha D}.$$

This expression may be applicable to an interpretation of observational results for  $\Delta(R_{2.0}/H_{2.0}) / (R_{2.0}/H_{2.0})_0$ , or  $R_{1.0}/R_{2.0}$  as far as we confine the event itself to the matter in the vicinity of Japan and neglect supposed small geomagnetic effect due to the local currents said above.

At last, rough estimations of the order of magnitude of possible effects before-mentioned will be made in the following. The induced e. m. f. due to the tidal motion of sea-water is given by

$$E = H \cdot v,$$

where  $H$  is the geomagnetic horizontal intensity of  $0.3\Gamma$ , and  $v$  the velocity of rising or falling of the sea-level height,  $h = h_1 \sin(2pt + \alpha_2)$ . So putting  $h_1 = 20$  cm for an average

solar semi-diurnal tide[54], and for conductivity of sea-water  $\sigma_s=0.03$  (35% salinity and  $10^\circ\text{C}$ ), the amplitude of induced e. m. f.  $E_2^s$  and current density  $I_2^s$  are as follows,

$$E_2^s=0.3 \cdot 2ph \cdot 10^{-8}=8.4 \cdot 10^{-2} \text{ volts,}$$

$$I_2^s=\sigma_s \cdot E_2^s=2.5 \cdot 10^{-13} \text{ Amp.}$$

If  $I_2^s$  be assumed to flow uniformly in the ground adjacent to the sea-side, potential difference along a stream line in the ground is

$$E_2^g=I_2^s \cdot \rho_t \cdot L=0.3 \text{ mV/km,}$$

where specific resistance of the ground  $\rho_t=10^4 \Omega \cdot \text{cm}$  is assumed, and  $L$  the length of a base line. As  $E_2^g$  is of order of  $0.5 \sim 2 \text{ mV/km}$ ,  $(E_2^g)_{D=0}$  is  $0.3 \sim 1.1 \text{ mV/km}$ , assuming  $(E_2^g)_{D=0}/E_2^g=0.54$ . This value is of the same order as  $E_2^s$ , but in the ground equal current density as that presumed in the sea is assumed, the conductivity of the latter being very much larger than that of the ground. So, this type of e. m. f. seems to be unsuitable for the sufficient interpretation of the matter.

The electrochemical potential difference due to a concentric cell is given by

$$e=KT \log\left(\frac{C_2}{C_1}\right),$$

where  $C_2$  and  $C_1$  are concentrations of a supposed solution around the corresponding two electrodes, and  $K$  a constant specified by the solution, and  $T$  the absolute temperature of the solution. Now, when the solution is taken as  $\text{NaCl}$  and  $T=291^\circ$ ,

$$e=\frac{u_- - u_+}{u_- + u_+} \cdot \frac{R}{F} \cdot T \cdot \log\left(\frac{C_2}{C_1}\right)=11.6 \log_{10}\left(\frac{C_2}{C_1}\right) \text{ (mV).}$$

If we suppose that  $C$  is given by

$$C=C_0 e^{-\beta D},$$

where  $D$  is expressed in unit of km.

So,

$$C_2/C_1=\frac{C_0 e^{-\beta D_2}}{C_0 e^{-\beta(D_2+\Delta)}}=e^{\beta \Delta}.$$

As before-mentioned, say putting  $e=0.3 \text{ mV/km}$  and base length  $\Delta=1 \text{ km}$ , we have

$$\beta=0.06,$$

$$C=C_0 e^{-0.06D}.$$

The value of  $\beta$  is nearly equal to  $\gamma$  in the expression of  $\Delta(R_{2,0}/H_{2,0})/(R_{2,0}/H_{2,0})_0$ ; a plausible explanation may be promised providing more comprehensive material.

T. Terada[55] has pointed out a possibility that luminous phenomena accompanying destructive sea-waves (Tsunami) may be explained by taking streaming

potential produced in the sea-bottom into account, which is proportional to the difference of water-heads of the high water of a tsunami and normal sea-level. For the present problem similar considerations may be applicable. In some cases meteorological water contained in the water-bearing layer may manifest a horizontal displacement towards the sea-side under the horizontal pressure gradient due to the difference of vertical pressure exerting upon the layer. On the contrary, high sea-water itself may permeate into the land in other circumstances. At any rate, expectable change of streaming potential in the ground due to the varied height of the sea-level may be given by

$$E = \frac{\zeta \cdot D \cdot \rho}{4\pi\eta} \cdot p,$$

where  $\zeta$  is the kinetic potential (mostly 0.01~0.05 volts),  $p$  the total hydrostatic pressure difference,  $D$ ,  $\rho$  and  $\eta$  respectively the dielectric constant, specific resistance, and coefficient of viscosity of the liquid. Taking  $p$  equals to the pressure exerting at the depth of sea-water of  $h_2=10$  cm, and besides, say, for the ground water,  $\zeta=0.03$  volts,  $\rho=10^3 \Omega \cdot \text{cm}$ ,  $D=81$  and  $\eta=0.01$  ( $t=15^\circ$ ), we have,

$$E=0.2 \cdot 10^{-3} \text{ volts.}$$

This is the same order as that requested from observations, but we have no reliable data to refer concerning actual motion of soil liquid in any horizontal level and some constants considered above. So the value is of very rough estimation at all.

# CHAPTER IV. SOME CHARACTERISTIC FEATURES OF THE DISTURBANCE FIELD OF EARTH-CURRENTS OBSERVED IN JAPAN

## §1. Introduction

In the preceding chapter all statements on various characteristics of earth-currents are obliged to be based on  $Sq$  field only in order to discuss the problem in a world-wide scale of data, since no systematic material of disturbing field has been published. However, in view of both geophysical interest and inductive nature of earth-currents, a study of the universal earth-currents is to be promoted along the line to analyse and interpret so-called short period variations with regard to their spectrums of period, frequency characteristics of some specified variations and etc. Recently, along his line of investigations various works have been carried on by the members of our observatory. In this chapter some newly found characteristics of  $SSC$  and  $SI$  changes of earth-currents observed at Kakioka and other stations in Japan will be reported.

## §2. Preliminary changes of $SSC$ and $SI$ of earth-currents

### (A). Preliminary change

Both  $SSC$  and  $SI$  changes are characterized by their first impulsive movements in geomagnetic field and earth-currents as well as their world-wide appearance. It has been commonly accepted that the first movement of  $SSC$  starts suddenly from some point on the magnetograph or electrogram, independent of the state of activity at that time. However, in the course of preparing long period material of  $SSC$ 's for the investigations of their diurnal and seasonal frequencies at Kakioka[56] it was found out that a

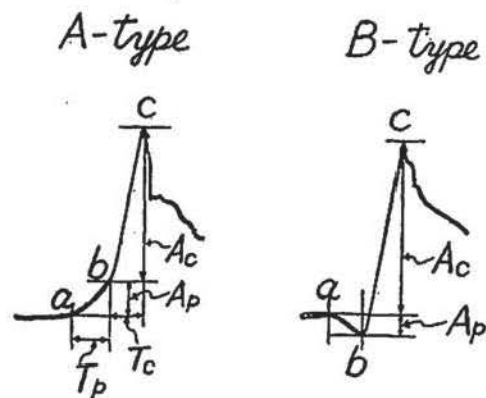
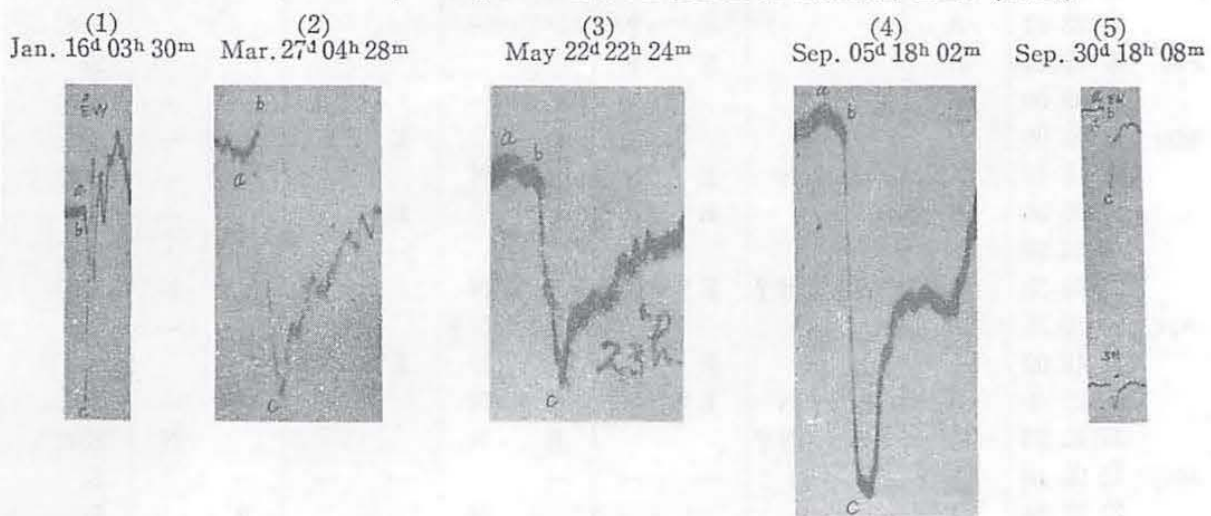


Fig. 58. Schematic figure of A-type and B-type of preliminary changes of  $SSC$  and  $SI$ .

kind of preliminary characteristic change was frequently followed by *SSC* or *SI* change. It was strange to us to see that even when they started on the very smooth electrograms free from any minor fluctuations, some *SSC*'s or *SI*'s were anticipated by small gradually increasing or decreasing preliminary changes lasting some minutes. Some typical

Plate 1~5. Preliminary changes for east-component at Kakioka, 1947. (U.T.)



Magnification factor : (1):1.0; (2):2.7; (3):2.7; (4):2.7; (5):0.8.

examples of these preliminary changes are shown in Plate (1)~(5), together with the exaggerated schematic expression in Fig. 58. In the figure the part *a*~*b* is meant by the present preliminary change of *SSC* or *SI*, and classified into A-type and B-type, respectively, according to its relative motion to the main first movement. As seen from the plate(5) the preliminary change is entirely distinguished from so-called a preliminary impulse or kick of *SSC*\* (arrow mark in *SN*), the latter being recorded almost as a segment of a line on the usual electrogram with revolving speed 1.5~2.0 cm per hour. Since the magnitude,  $A_p$ , and duration time,  $T_p$ , of the preliminary change approximately amount to a few percent of  $A_c$  and some minutes, respectively, the records were read out by means of a tenfold power micrometer. The preliminary changes adopted here are limited to all changes which have their duration times less than ten minutes and monotonously merge into the main impulses. When *SSC* or *SI* is occurred during disturbances, corresponding preliminary change is omitted. Of course, *SSC*\* with a preliminary inverse kick is included in A-type or B-type according to the criterion for the preliminary change.

In Table 23 are given the results of classification of the type of all available preliminary changes occurred in the sunspot maximum year, 1947, together with data

Table 23. Type of preliminary changes (P.C.) and distribution of inverse kicks of SSC\* and SI of earth-currents observed in Japan.

Date (U. T.)	Type of P. C.	Inverse Kick					Remark		
		Kakioka		Morioka		Haranomachi		Owashi	Miyakonojo
Jan. 14 11 16	A			? ?					SSC
16 03 30	A			E N					SSC
24 06 20	B			E? N	E				SSC
24 23 51	A			— ?		—			SSC
Feb. 07 08 14	A			? ?					SI
16 03 00	A					— —		— —	SSC
Mar. 02 04 00	?						E N	— —	SI
02 18 17	A	E N		E N	E N			— —	SSC
07 05 36	B			E N	E?		E	— —	SI
12 04 56	A						— —	— —	SSC
27 04 28	B	N? E?		E? N	E N			E N	SSC
Apr. 02 10 15	A			— —		N?		— —	SI
03 15 02	?			E N		N	E N		SI
08 21 49	A	E N		E? N	E? N			—	SSC
17 12 25	A	E N?			E N			N	SSC
May 15 00 18	?			— —	— —		— —	— —	SI
22 22 24	A					N		?	SI
23 02 40	B			E ?	— —			— —	SI
24 06 45	A	E N		? ?			E N	— —	SSC
Jun. 05 07 27	A	E N		E N			E N	— —	SSC
13 17 49	X	E N		E N	E N	E N	E N	— —	SSC
17 03 00	?			— —	E N	N		— —	SI
Jul. 17 10 37	A				E N	N	— —	— —	SI
17 17 49	B					N	— —	— —	SSC
Aug. 15 09 51	A			— —			N	E?	SSC
22 09 11	?			E E			N		SSC
Sep. 02 23 26	A					N		— —	SSC
04 13 45	A							— —	SI
05 18 02	A				N			— —	SSC
23 03 23	?							— —	SSC
30 18 08	A		N		N			— —	SSC
Nov. 09 08 56	A			— —	— —				SSC
11 06 51	B			— —	— —				SI
24 17 56	A		N				—	N	SI
27 18 35	B			— —	— —			— —	SI
Dec. 01 08 53	A			— —	— —			— —	SI
23 11 24	A						— —	— —	SI

UNIVERSAL EARTH-CURRENTS AND THEIR LOCAL CHARACTERISTICS 63

Table 24. Values of amplitude and duration time of the main impulse and preliminary change at Kakioka for east-component. unit : minute and mV/km

Date (U. T.) 1947			T <sub>p</sub>	T <sub>c</sub>	A <sub>p</sub>	A <sub>c</sub>	A <sub>p</sub> /A <sub>c</sub>	
Jan.	d	h	m					
	04	11	16	2.0	2.8	10.4	107.8	0.096
	16	03	30	1.6	1.6	16.5	154.2	0.107
	24	06	20	1.2	1.6	6.4	55.1	0.116
Feb.	24	23	51	1.5	0.8	9.2	78.8	0.116
	07	08	14	1.3	1.6	6.5	63.1	0.103
	16	03	00	0.8	0.9	13.9	102.0	0.136
Mar.	02	04	00	?	?	?	?	?
	02	08	17	1.1	1.1	6.5	24.1	0.025
	07	05	36	0.2	0.4	9.2	91.5	0.101
	12	04	56	4.4	4.4	10.2	74.2	0.138
Apr.	27	04	28	2.4	3.0	9.2	103.0	0.089
	02	10	15	1.9	3.1	1.8	37.6	0.048
	03	15	02	?	?	?	?	?
	08	21	49	1.2	1.6	2.7	127.0	0.021
May	17	12	25	2.1	1.9	5.4	279.6	0.020
	15	00	18	?	?	?	?	?
	22	22	24	4.0	4.0	6.7	85.2	0.067
	23	02	40	1.1	1.1	16.3	102.3	0.159
Jun.	24	06	45	1.1	1.6	20.1	233.3	0.086
	05	07	27	0.8	0.8	4.8	329.2	0.015
	13	17	49	—	—	—	—	—
	17	03	00	?	?	?	?	?
Jul.	17	10	37	1.9	1.7	2.8	37.6	0.074
	17	17	49	0.8	1.0	18.7	413.2	0.045
Aug.	15	09	51	2.2	1.6	8.2	161.0	0.051
	22	09	11	?	?	?	?	?
Sep.	02	23	26	2.2	2.2	8.2	92.4	0.089
	04	13	45	3.6	2.8	10.4	93.3	0.110
	05	18	02	3.2	3.2	4.5	66.3	0.068
	23	03	23	?	?	?	?	?
Nov.	30	18	08	2.8	2.4	1.1	95.0	0.012
	09	08	56	3.4	4.0	4.3	65.5	0.065
	11	06	51	2.6	2.9	6.4	71.2	0.090
	24	17	56	3.2	2.8	2.2	79.0	0.045
Dec.	27	18	35	4.2	4.8	1.8	48.8	0.037
	01	08	53	2.5	2.7	3.7	81.2	0.045
	23	11	24	1.3	1.3	3.7	97.0	0.038

of inverse kicks of sudden commencements. The type is determined from the record at Kakioka, and ? marks indicate some preliminary changes not measurable correctly for some reasons, say, faint image of record, accidental coincidence with time marking, masking effect by disturbances and etc. The cross mark indicates that it is difficult to attribute any type to the variation considered.

Concerning the frequency of each type it is surprising to see that out of available thirty preliminary changes twenty three belong to the A-type, which is too many to be expectable from the view of a mere chance. This is the first fact that we should pay our attention to the immediate part of an electrogram anticipated to any SSC or SI change.

[B]. Relation between  $T_p$  and  $T_c$

The results of readings of  $T_p$  and  $T_c$ , duration time of the main in impulse or east-component are given in Table 24. As seen in Fig. 59, there exists approximately a linear connection between  $T_p$  and  $T_c$ , and on the average,  $T_p \approx T_c$ . The relation seems to hold good for both A- and B-type. For purpose of reference it was checked by the data of 1946 with regard to the A-type. These are the second fact to suggest something about the existence of some anticipated phenomena for the world-wide disturbance, SSC or SI.

[C]. Relation of  $A_p$  to  $A_c$

The values of  $A_p$  and  $A_c$  for east-component at Kakioka are given in Table 24, and connection between them is graphically shown in Fig. 60.

Roughly speaking, there is a tendency that  $A_p$  increases with increasing  $A_c$ ,

although points in the figure are remarkably scattered. But the following two points are noticeable, (1)  $A_p$ 's of the A-type with kicks are very small as compared with others, making the lowest boundary line of the domain in which all observational points are contained; (2) Observational points seem to converge to a common point ( $A_p \approx 0, A_c \approx$

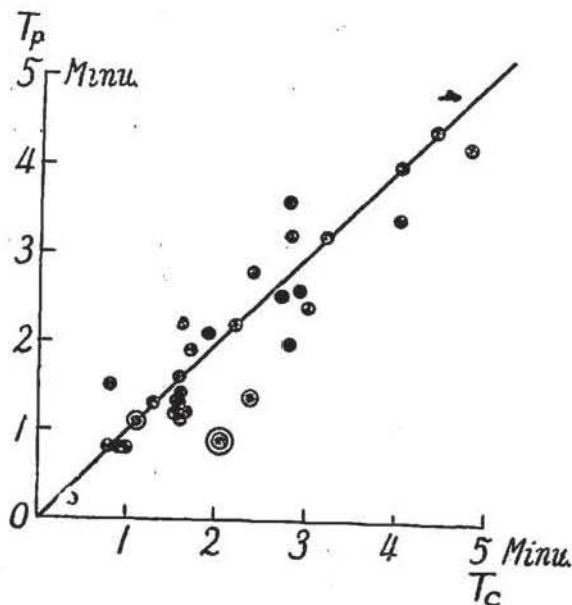


Fig. 59. Correlation between  $T_p$  and  $T_c$  of the preliminary change at Kakioka.

15 mV/km), in other words, at Kakioka  $A_c$  less than this value might not be accompanied with  $A_p$ , or such a small  $A_c$  might be forbidden to occur entirely. Concerning the item (2), the frequency spectrum with regard to the amplitude of SSC may be

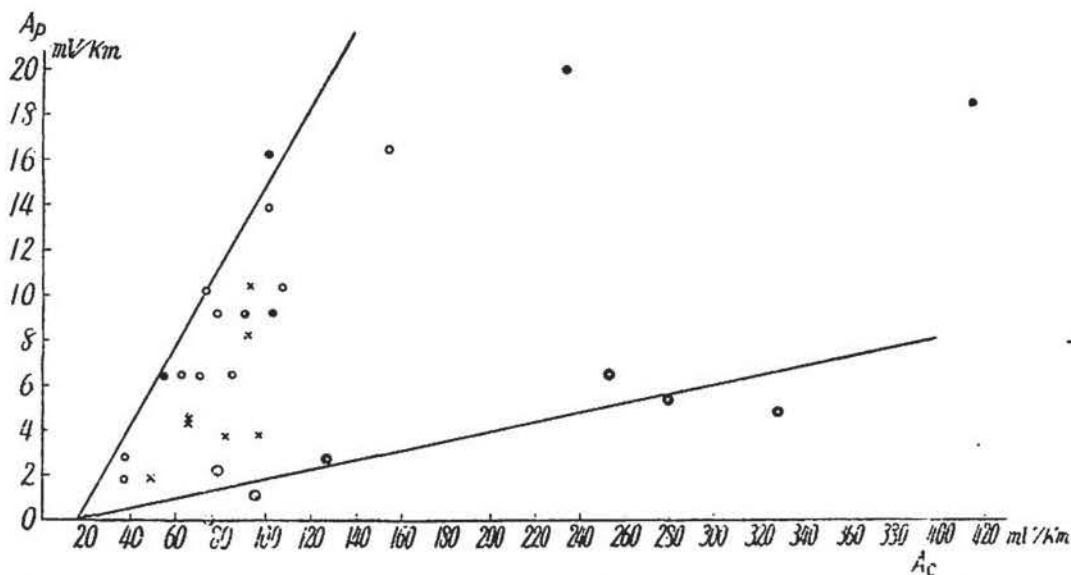


Fig. 60. Relationship between  $A_p$  and  $A_c$  of the preliminary change at Kakioka.

Table 25. Frequency spectrum of  $A_c$  for east-component at Kakioka, 1945~1949.

$A_c$ (mV/km)	0~14	15~19	20~24	25~29	30~39	40~49	50~59	60~69	70~79
Numbers	1	5	6	8	19	17	15	13	16
$A_c$	80~89	90~99	100~109	110~119	120~129	130~139	140~149	150	
Numbers	7	17	11	5	5	3	1	17	

advisable, which is given in Table 25 for the interval of five years from 1945 to 1949 centering in 1947. From this table it is obvious that  $A_c$  contained in the interval 0~14 mV/km occurred only once out of one hundred and sixty six, and so as the lowest magnitude of  $A_c$  for east-component at Kakioka may be taken as the same value as that defined by a common point before-mentioned. Regarding (1), it is considered that  $A_p$  may be decreased due to superposition of an inverse change of kick. These facts are the third point to suggest some preliminary changes immediately before SSC or SI.

[D]. Diurnal and seasonal variation of  $A_p/A_c$

The amplitude ratio,  $A_p/A_c$ , is plotted in Fig. 61(A) with regard to the nearest hour of occurrence, where the material for the A-type in 1946 is supplied to get more numerous points for each hour. The average curve shows a predominant maximum and minimum around noon and 18 hr, respectively. And the difference between two three-hour means of  $A_p/A_c$  centering at these hours is statistically high significant. Although the observational points are less numerous during night hours, the curve seems to have a minor maximum and minimum before midnight and near 6 hr, respectively.

Concerning the daily variations of  $A_p$  and  $A_c$  themselves, they are shown separately in Fig. 61(B), in which the daily variation of  $A_p$  shows a fairly good agreement with that of  $A_p/A_c$ , but not so distinct for  $A_c$  as far as the present data are concerned. Therefore, the mode of the daily variation of  $A_p/A_c$  presented here is mainly responsible for that of  $A_p$ , though a minimum of  $A_p/A_c$  around 18 hr may be more exaggerated by some larger values of  $A_c$  appeared near the hour.

Any definite seasonal variation of  $A_p/A_c$  could not be obtained from the present small material, and so is desirable a longer period statistics.

The solar daily variation of the amplitude of the preliminary change is the fourth fact to support the foregoing statement, considering a similar local time variation of that of sudden commencements.

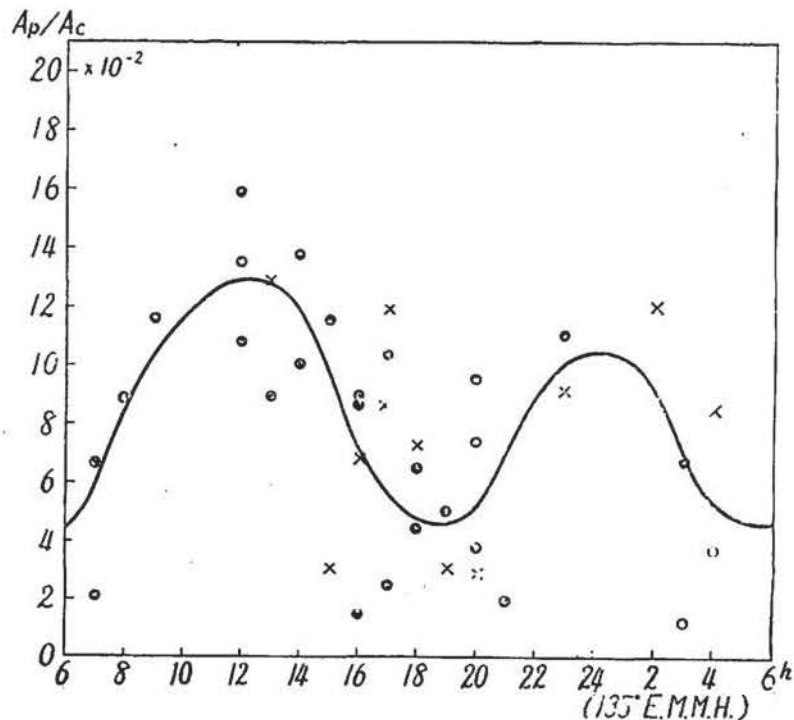


Fig. 61(A). Daily variation of  $A_p/A_c$  of the preliminary change at Kakioka.

### §3. Diurnal variation of $A_p$ and $S_q$ -variation

On the other hand it has been recently pointed out that so-called world-wide phenomena such as  $SSC$  or  $SSC^*$  of the geomagnetic field should not be left alone as they were, but re-examined taking such facts as their newly found local characteristics with regard

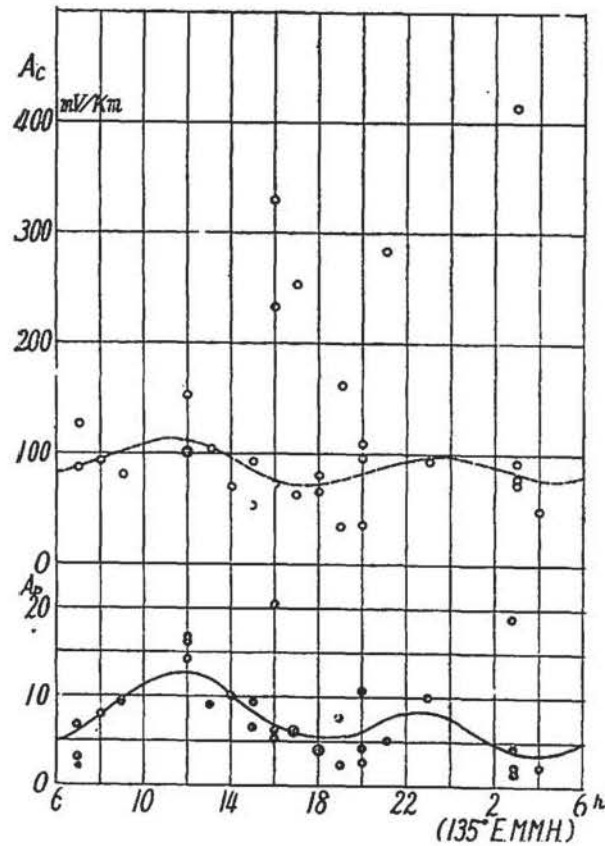


Fig. 61(B). Daily variations of  $A_p$  and  $A_c$  at Kakioka.

to the hourly frequency of occurrence as well as amplitude into consideration. The phenomena pictured up here may also introduce an another fact to be clarified from the same point of view. Here, the writer suggests that a part of the original current of  $SSC$  or  $SI$  may flow in our ionospheres.

If we compare the diurnal variation curve of  $A_p$  shown in Fig. 61 with that of  $S_q$ , we can easily find out a striking resemblance to each other except that the former lags about three hours behind the latter. So the correlation between  $A_p$  and each monthly mean  $S_q$ , of which phase angle is retarded three hours, is graphically shown in Fig. 62. A statistical test of significance of the linear correlation is made by the method of variance as shown in Table 26. The ratio of the variance (1) and (2) is 9.21. For 1 and 28 degrees of freedom the 5% and 1% values of  $F$  in the  $F$ -distribution are 4.20 and 7.64, respectively. It follows that the regression is significant, i. e. the tendency for large values of  $A_p$  to be associated with large values of the retarded  $S_q$ -variation is significant.

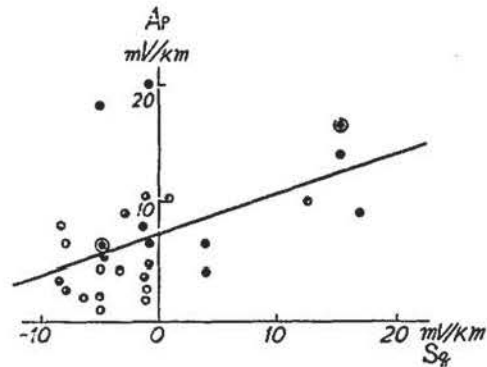
Table 26. Analysis of variance of regression.

Source of Variance	Sum of Squares	Degree of Freedom	Variance
(1) Due to Regression ( $C^2/S_x$ )	188.18	1	188.18
(2) About Regression ( $S_y - C^2/S_x$ )	571.70	28	20.42
Total	759.88	29	

$$S_x = \sum x^2 - (\sum x)^2/n, \quad S_y = \sum y^2 - (\sum y)^2/n, \quad C = \sum xy - \sum x \cdot \sum y/n,$$

$$x = \xi q, \quad y = Ap - 7.7, \quad n = 30.$$

Some years ago this writer suggested to consider anew the solar daily variation field or some radiation agency for the interpretation of the local time variation of the hourly frequency of SSC or SSC\* [57]. Yet no plausible opinion has been brought forward up to date, meanwhile a local time variation of  $A_p$  with a striking resemblance to  $S_q$ -variation has been newly presented here. Now, it may be further suggested that at least a part of currents responsible for  $A_p$ , probably for SSC or  $SI$ , flow in or near the E-layer.

Fig. 62. Relationship between  $A_p$  and  $S_q$  for 1947.

On the other hand it has been well known that the amplitude of SSC becomes larger with increasing latitude, and T. Nagata and his collaborators [83] have recently showed that Ds-field begins to appear in high latitudes from the very time of SSC, suggesting some corpuscular impinging upon the auroral zone ionospheres at the time. The origin of preliminary changes considered here may also be situated in high latitudes, and current distribution may take such a type as that of a polar storm. But the phenomena relies almost for its full account including an explanation of the phase angle mentioned above on the accumulated world-wide data in future.

#### §4. Preliminary inverse impulse, or kick of SSC\* of earth-currents

Regarding geomagnetic SSC\*, among all investigators, T. Nagata [59] recently carried out the most comprehensive investigations, and so here something about the

matter will be described from a standpoint of locality of earth-currents. From the data of 1947 at Kakioka four and nine *SSC\** for geomagnetic field and earth-currents can be respectively taken out, of which three *SSC\*\**'s occurred simultaneously in both fields. If geomagnetic *SSC\*\**'s corresponding to ? marks in Table 23 are counted in, the number increases to seven, of which five become to occur simultaneously with those of earth-currents. Therefore, it should be first admitted that all *SSC*'s of earth-currents are not always accompanied simultaneously with geomagnetic ones; the former being more numerous. The second point to be mentioned is that *SSC\*\**'s of earth-currents are not always simultaneously observed at all five stations in Japan as given in Table 23.

Concerning these local characteristics of earth-currents, following two explanations may be possible. (a): All *SSC\*\**'s are supposed to be occurred simultaneously in both earth-currents and geomagnetic field, but small rapid ones are apt to appear in earth-currents only. This opinion assumes first that by using suitable technique so numerous kicks are to be observed even in the geomagnetic field in the lower latitudes, and a lack of simultaneity of earth-currents in a rather small area such as Japan is responsible for some inhomogeneity of electric structure of the ground, or such local structure of the ionosphere over some specified region. (b): Even when there is no primary agency of *SSC\** in the geomagnetic field, there may be a good chance to observe *SSC\**-like kick of earth-currents in conjunction with the principal direction, provided some suitable direction and quickness of time change of the first starting vector of a geomagnetic *SSC*. These apparent *SSC\*\**'s may be superposed on primary ones.

For example, the direction of the first starting magnetic vector in Japan is generally north-easterly(60) and may change in some range of degrees. So at a station with the south-westerly principal direction will be more numerous such lucky chances for north-component than east-component(Table 23).

Unfortunately, there are few key points to decide which opinion is more plausible. The writer, however, is now inclined to consider the case (b) more promisingly than(a), although the latter would be more interesting from a geophysical point of view. At any rate, carefully conducted simultaneous quick-run recordings of both geomagnetic elements and earth-currents will answer to this question, especially provided high sensitive instruments and accurate timekeeping.

In conclusion it may be worthy to add some words about a question whether or not some other variations do manifest such changes as preliminary changes before-mentioned or kicks. Some well-known variations such as pulsations, solar flare variations, bays and etc. are unlikely to show such characteristic changes, but further efforts should be offered to examine for other rapid changes frequently observed during storms.

## CHAPTER V. CONCLUSIONS

1. It was endeavoured to collect recent data as many as possible from various parts of the world together with our Japanese observations, and to analyse them to deduce some general pictures of local characteristics as well as world-wide natures of the spatial distribution and time variations of earth-currents.

2. First of all the principal direction, or restricted direction of earth-currents, was examined by using the hodographs of the annual mean  $S_q$  observed at several stations in U. S. A., Europe, South-America, Japan, Australia and so on, as well as short period variations recorded at about two dozens of stations in Japan. In spite of apparently random distribution of the direction, we may finally deduce three groups of type, correlating to the actual distribution of land and sea, and topographical and geological circumstances together with earth-resistivity surveys around the stations. At several stations the direction is almost constant even for each individual harmonic wave of  $S_q$ , and if except for the diurnal waves at some stations, twelve stations out of seventeen ones belong to this catalogue. So there are few stations at which principal directions deduced separately from each harmonic wave are not always equal, but somewhat different one another; for example, at Kakioka both diurnal and semidiurnal harmonics in winter are responsible for this inequality

3. Comparing the year-to-year change of the maximum range of the  $S_q$ -variation of earth-currents to that of relative sunspot numbers, we obtained a nearly linear correlation between them, of which proportional constant to  $S$  approximately depends neither upon the base direction nor coordinates of latitude of stations. The east-component at Kakioka, however, was found to be exceptionally small compared with an expectable value from the linear expression said above, and to be attributed to the winter characteristics of the mode of  $S_q$ . Of course, a similar consistent result

can be obtained for each harmonic wave of Sq. The facts lead us to study how does the mode of Sq change in the long course of years at any station situated near the locus of the wandering focus of the equivalent current system of the Sq field.

4. There is found a remarkable long period variation of  $T_{\min}^B$  of Sq, time of occurrence of the extreme minimum for east-component in winter at Kakioka, which has a distinct maximum about two years before the maximum of  $S$  and shows a good parallelism with the change of  $\Delta S/\Delta t$ , not  $S$  itself, where  $S$  is the relative sunspot number and  $t$  time in unit of year. We have no such a change for  $T_{\max}^B$ , time of occurrence of the extreme maximum for east-component of Sq in winter. There is also found a similar variation in the geomagnetic Sq field, especially in the horizontal intensity at Kakioka, and a tendency of less significance at Tucson, an another similar middle latitude station.

5. An another interesting aspect of the secular variation of the mode of Sq in winter at Kakioka is that there exists some shorter period, namely, four-year period variation superposed on the long period change before-mentioned. We can detect similar periodic variations in both geomagnetic Sq at Kakioka and  $f_{F_2}^2$  at Kokubunji, Tokyo, as well as relative sunspot numbers  $S$ .

6. On the other hand, phase angles  $\varphi_n$ 's of harmonic waves of Sq show no systematic connection with  $S$  as a whole, contrary to the amplitude changes, though  $\varphi_1$  manifests apparently random large fluctuations, especially in north-component. However, the year-to-year change of  $\varphi_n$  is fairly systematic for each wave, but there is a remarkable dissimilarity between  $\varphi_1$  and other  $\varphi$ 's, namely, the former manifests the long period change before-mentioned, while the latter 4-year period changes. These two characteristics correspond to those of  $T_{\min}^B$ , namely,  $n$  or  $N$  and  $\Delta n$ , respectively, showing distinct different contributions from different harmonic waves to an apparent secular change of the mode of Sq at Kakioka. At Tucson, however, there is found no such 4-year period changes for  $\varphi_n$ 's, while  $\varphi_1$ 's at both stations show the similar long period change. This discrepancy may be responsible for the different behaviors of the ionospheres in winter over the stations. Further investigations will be desirable from both sides of the geo-electromagnetic field and ionosphere by gathering longer period data from various places in the world.

7. Concerning the solar daily variations observed at seventeen stations, the magnitude of the resultant potential gradient  $R_{n,o} = \sqrt{C_{n,o}^N{}^2 + C_{n,o}^E{}^2}$  is of order of some millivolts per kilometer at most, except for two stations, Toledo and Nemuro with exceptionally small and large values, respectively. The average values for twelve middle latitude stations are as follows.

Period (hrs) .....	24	12	8	6
Amplitude (mV/km) .....	1.51	1.86	1.22	0.43

8. It is confirmed that the ratio of  $R_{n,o}$  to  $H_{n,o} = \sqrt{C_{n,o}^X{}^2 + C_{n,o}^Y{}^2}$  is approximately proportional to  $1/\sqrt{T_n}$  even in many different localities in the world as far as such a range of  $T_n$  that covers those of principal harmonics of the Sq-variation is concerned. This relationship, however, deviates from its lineality with increasing  $1/\sqrt{T_n}$ ; for example, at all four stations in Japan the specific resistance of the ground increases with increasing depth from the surface. Assuming a proper uniform specific resistance of the upper several kilometers depth, a presumed two-layer structure of the ground fits fairly well to each station.

9. Apparent resistivities  $\rho_a$ 's calculated from  $R_{n,o}/H_{n,o} = \sqrt{\rho_a/2T_n}$  are of order of  $10^4 \Omega \cdot \text{cm}$  at nine stations out of fifteen, while they are as small as  $3 \sim 4 \cdot 10^3 \Omega \cdot \text{cm}$  at Huancayo and Toledo. The average value of  $\rho_a$ 's for twelve middle latitude stations gives  $4 \cdot 10^4 \Omega \cdot \text{cm}$ .

10. There is a fairly intimate connection between  $\rho_a$ 's and earth-resistivities  $\rho_{obs}$ 's, which are observed in the shallow upper portion of the earth up to some hundred meters or more below the surface, as far as the present observed earth-resistivities are concerned.

11. The second harmonic wave of Sq near the sea-coast contains a factor of which amplitude decreases towards the inner part of the land with increasing distance measured from the nearest sea-coast to the respective stations. Since it is examined in vain to get such a regular distribution for the other waves, it is suggested that some local earth-currents due to, say, electrochemical actions or capillary fluid motions may be produced near the sea-coast by the solar tidal motion of the sea-water.

12. It is pointed out that SSC and SI changes are generally anticipated by small gradually increasing or decreasing preliminary changes lasting some minutes. These preliminary changes are characterized by four observational facts which suggest us to

pay our attentions to the immediate parts of the electrogram anticipated to SSC and *SI* changes. The four observational characteristics of the preliminary change are as follows, (1) Preponderance of the frequency of one specified type of the variation, A-type; (2) Duration time of the variation,  $T_P$ , is almost equal to that of the main impulse,  $T_O$ ; (3) Amplitude of the preliminary change,  $A_P$ , is distributed within a definite domain of the  $(A_P, A_O)$  diagram; (4) The solar daily variation of the amplitude of the preliminary change.

13. The solar daily variation of  $A_P$  shows a striking resemblance with  $S_q$ -variation, though the phase angle of the former lags about three hours behind the latter. This suggests that at least a part of currents responsible for  $A_P$ , probably SSC or *SI*, may flow in or near the E-Layer.

14. All SSC\*'s of earth-currents are not always accompanied simultaneously with geomagnetic ones, the former being more numerous. SSC\*'s of earth-currents are not always simultaneously observed at all five stations in Japan. These local characteristics of earth-currents may be considered to be mainly controlled by suitable combinations of the direction and quickness of the first impulse change with the electric structure of the ground around the very station.

## ACKNOWLEDGEMENTS

The writer wishes to acknowledge his indebtedness to Dr. S. Imamiti, the former director of the Kakioka Magnetic Observatory, for his constant interest and encouragement throughout the course of this investigation extending over several years. He also cordially thanks Dr. M. Hasegawa, Dr. H. Hatakeyama, Dr. T. Nagata, Dr. T. Rikitake and other colleagues for their valuable suggestions and criticisms given him at the general meetings of the Society of Terrestrial Magnetism and Electricity of Japan, and in private conversations. The writer extends his hearty thanks to all members of our observatory at Kakioka and its attached observatories for their kind aids in the preparation of the paper.

## References

- [ 1 ] Terr. Magn. 36, No. 2 (1931), 1907.
- [ 2 ] Terr. Magn. 33, (1928), 205~209.
- [ 3 ] Terr. Magn. 32, (1927), 143~145.
- [ 4 ] Terr. Magn. & Elect., Chapter VI Earth-Currents (1949).
- [ 5 ] Ency. Britanica, Vol. VIII, 815 (8th Ed.)
- [ 6 ] Jour. Met. Soc. Jap. 12, No. 1; Ann. Rep. of Toyohara Mag. Obs.
- [ 7 ] Ann. Rep. of Kakioka Mag. Obs.
- [ 8 ] Terr. Magn. 40, No. 3 (1935), 317~324.
- [ 9 ] Corrientes Teluricas Año 1948, Observatorio Central Geofísico de Toledo.
- [10] K. Maeda, 地震 (Earthquake), 9, No. 7 (1937).
- [11] T. Nagata, 地震 (Earthquake) 15, No. 11 (1943).
- [12] Y. Yokouchi, Memo. Kakioka Mag. Obs., 5, No. 1 (1943)
- [13] Y. Kato, Jap. Jour. Astr. & Geophy., 1, No. 4 (1943).
- [14] Yamakawa Ionospheric Obs.
- [15] K. Hirao, Geophy. Notes, Tokyo Univ., No. 29 (1947).
- [16] K. Hirao, Special Committee for the study of the Fukui Earthquake (1950), 181.
- [17] Terr. Magn. 40, No. 3 (1935), 237~254.
- [18] Terr. Magn. 32, No. 1, 49~63.
- [19] Terr. Magn. 27, 1~30 (1922).
- [20] Ann. Rep. of Toyohara Mag. Obs., 1933~1936.
- [21] 理科年表 (Rika Nenpyo), 1955.
- [22] M. Hasegawa and M. Ota, Read before the meeting of the Section of Terr. Mag. and Elect., N. P. C. Japan (Feb. 1941)
- M. Ota, Rep. of Ionosphere Res. Japan, 3, No. 1~2 (1949)
- T. Nagata, Geophy. Notes, Tokyo Univ., No. 36 (Feb. 1948)
- [23] [22]
- [24] W. J. Rooney, Reseaches of Dep. Terr. Mag., Carnegie Inst., Washington, Vol. IX.
- [25] Terr. Magn. 50, No. 3 (1945), 175~184.
- [26] [21]
- [27] [21]
- [28] Kakioka Magnetic Observatory Annual reports and five-year's reports of "Goelectricity,"
- [29] Boletín Mensual Vol. 6~7 (1951~1952), Observatorio De Física Cosmica De San Miguel (R. Argentina).
- [30] Canadian Polar Year Expeditions, 1932~1933, Vol. II.
- [31] Geomagnetismo Año 1949, Obs. Cent. Geof. de Toledo.
- [32] L. A. Bauer, Terr. Magn, 27 (1922), 1~30.
- [33] Year Books for Tucson (Ariz.), 1919~1920, U. S. Coast and Geodetic Survey.
- [34] Ann. Rep. Toyohara Mag. Obs.
- [35] Ann. Rep. Kakioka Mag. Obs.

- [36] Res. Dep. Terr. Magn. Vol. VII-A, Carnegie Inst., Washington.
- [37] Res. Dep. Terr. Magn. Vol. X-A, Carnegie Inst., Washington.
- [38] L. Cagniard, Geophysics Vol. XVIII, No. 3 (1953), 605~635.  
T. Rikitake, Bull. Earthq. Res. Inst. Tokyo Univ., Vol. XXIX (1951)
- [39] Corrientes Teluricas Año 1949, Obs. Cent. Geof. de Toledo.
- [40] Terr. Magn. 32, No. 1 (1927), 49~63, ; 33 (1928), 79~90.
- [41] Terr. Magn. 39, No. 3 (1934), 199.
- [42] Terr. Magn. 35, No. 2 (1930), 61~72).
- [43] [40]
- [44] M. Hirayama, Jour. Met. Soc. Jap. 12, No. 1 (1934), 16~22.
- [45] S. Omote, Bull. Earthq. Res. Inst. Tokyo Univ., Vol. XXIX, Part I (1951)
- [46] Terr. Magn. 43, No. 2 (1938), 107~118.
- [47] J. Egedal, Terr. Magn, 42 (1937), 179~181.
- [48] Y. Yokouchi, Memo. Kakioka Mag. Obs. 2, No. 2, 3 (1939), 65~18.
- [49] M. Hasegawa, Rep. Jap. Ass. Adv. Sci., 14, No. 2 (1942).
- [50] Y. Yokouchi, Read before the 16th general meeting of Soc. Terr. Magn. & Elect. Japan (1954).
- [51] S. Ogura, 潮汐 (Ocean Tide).
- [52] [51]
- [53] Z. Yasukura, Tech. Rep. Kyushu Univ., (1934), 1~11.
- [54] [51]
- [55] T. Terada, Bull. Earthq Res. Inst. Tokyo Univ., Suppl. I (1934), 25~34.
- [56] T. Yoshimatsu, Journ. Geomag. Geoelec., II No. 2 (1950), 54~60.
- [57] [56]
- [58] For example, T. Nagata and N. Fukushima, Indian J. Met. Geophys., 5, Special. geomagnetic number (1954), 75~88.
- [59] T. Nagata, Rep. Ionosphere Res. Japan, VI, No. 1 (1952), 13~30.
- [60] Y. Yokouchi, Memo. Kakioka Mag. Obs. 6, No. 2 (1953), 204~248.  
T. Yumura, Memo. Kakioka Mag. Obs. 7, No. 1 (1954), 27~48.

# APPENDIX

## THE MEASUREMENT OF EARTH-CURRENT POTENTIALS AND ITS RELIABILITY

### § 1. Introduction

Superficially the method of the earth-current measurement is simplicity itself and does not differ in principle from an ordinary physical measurement of potential difference in the first kind or second kind of conductor. We must, however, take seriously into considerations following some characteristic points in these fields of science.

In the first place, the earth may be probably considered to be a complex semiconductor; especially the electric state of its upper layer, in which some of the main parts of the measuring equipments are installed, is mainly governed by its constituents and quantities of electrolytic substances contained. And generally it is apt to vary over rather wide limits beyond our control, so that it tends to rise various extraneous effects at the electrodes. Much efforts, therefore, have been done by many investigators to get electrodes free from any such contact potentials, but, unfortunately no satisfactory success has been done, at least in the permanent installation, though the non-polarizing liquid electrode is surely superior for the temporary observation in respect to its small contact potentials. We must, therefore, allow for some of these contact potentials and try to minimize them as possible as we can, and more practically as constant as possible compared with other portions of potentials considered(1). Although these statements seem to be rather negative for us, in practice even this last requirement is not so easily realized as it is the case. These anomalous variations, however, are used to be distinguished from other portions of potentials by comparing two or more independent bases in the same direction. One of the most fundamental and urgent necessity for earth-current measurement is to improve the method of electrode installation to be suited for the permanent routine observation in the very place.

As to other requirements for the satisfactory measurement, similar careful practices must be done for the installation of the underground wires protected from any fault insulation and natural corrosions, and sometimes for the construction of some suitable shaped electrodes of small contact resistances compared with that of the remainder of the circuit. These two requirements seem to be more or less easier to artificially control

than contact potentials, but various initial testing and practice of the former should be most carefully carried out as well as that of electrodes themselves, because of the difficulty of testing their correct order of function at any time when once buried in the ground.

Besides of these points, various kinds of minute techniques may be required in practice for the method of recording and installation, corresponding to the apparatus used and the different geological, topographical and hydraulic states at the very station. From these points of views, in this paper are given some observational simple experiments and notes on the essential points, on which the accuracy of the measurement depends mainly but not so systematically have been treated, and general description of the method and equipment made at the Kakioka Magnetic Observatory, through which important data used in this paper are supplied.

## § 2. Some experiments and notes on the measurement of earth-current potentials

### 1. *Base length*

Generally speaking, it is difficult to say in a word how long and in what directions the base lines should be installed. The matter differs for different subjects of investigation and localities of the subterranean structure in the neighbourhood of the station. For instance, at the ordinary observatory recording of such sorts of earth-currents as the world-wide and rather short period variations, one to ten Km lines running in northward and eastward directions are usually installed [2]. On long lines, running scores or hundred kilometres long, we have some advantages in such points as the negligible small electrode potentials compared with universal earth-current potentials, low sensibility of instruments used, more representative features of the current flow in the vicinity of the station and so on. For the permanent routine work, however, it may be more desirable to construct cheaply and to keep permanently the lines in satisfactory conditions, even it is required to use somewhat higher sensitive instruments or recording apparatus. Hence, from only this point of view, and further from the need of uniformity of the structure in the area included in the measurement, it may be apparently said that the more the line is short, the better it goes. Of course, we may frequently encounter with troublesome and difficult events to overcome for the satisfactory measurements of small quantities

considered (3), if unduly short lines were operated without any sensible precaution against various extraneous effects. In order to harmonize those merits and failures, at an ordinary observatory it may be safe to choose the base length as long as a few kilometres at most, provided careful precaution and patient endeavour for maintenance of all parts of the equipment.

On the other hand, at a place where the subterranean structure is so complex that the distribution of its electrical conductivity becomes heterogeneous or even anisotropic, we may have a few base systems with different base length and direction of the line. The need of these auxiliary equipments can be justified by the precise knowledge about the distribution of the current flow in respect to that of conductivity in both horizontal and vertical directions. A more important point in some sense is that these duplicate or multiple systems can manifest themselves as a powerful tool for the investigation of local or sometimes regional character of earth-currents.

## 2. *Geomagnetic and atmospheric electric induction on the overhead line*

It is unquestionably desirable to use the highly insulated cable lines for connection between the recording instruments and electrodes, because when the aerial lines are used the following points should be cared of; electromagnetic induction on them due to the time changes of the geomagnetic field or mechanical motion of the lines in the permanent geomagnetic field, electrostatic induction effects of atmospheric electricity, and some mechanical damages of leading wires and their supporters. But frequently are used the overhead lines instead of cables, because of the expense entailed and serious injury upon the crops.

### (A). *Geomagnetic induction on the line*

#### (i). Induction due to the transient geomagnetic field changes

Two test base lines were set in the compound of the Kaḳioka Magnetic Observatory, one of which formed a vertical rectangular loop of the area  $100 \text{ m}^2$  with its overhead line and the ground, while an insulated wire for another base was laid down on the surface of the ground in a straight line, running in the same direction as the former base. Earth-current potentials for each base were photographically recorded by means of two sensitive galvanometers with the same instrumental constants as shown in Table 1;

Table 1.

Galvanometer	Period	C. D. Res.	Coil Res.	Current sens.	Scale value
	7.5 <sup>s</sup>	110 $\Omega$	104 $\Omega$	1.1.10 <sup>-6</sup> amp/mm	2.8.10 <sup>-5</sup> volt/100m/mm
Speed of Recording	6.0 mm/minute				

Considering the fact that the more the magnetic field changes quickly, the more induced current in a loop becomes large, the amplitudes of the same short period variations with their time duration ranging from ten seconds to one minutes were read out from the two records. The amplitudes of the selected variations are given in three groups in Table 2.

Table 2. Comparison of amplitude of potentials, A, of the universal short period variations observed with two sets of lines; the one makes a vertical loop with the ground, while another makes no loop.

A: expressed in mm unit.

Range	A <sub>γ</sub>	A <sub>0</sub>	Range	A <sub>γ</sub>	A <sub>0</sub>	Range	A <sub>γ</sub>	A <sub>0</sub>	Mean	A <sub>γ</sub>	A <sub>0</sub>
0-5.0	4.0	4.0	5.1-10.0	5.2	5.3	>10.1	12.1	12.3	0-5.0	3.81	3.79
	2.0	2.1		7.0	7.0		13.9	14.0	5.1-10.0	7.14	7.16
	5.0	5.0		6.0	6.0		10.1	10.3	>10.1	14.56	14.54
	2.8	2.8		7.0	7.0		10.2	10.2			
	3.0	2.8		8.0	8.0		22.8	22.5			
	5.0	5.0		6.0	6.0		16.9	16.7			
	4.0	4.0		7.0	7.0		15.8	16.0			
	4.0	4.0		8.1	8.0		14.0	13.9			
	5.0	5.0		10.0	10.1		11.0	11.0			
	3.3	3.2					22.2	22.0			
				11.2	11.0	Total Mean			8.75	8.74	

A<sub>γ</sub>: Line with a loop.

A<sub>0</sub>: Line with no loop.

As it had been expected before the experiment, we could not detect any appreciable difference in amplitude between two sets of base lines as far as the accuracy of the measurement was concerned. We could also find no phase differences between two records in the limit of error, four seconds. From the theoretical standpoint of view, however, the magnitude of induced electromotive force, V, in a coil due to the varying magnetic force, H, which passes perpendicularly through the coil can be expressed as follows,

$$V = S \cdot N \cdot \frac{dH}{dt} \cdot 10^{-8} \text{ volts,}$$

where S and N are the area and number of turns of the coil. Then, in the case of the above experiment, V can be calculated as V=10<sup>-7</sup> volts for S=100 m<sup>2</sup>, and 4.5.10<sup>-8</sup> volts

for  $S=4500 \text{ m}^2$ , respectively, when  $N=1$ ,  $\frac{dH}{dt} = 10^{-5}$ .

The maximum area of the loop in the sense said above is approximately  $4500 \text{ m}^2$  for the regular east base line of one and half kilometers long at Kakioka. At any rate, therefore, it is clear that induction effect due to the varying geomagnetic field with period as low as ten seconds is not so important.

(ii). Induction due to the motion of the line in the permanent geomagnetic field

On the other hand, we have an another equivalent induced electro-motive force due to the relative motion of the overhead line to the permanent geomagnetic field when the wind and other mechanical forces act to oscillate the line in favourable conditions. The line is more or less flexible and not always bound on the insulators in the same manner at each point and, moreover, the external mechanical forces, of which most effective one is wind, usually change their directions and magnitudes with respect to time and space. Consequently, the loop formed between the line and the ground changes its area with time, and then the induced E.M.F. will become so irregular and indefinite that it would not be so easy to grasp the exact mode of the matter. Nevertheless, the order of magnitude of the induced E.M.F. may be estimated as follows. For example, at the Kakioka Magnetic Observatory we have an eastward line of one and half kilometer long as above-mentioned of which wire is fixed at fifty one points on the insulators. The mean area of each segment of the line formed between it and the horizontal line connecting two consecutive points amounts to about  $3 \cdot 10^4 \text{ cm}^2$ . For simplicity's sake, if we assume that each segment has the same area said above and as a rigid body oscillates about the horizontal axis in the plane perpendicular to the geomagnetic meridian with the same phase, then the induced E.M.F. in the whole line can amount to the order of millivolt. The magnitude estimated in this idealized case is not so small enough to be neglected compared with other kinds of universal earth-currents. In practice, however, such an idealized uniform condition can not be realized, and moreover, owing to the rapidness of the motion of the segment, only a few percent of this amount will be actually recorded by an ordinary galvanometer or such like apparatus with its proper period of a few seconds. Actually, during the long period of observation at Kakioka we could not detect any remarkable trace on the electrogram even when rather strong wind blew

It is necessary, however, to take these effects into account when the small and rapid variations such as micropulsations comparable with those of the earth ground are to be recorded.

(B). *Atmospheric electric effects upon the line*

Accompanying with the disturbances in atmospheric electricity in such bad weathers as thunderstorms, heavy rains, snowfalling, solid precipitation and etc, we have frequently recorded some irregular and rather larger variations in both components at Kakioka. The amplitudes of these variations differ markedly in different localities, and depend upon the prevailing meteorological conditions, topography, height of the overhead line and etc. On the meteorologically calm days, however, no such remarkable abnormal changes can be observed. Therefore, such kinds of local effects due to the changes of atmospheric electricity, of which major part may due to the antenna-earth current, are only occurred in very specified time intervals, and then give no serious handicap for the discussion of the general aspects of earth-currents.

Generally speaking, however, we have some possibilities to suppose more extended spatial correlation, or rather world-wide relation between earth-currents and atmospheric electricity through the transfer of electricity between the air and the earth, but the discussion for these problems are out of the scope to be treated in the present paper.

An example at the Kakioka Magnetic Observatory is shown in Fig. 1, which was accompanied with the precipitation of hailstone of moderate intensity. The

maximum ranges of this variation recorded by some lines are given in Table 3. It shows how much differ these variations in different localities. In reference to this, the topographical and geological features near the observatory are shown in Fig. 2 together with the site of the observatory. For convenience's sake for the further statement, some of the regular and temporary base lines drawn in the figure are numbered and their base lengths are also given in Table 4.

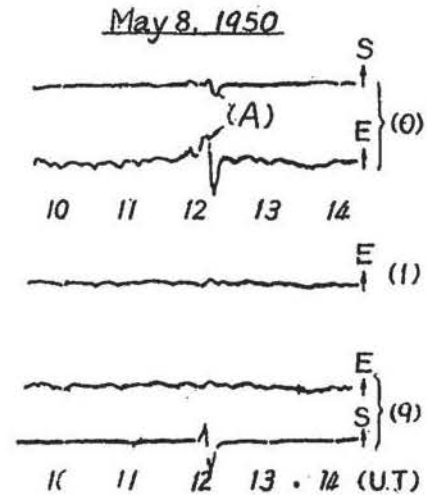


Fig. 1. Abnormal variation of earth-current potentials accompanied with hailstones of moderate intensity, (A). Arrows show the direction of current flow.

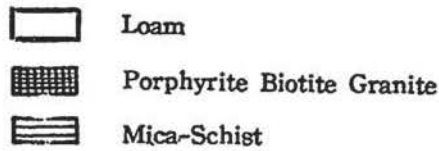
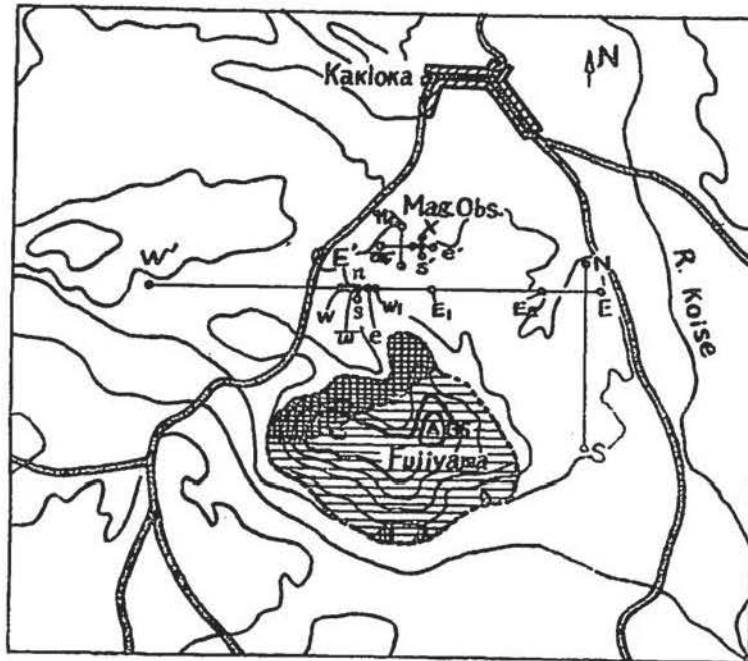


Fig. 2. Arrangement of regular and temporary earth-current lines, and geological and topographical sketch near the Kakioka Magnetic Observatory.

Table 3. Local abnormal variations of earth-current potentials accompanied with hailstones at Kakioka

Base line*	Base length		Max. range, mV/km		Amplitude ratio of universal currents	
	EW	NS	EW	NS	EW	NS
(0)	1.50km	1.10km	79.8	36.8	1	1
(1)	100m	100m	0.6	—	0.70	0.92
(9)	100m	100m	0.6	160.5	1.24	0.64

\* Refer to Table 4.

Table 4.

Base line		Designated number of base lines
Component	length	
EW NS	1.50km 1.10km	(0)
ew ns	100m 100m	(9)
e'w' n's'	100m 100m	(1)
E <sub>1</sub> W <sub>1</sub>	350m	(3)
E'W'	1.35km	(2)
E <sub>2</sub> W <sub>1</sub>	1.05km	(4)
e <sub>1</sub> w <sub>1</sub> n <sub>1</sub> s <sub>1</sub>	210m 210m	(5)

In connection with this phenomena, it should be remembered that some abnormal variations in bad weathers are often mistaken as those due to atmospheric electricity, but they are really caused by fault insulation of the line and insulators.

### 3. *Insulation*

It is one of the most important requirement for the satisfactory measurement of earth-currents to keep the total circuit in adequate insulation throughout the measuring period notwithstanding any unexpected changes in the natural and artificial circumstances under which the measurements are regularly carried on. The difficulties in obtaining adequate insulation are mainly encountered in the field equipments, that is, overhead and underground lines, together with insulators and leads joining the electrodes to the lines. Sometimes the faulty insulation of the overhead lines may be introduced unconsciously by touching and injuring their coating with something like branches of trees, except the gradual decrease of insulation resistances of the lines and insulators due to the changes of their materials over a period of years. As to the underground lead joining the electrodes proper to the lines, the matter is very troublesome, for its insidious effects are influenced by various kinds of changes of physical and chemical states of the surface layer of the earth. The following experimental results may give an idea of the order of error to be introduced in the measurements due to faulty insulation.

(A). Error due to faulty insulation of the line and insulator

(i). Simple circuit

The simplest case of measuring arrangements will be considered; more complicated ones can be treated in the similar manner. In Fig. 3, the overhead line is supposed to be earthed between Px and Qx through the total-resistance X, then the current  $i_g$  flowing in the line can be expressed as follows;

$$i_g = \frac{v}{R_0} \left\{ \frac{X + C_1 \frac{v_x}{v}}{X + C_1 \left(1 - \frac{C_1}{R_0}\right)} \right\} \equiv \beta \frac{v}{R_0},$$

where  $v_1$ ,  $v_2$  and  $v_x$  are earth-current potentials at the points of electrodes  $E_1$ ,  $E_2$  and earthed point Px;  $C_1$  and  $C_2$  the contact-resistances at the respective electrodes. Since the condition  $\beta \leq 1$  is usually fulfilled for  $C_1/R_0 \ll 1$  in practice, though the case of  $v_x > v_1$  when  $v_1 > v_2$  can be possible along some path of the overhead line,  $i_g$  will become generally small compared with the case when the line is kept in perfect insulation, i. e.,

$$i_g < (i_g)_\infty = \frac{v}{R_0}$$

It is to be noted that the reduction coefficient  $\beta$  is almost determined by the ratio of the contact resistance at the electrode to the insulation resistance at the pole or some point on the line.

(ii). Model experiment

These considerations were illustrated in the following simple model experiment of which arrangement is shown schematically in Fig. 4. Two similar rectangular copper electrode  $P_1$  and  $P_2$  (2.0 cm  $\times$  2.0 cm) was immersed at a horizontal distance  $l$  apart in the concentric  $\text{CuSO}_4$  solution in which an approximately uniform electric field was set up between copper electrodes  $E_1$  and  $E_2$ . All splices joining  $P_1$  and  $P_2$  to heavy rubber doubly coated wires  $m_1$  and  $m_2$  was thickly coated by high quality pitch to be impervious to the

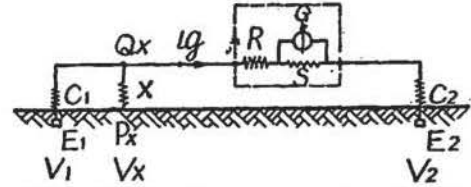


Fig. 3. Simple gavanometer circuit.  
R: High manganin series resistance.  
G: Coil resistance of galvanometer.  
 $C_1, C_2$ : Contact resistance at the electrode  $E_1$  or  $E_2$ .  
S: Universal shunt resistance.

$$v = v_1 - v_2, \quad v_x = v_x - v_2$$

$$R_0 = R + \frac{GS}{G+S} + C_1 + C_2$$

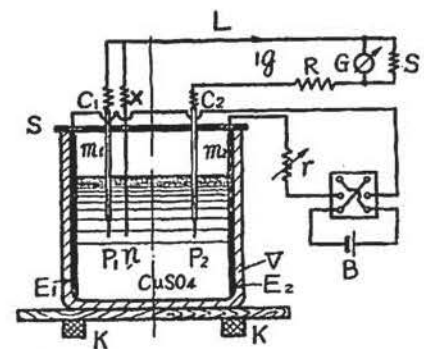


Fig. 4. V: Glass vessel, 18cm  $\times$  21cm  $\times$  21cm.  
S: Wooden plate cover.  
E's: Copper plate electrodes.  
m's: Heavy rubber wire.  
p's: Copper plates.  
n: Copper wire.  
K: Porcelain insulator.  
 $l = P_1P_2$ ,  $x = P_1n$ .

solution. A copper wire  $n$ , 1 mm in diameter, was then dipped into the solution at the distance  $x$  from  $P_2$  on the line joining  $P_1$  and  $P_2$ . The current  $i_g$  passing through a galvanometer  $G$ , its sensibility being  $1.50 \cdot 10^{-3}$  Amp. per mm and period 2 seconds, was measured for two cases when  $n$  was connected to the base line  $L$  and disconnected from it, corresponding to the actual cases of faulty and perfect good insulation. Some examples of the results thus obtained and calculated values by the expression of  $i_g$  in (i) are given in Table 5. The example A shows the linear functional relation between  $i_g$  and  $x$ . The examples  $B_1$  and  $B_2$  were carried out to check the asymptotic variation of  $i_g$  by increasing  $X/C_1$ , all tabular values of currents being expressed by divisions of the deflection.

Table 5A. Relation between  $i_g$  and  $x$ 

$(i_g)_\infty$	$x(\text{cm})$	$i_g$	
		obs.	cal.
18.5	6.1	16.4	16.6
18.4	5.3	15.5	15.6
18.4	4.4	14.9	14.7
18.4	2.9	13.1	13.1

$X=17\Omega$   
 $C_1=C_2=14\Omega$   
 $R+\frac{GS}{G+S}=11000\Omega$   
 $l=8.0\text{cm}$   
 one div= $0.6 \cdot 10^{-3}$  volts.

Table 5B<sub>1</sub>. Relation between  $i_g$  and  $X/C_1$ 

$X_0(\Omega)$		$5 \cdot 10^2$	$1.5 \cdot 10^3$	$3.5 \cdot 10^3$	$7 \cdot 10^3$	$2 \cdot 10^4$
$i_g$	obs.	16.1	17.0	17.8	18.2	18.4
	cal.	15.9	17.2	17.8	18.3	18.4
$(i_g)_\infty$		18.8	18.8	18.6	18.7	18.6
$X/C_1$		0.75	2.20	5.10	10.15	29.0

$C_1=690\Omega$ ,  $R=14000\Omega$ ,  $l=8.0\text{cm}$ ,  $x=5.5\text{cm}$   
 $X=X_0+C_n$ ,  $C_n=17\Omega$ ; contact resistance at  $n$ .

Table 5B<sub>2</sub>.

$X_0(\Omega)$		$10^2$	$5 \cdot 10^2$	$10^3$	$5 \cdot 10^3$	$10^4$	$5 \cdot 10^4$	$3 \cdot 10^5$	$10^6$
$i_g$	obs.	13.3	14.0	14.8	17.0	17.8	18.5	18.9	19.0
	cal.	13.2	14.0	14.7	17.0	17.8	18.7	19.0	19.0
$(i_g)_\infty$		18.9	18.9	18.9	18.9	18.9	19.0	19.0	19.0
$X/C_1$		0.04	0.17	0.34	1.67	3.32	16.7	99.5	332

$C_1=3014\Omega$ ,  $R=14000\Omega$ ,  $l=8.0\text{cm}$ ,  $x=4.5\text{cm}$ .

In the above experiments contact resistances at  $P_1$  and  $P_2$  were assumed to be equal and one half of the effective resistance between  $P_1$  and  $P_2$ . The contact resistance at  $n$  was calculated in the same way by subtracting the contact resistance at  $P_1$  from the effective resistance between  $P_1$  and  $n$ . The good coincidence between the experiment and calculation proved that the uniform electric field was fairly well established in the solution, and it was not disturbed by the arrangements of the experiment and the current flowing in the circuit, showing no appreciable polarization effect at electrodes. Indeed, as it is seen in Fig. 5 the potential drop between the electrode  $P_1$  and  $n$  ( $V_1 - V_x$ ) was increased linearly with the increasing distance between them.

(iii). Field experiment

A similar field experiment was carried out for the east component of the universal earth-currents at Kakioka. Some experimental details are given in Table 6 where all resistances were measured by the Kohlrausch's bridge, notations being to be referred to Fig. 3 or the expression of  $i_R$ .

Table 6.

$C_1$	$X$	Distance $E_1 E_2$	Distance $E_2 P_X$	$R_0$
$1.2 \cdot 10^3 \Omega$	$1.2 \cdot 10^3 \Omega$	100m	57m	$301.1 \cdot 10^3 \Omega$

The decrement of the amplitude of the short period variations when  $X$  was connected to the line is clearly seen in Fig. 6, where the amplitude is plotted referred to the same variations recorded by another independent adjacent eastward line of equal length as a reference base. From these two linear relations we obtained the coefficient  $\beta=0.80$ , while the calculated value is  $\beta=0.79$ .

When the measurement is under fear of low accuracy by large contact resistances or low insulation resistances, the scale value, or voltsensibility of the electrogram is frequently calibrated by impressing the known electromotive force in the total circuit including the earth instead of substituting it only across the galvanometer unit in place of lines (Fig. 7). In the former method of scaling, scale value is apt to be disturbed

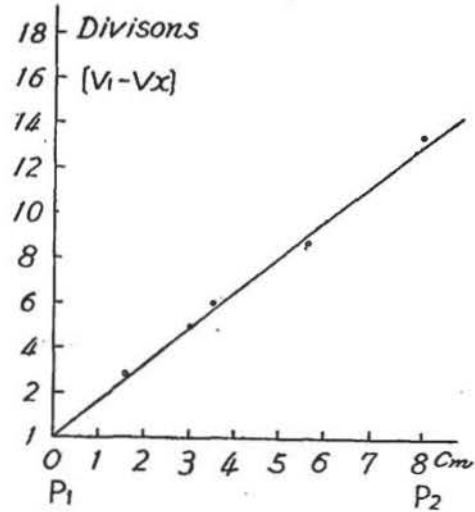


Fig. 5. Potential drop between  $P_1$  and  $n$ , ( $V_1 - V_x$ ), and distance between  $P_1$  and  $n$ .

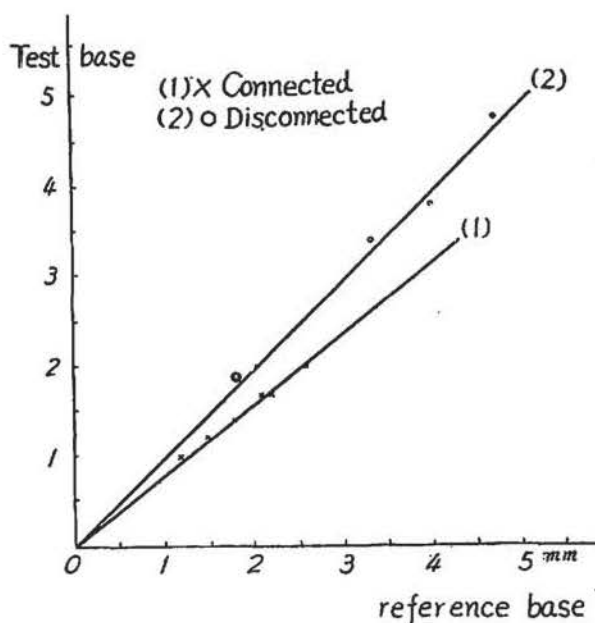


Fig. 6. Decrement of amplitude of the universal earth-current potentials when the line is artificially earthed through the insulating resistance  $X$ .

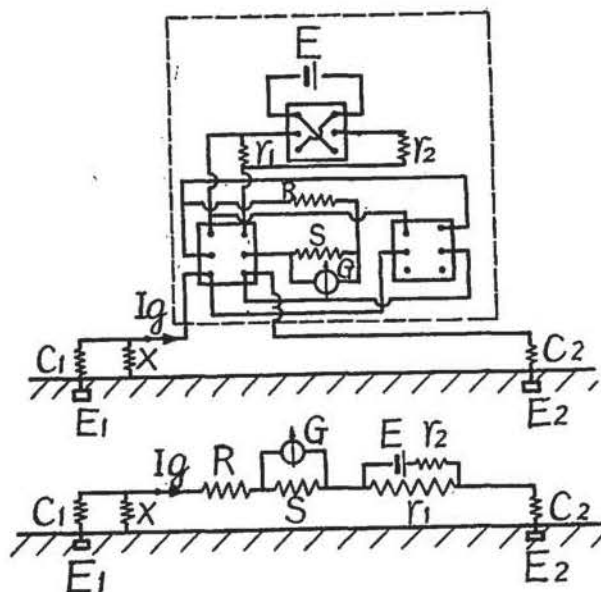


Fig. 7. Galvanometer method with the calibrating circuit for the total resistance including the earth.

during the time of operation by the short periodic fluctuation of the universal currents themselves, and sometimes polarization currents. If we keep the resistance of the circuit in such a way that,

$$R + \frac{GS}{G+S} + \frac{r_1 r_2}{r_1 + r_2} \gg C_1 + C_2,$$

the scale value determined by the latter method becomes approximately independent of contact resistances  $C$ 's and  $X$ .

At any rate, from these considerations it can be concluded that the contact resistances at electrodes should be minimized as possible as we can in order to avoid both unstable potentials due to the variations of contact resistances and insidious errors caused by the faulty insulation of the lines and insulators, provided no unstable contact potentials are consequently introduced in the circuit.

#### [B]. Errors due to faulty insulation of measuring apparatus

Although it seems apparently to be much easier to keep the measuring apparatus in the room than to keep the outdoor equipments in adequate insulation, we must take care of the occurrence of faulty insulation effects during the long period of observations, especially when potentials are to be recorded photographically by means of sensitive galvanometers in a dark room. Most of events happened at Kakioka and other places were due to the unsatisfactory conditions of the galvanometer set, that is, damage of

insulation between two terminals of a galvanometer, leakage through the tripods and leading wires connected from the shunt resistance to the galvanometer, and so on. These unsatisfactory conditions were all caused by the accumulation of very small dust particles on the surfaces of insulators in the course of long time recording in a dark room, of course, the events being promoted by the moisture content in the air. The rest minor parts were due to the faulty insulation at terminals of various connections and natural decreament of insulation resistance of insulators used.

These insidious errors due to faulty insulation, however, can be detected and preventable by the effort of constant and careful cleaning the main portions of galvanometer sets and all terminals in the circuit and checking for the constancy of daily scale values, jointly using the suitable devices for protecting the all apparatus from the dust accumulation, variations of air humidity and temprature. For example, coating bared portions of the leading wire near the terminals and tripods with high quality liquid insulator, sealing the wax on the surface of concrete block on which the galvanometers were set, and sometimes setting the galvanometers in a suitable thermostat, or in a semi-underground house in which temperature and humidity were kept approximately constant, and etc., were all experienced to be simple and useful for the present problem.

At last, it is not to be forgotten that in some case all dry cells or batteries, usually 1~6 volts, used in the calibrating circuit or potentiometer circuit should be carefully insulated.

#### 4. *Contact resistances and their time variations*

Some examples of the effective contact resistances between two electrodes and their time variations measured at Kakioka are given in Table 7, which were all measured by the Kohlrausch's bridge with the alternating current source of ten thousand cycles. As is seen in the table, their mean values extend from the minimum five hundred ohms of ew component to the maximum seven hundred ohms of ns, while for each base he maximum deviation from its mean in the course of the year approximately amounts .o 20%. Thus, in this case the effective contact resistance of EW, or ns component above-mentioned only amounts to less than one percent of the high series resistance inserted in the circuit, and at least the seasonal variations of all components can be neglected in the measurement of potentials. As it is well known, the contact resistance

is principally controlled by the surface area of the electrode, closeness of contact between the surface of the electrode and its adjacent part of the soil, amount of moisture content, kinds of salts contained in it, and so on. Then, at different places and by different process of installation, we may have sometimes so large contact resistances, or their remarkable time variations that the accuracy and stableness of the measurement are principally decided by the unavoidable changes of chemical and physical states of the ground. In practice, however, it may be more important to keep the constant contact resistance in long period than to make it as small as possible, if we can not realize simultaneously these two conditions. Any extraneous effect at the electrode, which may be accidentally introduced by making mechanically the contact resistance as small as possible, should be avoided, because any unstable contact potential is usually much troublesome to treat than to avoid the effect due to a rather large contact resistance.

Table 7. Effective contact resistances (R) in some independent base lines at the Kakioka Magnetic Observatory. ( $\times 10^3 \Omega$ )

Date	1948											1949				
	19/IV	29/V	28/VI	31/VII	28/VIII	31/VIII <sup>(1)</sup>	16/IX <sup>(2)</sup>	17/IX <sup>(3)</sup>	19/IX	30/X	24/XI	8/XII	22/I	22/II	23/III	
Base * line	EW	0.64	0.62	0.56	0.60	0.63	0.60	0.55	0.45	0.48	0.54	0.51	0.54	0.55	0.60	0.63
	ew	0.57	0.55	0.50	0.49	0.44	0.45	0.42	0.44	0.44	0.49	0.50	0.53	0.58	0.59	0.60
	ns	0.82	0.78	0.67	0.64	0.59	0.59	0.54	0.56	0.57	0.60	0.65	0.68	0.75	0.75	0.76
Remarks	(1) after rain; (2) heavy rain; (3) after heavy rain															

\* Refer to Table 4.

Referring to the further continued data[4], the contact resistance generally undergoes a rather simple seasonal variation with a maximum in the interval from the later spring to the early summer, and a minimum in the autumn months, though some irregularities are found in the period from the later summer to the early autumn (Table 7). And the mean amplitude of the seasonal variation seems to make no remarkable change from year to year as far as these electrodes are concerned. On the occasions of heavy rains, however, the contact resistance of the regular eastward base, (O)-line, decreased rapidly and recovered gradually, of which mechanism may be connected to the irregularities appeared in the period from the latter summer to the early autumn above-mentioned.

Although we have no need in this paper to touch the further details of the contact resistance, it may be worthy to see a similar seasonal variation of the earth's

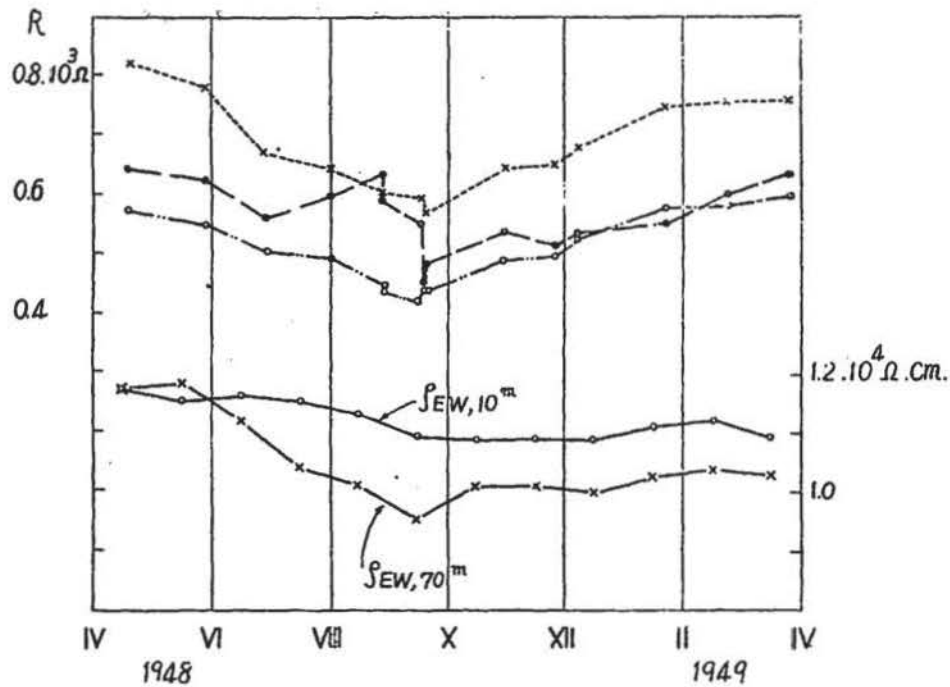


Fig. 8. Seasonal variation of effective contact resistances and earth-resistivities at Kakioka.

resistivity of the upper layer of the earth. In Fig. 8 are shown the seasonal variations of both effective contact resistances ( $R$ ) and resistivities ( $\rho$ ) which were measured by the method of Wenner-Gish-Looney with a megger type ratiometer (L-10 type resistivity meter by the Yokogawa Electric Works). In the vicinity of the observatory the uppermost layer up to the depth about one hundred meters below the surface has a rather uniform resistivity of about  $10^4 \Omega \cdot \text{cm}$ . It may be expected from this figure that the seasonal variation of the contact resistance can be principally controlled by that of resistivity, but depends locally upon the physical and chemical states in the adjacent part of the ground to the electrodes.

##### 5. Variations of contact potentials

From the electrochemical point of views, there should be no potential difference existing between two electrodes which are identically equal in their physical and chemical states and made to contact with a homogeneous and isotropic medium. However, this is not practically realized in earth-current measurements, even if we use two identically equal electrodes. Therefore, it is a common sense among the earth-currentists that one of the most important points in the earth-current measurement is how to minimize the contact potentials and how long to keep it in a constant state, because it is

practically impossible to bury the electrodes in the ground without some contact potentials between any two electrodes. In order to get a pair of electrodes to meet these troublesome demands, skilful methods have been proposed by some authors (5).

In our routine works it was frequently effective in practice to bury both electrodes in some artificially prepared substances in place of the natural soils. At Kakioka two electrodes were buried in large volume of charcoal fine gravels, of which some details of performance will be described in the next paragraph. For another example, at Owashi ( $\lambda=136^{\circ} 12'E$ ,  $\varphi=34^{\circ} 04'N$ ), a branch station of the Magnetic Observatory, by replacing the very sandy ground of about three cubic meters with the fine clayey soil, in which double-carbon electrodes were installed, large contact potential variations were almost disappeared in the eastward line (Fig. 9a). Before this reconstruction of electrodes the record of this base showed the very typical and large contact potential variations due to the rainfall as shown in Fig. 9b. For the northward base, however, there was seen no remarkable improvement, because we made no replacement of soil for the south elec-

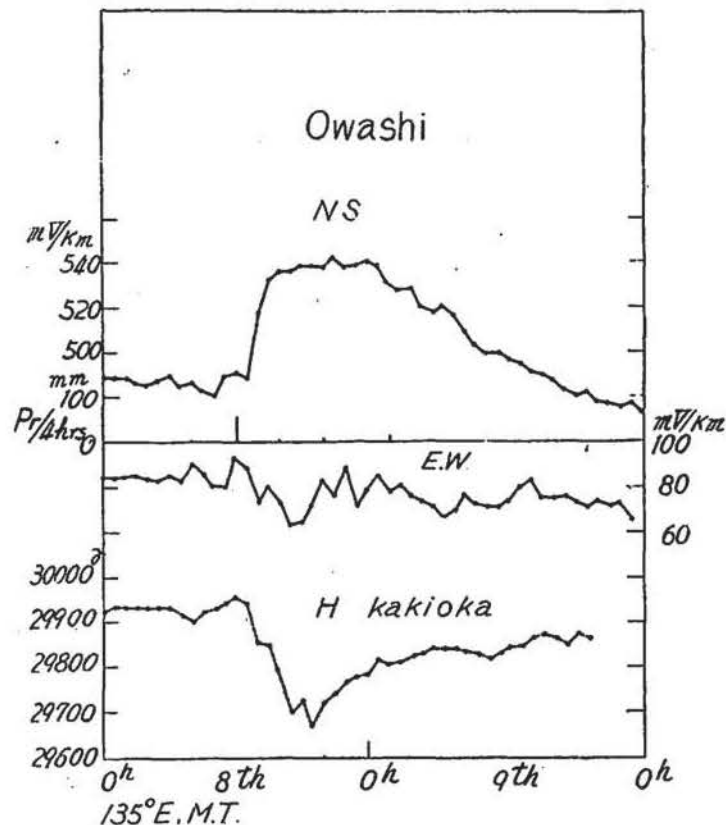


Fig. 9a. An example showing improvement of electrode performance by replacing the natural ground with other substances at Owashi.

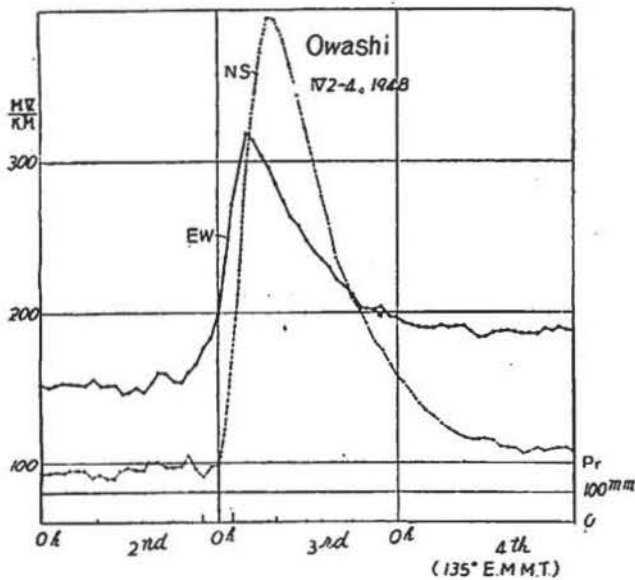


Fig. 9b. Large and rapid abnormal changes of earth-current potentials due to rainfall at Owashi.

which recording was started in April, 1950. This base was situated on the line extended westwards of the regular eastward line, (0)-line, and its east-pole was set down about ten meters eastwards to the west-pole of the latter. The electrode used is schematically shown in Fig. 10. Two carbon rods were buried in charcoal gravels, which were carefully packed in a hollow concrete cylinder enclosed by sand layer, and connected parallel with the overhead line. All outer surface of the concrete cylinder and its cover were coated with pitch to protect the vessel from the percolation of moisture from the surrounding soil, except the bottom side. For the underground leading wire was used the lead cable wire. As it is

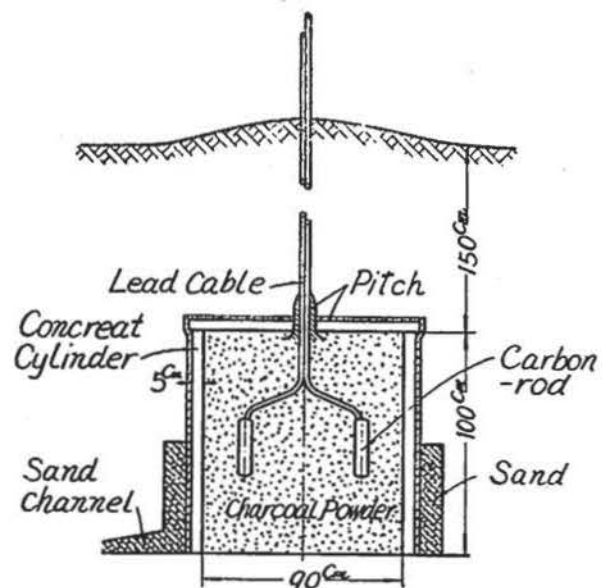


Fig. 10. A "pot" electrode buried upside down.

seen in Fig. 11, variations of daily mean values of potential gradients observed by this line and the regular EW line, (0)-line, are fairly in good accordance each other in spite of the latter base being set down about sixteen years ago. As a whole,

trode only. This improvement for the eastward base may be explained by the very small change of moisture content in the carefully compacted clayey volume said above due to its smaller coefficient of permeability compared with that of the very sandy part surrounding it.

An another example of similar, but more elaborate electrode performance was carried out at Kakioka for the equipment of the sub-regular eastward line, (2)-line, of

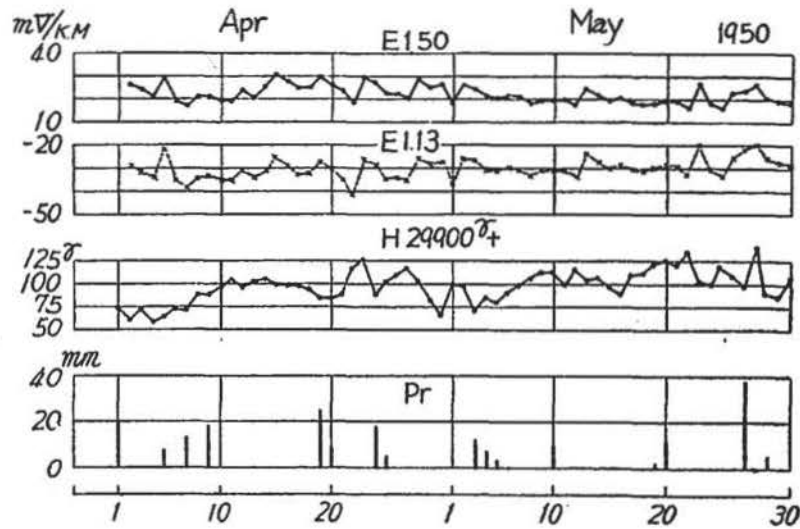


Fig. 11. Comparison of daily mean values of two independent base lines with different electrodes, "pot" electrode and copper-charcoal electrode.

they made also no appreciable long period variations due to some extraneous effects near the electrodes, showing hardly connection with neither the corresponding daily means of the horizontal intensity of geomagnetism, nor amount of rainfall.

These examples, therefore, tell us that if we can pay our careful and proper considerations to both construction and installation of electrodes, and together with to the circumstance of the place, we can expect a possibility to get a fairly good condition of electrodes, and consequently stable contact potentials.

Concerning to the electrode performance, it must be also noted that though it is frequently less emphasized to protect splices joining the underground wire to the electrode proper from permeation of soil moisture, remarkable contact potentials can be appeared especially when the soldered joints are imperfectly exposed to the ground. Referring to this point, the following simple experiment was carried out. By the same arrangement shown in Fig. 4, contact potential between  $P_1$  and  $P_2$  was measured when soldered jointed points between  $m$ 's and  $p$ 's were exposed to the solution by tearing off the pitch layers coated on their surfaces. Some of the results are given in the following Table 8.

Table 8. Variations of contact potential due to imperfect insulation at splices.

Pitch layer	Contact potential between P <sub>1</sub> and P <sub>2</sub>	
(1) exist on both side of P <sub>1</sub> and P <sub>2</sub>	0.06mv	P <sub>1</sub> negative
(2) no layer on one side of P <sub>1</sub> only and P <sub>2</sub> unchanged	19.60	P <sub>1</sub> negative
(3) no layers on one side of both P <sub>1</sub> and P <sub>2</sub>	0.35	P <sub>1</sub> positive
(4) no layers on both sides of P <sub>1</sub> and one side of P <sub>2</sub>	15.33	P <sub>1</sub> negative
(5) no layers on both sides of P <sub>1</sub> and P <sub>2</sub>	0.18	P <sub>1</sub> positive

Therefore, when we have some different materials with different physical and chemical states at some parts of electrodes or its underground wires, serious precaution must be paid for the electrode performance, for instance, when the lead electrodes are used.

As it is easily understood by the above experiment, similar precaution should be paid for the perfect protection of underground wires from the abrasion and corrosion, even no different materials being contained in them. If a part of the copper wire directly or through low insulation is exposed to the soil, at which depth it might has different physical and chemical states from those at the electrode proper, the very part of the wire would take a role of an another electrode. The contact potentials thus produced may be apt to vary especially near the earth's surface, accompanying with the variations of various kinds of meteorological elements, i.e., temperature, amount of rainfall, content of soil moisture and so on. An actual example will be shown in Fig. 12 in which all curves are drawn by the original millimeter readings. In the compound of the Kakioka Magnetic Observatory, a temporary eastward line, 100 meters long, was installed in October, 1944, adjacent to the sub-regular base, (1)-line. In this case as the underground wire was used a simple lead cable, thickness of the outer lead cover and inner single layer gum were 0.6 mm and 1.0 mm, respectively. At first, registrations were found normal, but seemed gradually to become out of order before not so long time passed after installation. In the figure D's curves will be responsible for the samples showing these different processes. The curves, D's, are calculated from the hourly values of both sub-regular base and temporary one by the following expression,

$$D_1 \equiv e_1 - \alpha e_2 = s_1 (I_1 - I_2 / \beta), \quad \beta = \frac{\Delta I_2}{\Delta I_1}, \quad \alpha = \frac{\Delta I_1 \cdot s_1}{\Delta I_2 \cdot s_2} = \frac{1}{\beta} \frac{s_1}{s_2},$$

where

- $e_1$ : hourly absolute values of the sub-regular base line.  
 $e_2$ : hourly absolute values of the temporary base.  
 $l_1$ : length of ordinate in mm on the recording paper for  $e_1$   
 $l_2$ : length of ordinate in mm on the recording paper for  $e_2$   
 $\Delta l_1$ : mean length of ordinate in mm corresponding to the amount of changes of short-period variations of the universal earth-currents for the sub-regular base line.  
 $\Delta l_2$ : corresponding value to  $\Delta l_1$  for the temporary base line.  
 $s_1$ : scale value (mv/km) for the sub-regular base line.  
 $s_2$ : scale value (mv/km) for the temporary base line.

Since it is reasonable to suppose that the electric conductivity of the earth is constant during the time interval, now two days, as far as the present bases are concerned,  $D_1$  can be responsible for a kind of residual potential which depends upon the local potentials, mainly contact potentials. Then, if the curve  $D_1$  shows a straight line, both bases relatively have no variable contact potentials, while when it does not so, both or either of them contain some variable potentials in the interval of time concerned. In the figure the upper  $D_1$  curve (Dec. 19-20, 1944), which corresponds to the normal state at the beginning of the installation, shows almost a straight line in the limit of error, while on the contrary, the lower  $D_1$  (Dec. 9-10, 1950) changes with a large diurnal variation. On the other hand, we have no such a diurnal variation in the  $D_2$  curve which is calculated in a similar way as done for  $D_1$  by combing the sub-regular base, (1)-line. and regular EW base, (0)-line. Then this large diurnal variation of  $D_1$  must be originated in the temporary base only. Indeed, it is very reasonable to see an intimate correlation between  $D_1$  (Dec. 9-10, 1950) and the simultaneous variation of soil temperature as shown in the lowest curves, because the reexamination of the underground lead wires showed clearly faulty insulation at two parts of the west pole wire. It is to be especially noted here that the "residual potentials", or "D-curve" method proposed here will be useful for the detection of various kinds of local changes superposed on other parts of potentials, which may otherwise be overlooked even by a keen observer due to their small amplitude or indefinite occurrence[6].

*6. Comparison of universal earth-current potentials observed with different kinds of electrodes and apparatus*

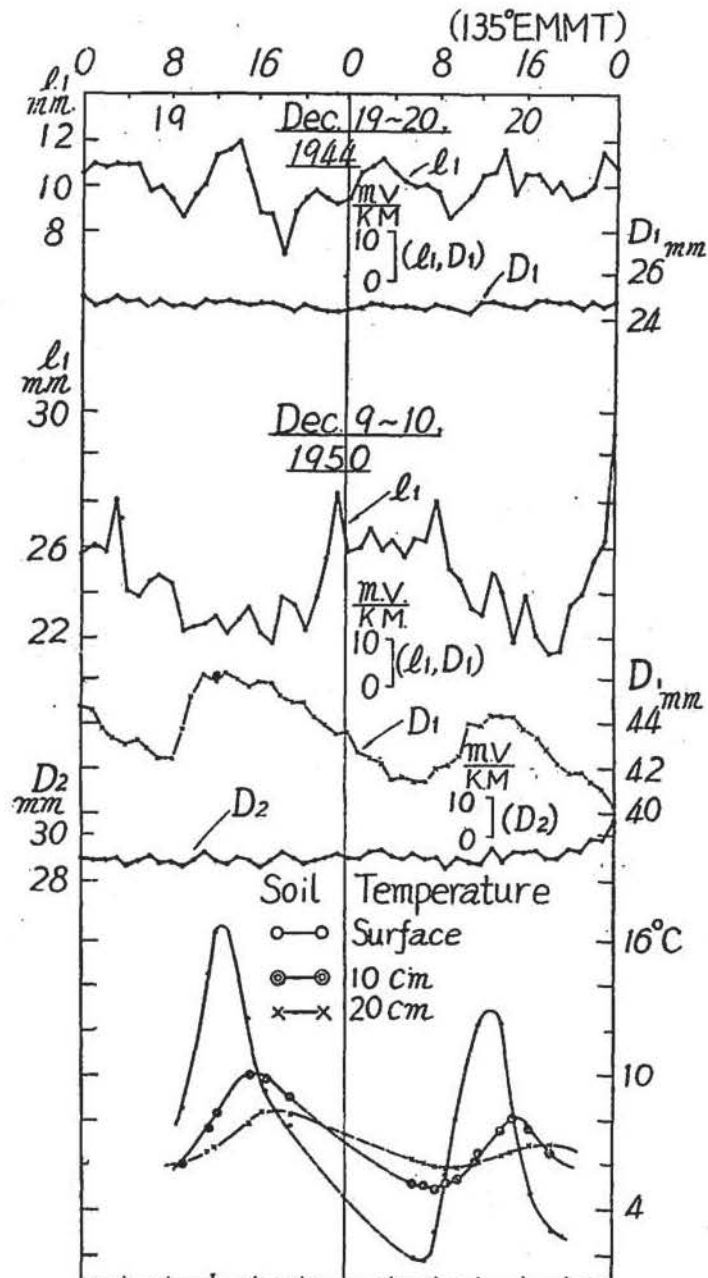


Fig. 12. An example showing abnormal variations of earth-potentials due to faulty insulation of an underground loading wire.

(A). Galvanometer method with different kinds of electrodes

In order to check whether some independent records obtained by the usual simple galvanometer method with different kinds of electrodes and different order of magnitude of current flowing in the circuit do accord with each others, or not, three temporary continuous observations were carried out in the compound at the Kakioka Magnetic Observatory. Each of the lines is equally of 100 meters long and laid almost

in the same east-west vertical plane. In order to get accurate readings avoiding any error due to gradual change of absolute values, only short period variations continued less than thirty minutes were selected on the records. The calibration of potentials was made for the total circuit including the ground. The electrodes used were of following three kinds, saturated  $\text{CuSO}_4$  non-polarizing single electrode[7], carbon rod double electrodes[8] and copper plates burried in charcoal powder; their structures are schematically shown in Fig. 13. Some details of the measurement and mean relative ampli-

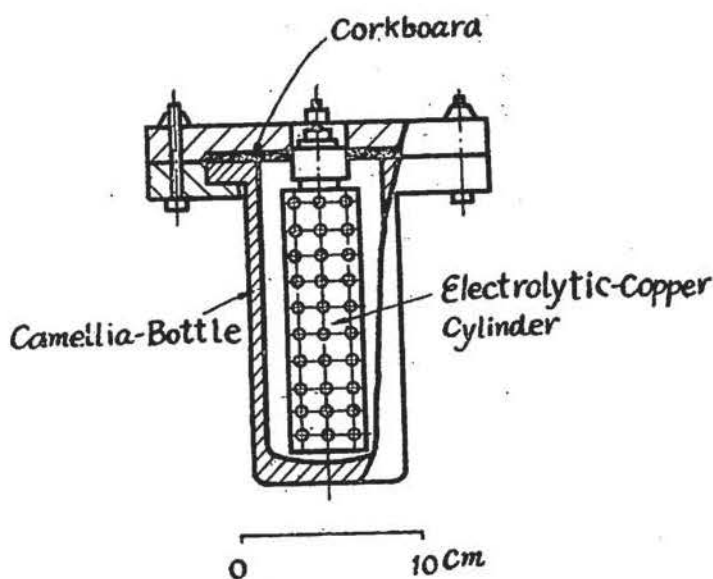


Fig. 13a.  $\text{CuSO}_4$  non-polarizing camellia-bottle electrode.

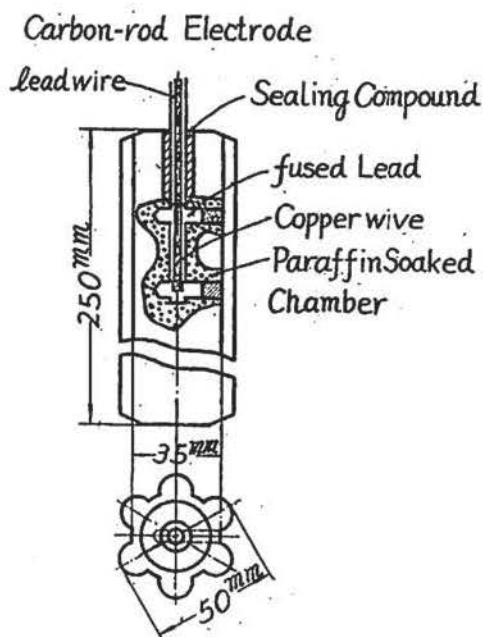


Fig. 13b. Carbon rod electrode.

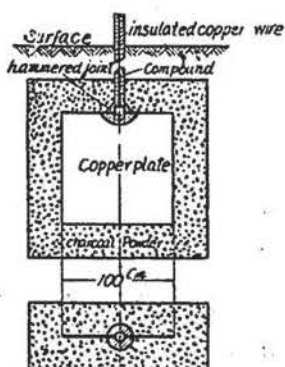


Fig. 13c.  
Copper-charcoal electrode.

tude ratio which are derived from the mean values of potentials for each specified interval of amplitude range are given in the following Table 9. As it may be expected only from the table, we can find no statistical significant difference between any two mean values of potentials among the three observations. In addition to the above experiment, further test observations were carried out for shorter lines down to ten meters long, and the former result was satisfactorily justified. As it is reasonably expected, therefore, it may be

Table 9. Mean relative amplitude ratio for short period variations of universal earth-currents.

		Amplitude range: $mp/km$				Sc (Amp/mm)	Ea (Amp.)	h (cm)
		0-1.99	2.00-3.99	4.00-5.99	>6.00			
Number of obs.		12	8	3	2			
Electrode	CuSO <sub>4</sub>	1	1	1	1	$1.0 \cdot 10^{-9}$	$2.5 \cdot 10^{-8}$	20
	Carbon	0.97	0.98	0.95	0.98	$12.0 \cdot 10^{-8}$	$4.0 \cdot 10^{-8}$	57
	Copper	0.99	0.99	0.97	0.98	$1.3 \cdot 10^{-7}$	$1.2 \cdot 10^{-6}$	350

Sc: Current sensibility of galvanometer.

Ea: Mean absolute value of potentials expressed by current.

h: depth of electrode at their middle points.

sarely said that the method of continuous galvanometric recording of earth-current potentials can afford the same result within the limit of error when the field equipment is in favourable conditions, notwithstanding that the nature of material, dimension and arrangement of electrodes themselves and, in a certain case, the magnitude of the current flowing up the circuit, are all different in wide range.

#### (B). Micromax self-recording potentiometer method

At Kakioka we compared the amplitudes of the universal earth-currents measured by two independent methods, the one was the simple galvanometric method above-mentioned and the other that of the self-recording potentiometer of micromax type[9]. The current sensibility of the galvanometer attached to the potentiometer is about  $10^{-7}$  amp/mm, which corresponds to 0.6 mv/mm on the recording paper, and the balancing operation can be repeated every two seconds. The potential differences to be measured are intermittently marked on the sheet every fourty five seconds by synchronous devices. The bases used for comparison are two eastward lines of which one is the regular line, (0)-line, and the other running 1.05 km long easterly from the point 150 meters east to the east pole of the former base. An example of comparison for the diurnal

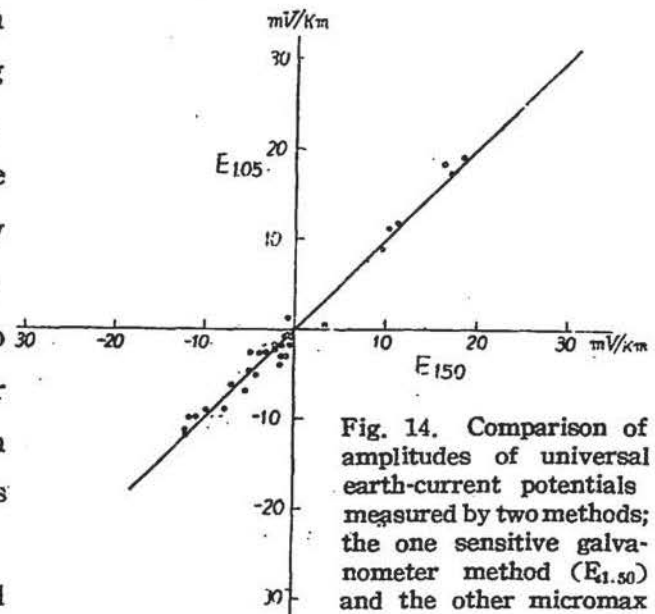


Fig. 14. Comparison of amplitudes of universal earth-current potentials measured by two methods; the one sensitive galvanometer method ( $E_{1.50}$ ) and the other micromax self-recording potentiometer method ( $E_{1.05}$ ).

variation is shown in Fig. 14 in which for the galvanometer method all available hourly departures from the mean in the whole period are given at just times, while for the potentiometer method each corresponding value is interpolated by two consecutive points before and after the just time. As it is seen in the figure two methods afford a good coincidence as a whole; their mean values of the absolute magnitude of departures are  $E_{1.05}=6.79$  mv/km and  $E_{1.50}=6.85$  mv/km, respectively. Moreover, more direct comparison by using the same instantaneous values for short period universal variations showed better coincidence even for each individual observation. On the other hand, similar comparisons between two observations made by the galvanometric method only give no differences nearly within the limit of error [10].

### 7 Polarization

At last but not least a word should be added to the above-mentioned statement that we could hardly find any appreciable amount of so-called polarization effect as far as the above experiment was concerned. In order to avoid or minimize polarization it is desirable on principle to measure statically or to keep the amount and duration of current flowing in the circuit as small as possible; in practice the latter, that is, potentiometric method will be better for the measurement. Nowadays, some types of self-recording potentiometers with skillful mechanical or electronic devices may be applied to it. For the observation of rather long period phenomena, an intermittent recording may be better for the aim of minimizing polarization, but at the ordinary observatory continuous recordings of such short period variations as their duration time less than some minutes are needed as well as those of diurnal variations. From this point and other technical reasons, the sensitive galvanometric method is conveniently used, and can be also effective, as already written, for minimizing polarization, provided satisfactory performance of electrodes, small contact potentials and perfect insulation. Some experiments [11] and field works suggest that a part of polarization can be controlled by the physical and chemical natures of different soils or artificially introduced materials around the electrodes. At any rate it is possible to make polarization as small as to be practically neglected by using suitable method, proper apparatus and electrodes.



empties into the Lake Kasumigaura at the distance about 20km from the observatory. A small hill, 136 metres high above the sea-level, stands about one kilometre apart in due south from the observatory, along its foot being laid down the regular eastward line.

According to the geological survey carried out in the neighbourhood of the Tsukuba mountain blocks by the Geological Survey Bureau[12] and to our preliminary measurement of earth-resistivity made in the vicinity of the observatory, it was shown that the geological structure in the hilly parts are more or less complex due to abundance of granite and mica-schist. The land near the observatory is, however, covered with the superficial uniform layer of loam, except the upper part of the hill, where rocks lay bare at several points of the surface. It can be presumed that the magnitude of universal earth-current variations or their direction of current flow may be locally modified by such geological structures of subterranean masses with high resistivity.

#### (ii). Layout and equipment

Some essential points of the equipment for the regular base only will be described here we make no touch to the sub-regular short base, (1)-lines, installed as early as in 1932. The system of installation of the base is of a cross type, but not a right angle common electrode one[13]; the east and north lines intersect perpendicularly at a point 70 meters west of the east electrode and 90 meters south of the north one. The base length of the north component line is 1.10 km, its direction being north five degrees west. The east line is 1.50 km long and runs to north eighty five degrees east. This orientation of the lines was adopted to be suited to the topography and low expense, but has no inevitable need for the observation. The area in the immediate vicinity along the lines is more or less flat, the maximum range of its ruggedness being less than ten metres at most, and quite negligible compared with the base length. The overhead lines, doubly coated rubber insulated copper wires, are supported by porcelain double cup insulators fixed on wooden pillars at a height about four metres above the surface. The maintenance of all field equipments in good conditions has been carried on by laborious tour of inspection along the long course of lines and careful testing for their damages and faulty insulation.

The electrode in use is of double-electrode type, that is, consists of two copper plates of one metre square connected parallel to the main line. Each plate is buried vertically

in fine oak charcoal gravels of three or four hundred kilograms at the depth of about three meters or more below the surface, the horizontal distance being five meters apart. The part of lead-covered cable from each plate was tested for its insulation and coated with asphalt of superior quality to protect the part from corrosion and leakage. The soils in the immediate vicinity of the east and north electrodes are rather brown colour loam to the depth about two meters from which it becomes sandy, while the uppermost layer at the south and west electrodes are more clayish brown loam up to the depth three metres. During the installation the charcoal fine gravels were packed firmly and uniformly around the electrodes with careful and patient endeavour to make a pair of electrode as equal as possible. The digged soils were returned back in the hole in their natural order of deposit and harden by falling a heavy weight uniformly upon the whole area of the hole.

As the method of recording is used a galvanometric one. The sensibility of the galvanometer is enough for the ordinary recording at the order of  $10^{-8} \sim 10^{-9}$  amp./mm, because amplitude of earth-current potentials is relatively large; especially for the east component mean maximum range of the diurnal variation amounts to 19.1mv/km in the sunspot minimum year 1943. In each circuit is inserted a series resistance of manganin wires of some ten thousand ohms. It is so large compared with the effective contact resistances of the electrodes that the total resistance of the circuit becomes almost equal to the series resistance itself. The earth-potentials are photographically recorded and calculated by the deflections of the galvanometer and the scale values, which are frequently calibrated by a standard electromotive force impressed across the galvanometer unit in place of the line. The hourly zero positions of the galvanometer, from which hourly values are read, are automatically marked on the recording paper by opening the circuit for two minutes from just hour with the clock-controlled mercury relay. The recording is made on the floor in a semi-underground house at the depth two metres below the surface. A model of the simple circuit is shown in Fig. 16.

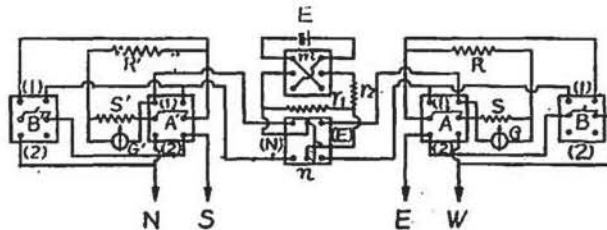


Fig. 16. A model circuit for the galvanometric method making possible to have two kinds of calibration; the one for total circuit including the earth and lines, while the other excluding them.

Regarding the measurement of earth-resistivity some details will be given elsewhere.

2. *Routine observations of earth-currents at the observatories attached to the Magnetic Observatory (Kakioka)*

At present routine observations of earth-currents are going on at following three places, Memambetsu in Hokkaido District, Kanoya in Kyushyu District and Haranomachi in the middle part of Japan Island. Their geographical coordinates and base length are given in the following Table 10. The equipments at these places are rather similar with those at Kakioka, but electrodes themselves used are of double carbon rods (Fig. 13b) except copper cylinders at Memambetsu.

Table 10.

Observatory	Lat. (N)	Long. (E)	Base length	
			EW*	NS*
Memambetsu	43° 55'	144° 12'	160m	195m
Kanoya	31 25	130 53	1.65km	2.80km
Haranomachi	37 37	140 56	1.33km	0.85km

\* Geographical west-east and north-south

Due to the violent meteorological disturbances, in the specified period of a year the maintenance of the regular recording is so difficult and frequently spoiled at Memambetsu and Kanoya. At these places underground cables and special devices of the construction and performance of electrodes are strongly demanded.

#### Concluding Remarks

In this paper are discussed the fundamental problems of earth-current measurements, that is, the method and apparatus used, performance and maintenance of field equipment and various kinds of errors which may be introduced in the measurement. In some sense, though they seem to be simple, they have not hitherto been treated so systematically that even at present there remain some obscurities to prevent the active improvement in this field of geophysics. The experimental and actual field informations will make better service to the observations of various kinds of earth-current potentials, and further precise understanding of this branch of science.

## References

- [1] a. J. E. Burbank, *Terr. Mag.*, **10** (1905).  
 b. O. H. Gish, *Terr. Mag.*, **28** (1923), Sept.  
 c. O. H. O. Gish and W. J. Rooney, *Terr. Mag.*, **35** (1930), Dec.  
 d. S. K. Bnerji, *Memo. India Met. Dep.*, **26** (1933), 1.  
 e. K. Burkhart, *Geofisica*, **19** (1951).
- [2] J. A. Fleming, "Terrestrial Magnetism and Electricity" (*Physics of the Earth VIII*), 270-306 (1939).
- [3] a. [1] a.  
 b. G. Arnold, *Beit. z. Geopys*, Bd. 49, Heft 1/2 (1937).
- [4] M. Kitamura, *Memo. Kakioka Mag. Obs.*, **6**, (1951), 1.
- [5] [1] c; [1] d.
- [6] T. Yoshimatsu, *Jour. Met. Soc. Jap.*, **15** (1937), 4.
- [7] By the courtesy of Dr. M. Iwase it was used in experiment.
- [8] Z. Kishimoto, "Musen to Zikken", Tokyo, **30** (1943) 1. (in Japanese)
- [9] Leeds and Northlap type manufactured by the Y. E. W., Tokyo.
- [10] K. Yanagihara, *Memo. Kakioka Mag. Obs.*, **6** (1951), 1.
- [11] H. Hatakeyama and T. Yoshimatsu, *Jour. Met. Soc. Jap.*, **11** (1933), 5.
- [12] Geological Map, "Tukuba", Zone 22 Col. 4, Sheet 99 (1927), (Geological Survey by H. Sato in 1924).
- [13] a. [2], p. 284.  
 b. O. H. Gish and W. J. Rooney, *Teir. Mag.*, **35** (1930), Dec.